THE PROCEEDINGS OF
THE PHYSICAL SOCIETY

Section A

VOL. 65, PART 8 1 August 1952 No. 392A

Some Post-War Developments in Magnetism

BY L. F. BATES
University of Nottingham

Presidential Address, delivered 20th May 1952; MS. received 31st March 1952

ABSTRACT. A survey is given of some of the more outstanding developments in magnetism during the post-war years, including the great extension of our knowledge of the ferromagnetic domain through the theoretical work of Néel and others and by the systematic use of the Bitter powder figure techniques; the main ferromagnetic, paramagnetic and nuclear resonance phenomena and experiments on the diffraction of neutrons by antiferromagnetic crystals are also described.

§1. INTRODUCTION

In choosing the subject of this Presidential Address I had in mind the fact that in 1939 an 'International Réunion d'Etude' was held at Strasbourg, when practically every branch of magnetism was surveyed in a then up-to-date manner. In 1950 a somewhat similar international colloquium was held at Grenoble, and on this occasion the subjects of ferromagnetism and antiferromagnetism were widely discussed. I had the good fortune to be present at both conferences, and so I want to talk to you today about the developments in certain branches of ferromagnetism which have taken place in the past ten or twelve years, and which have more particularly interested me. The fact that time will not permit me to deal with all important branches today must not be taken to indicate that I have not been interested in them.

§2. THE STUDY OF DOMAINS

I should like first of all to deal with some rather beautiful and striking extensions of our knowledge concerning ferromagnetic domains. We all know that Pierre Weiss put forward the idea of a ferromagnetic domain in 1907 in order to explain the fact that we may easily magnetize a specimen of fairly pure iron to a high degree of technical saturation by the application of a very small external field. In 1935 Landau and Lifshitz* published a remarkable paper which was almost completely ignored for ten years, and has only recently found its way into English papers and treatises on magnetism. They asked the following question. Why should several domains instead of one be formed in a small specimen of a single crystal which has once been magnetized to saturation The answer they gave was that a single domain is extremely improbable because of the huge magnetostatic energy which would in such a case be associated with free poles on the exterior of the specimen. By a series of simple diagrams they proved that a single domain must inevitably break down into many domains, magnetized consecutively in opposite, or as we say in antiparallel directions. Consequently, the positive and negative magnetizations at the ends of many such domains neutralize one another, and Landau and Lifshitz showed how the effects of these magnetizations might be still further reduced by the establishment of closure domains which ensure that little or no magnetic flux leaves the surface of a specimen.

---

* See note at top of References at end of paper.

It might at first sight appear that any specimen would therefore contain an infinite number of domains, but we have to take account of the fact that neighbouring antiparallel domains must be separated by a wall. Now, energy is necessary for the formation of such a wall, a Bloch wall as it is called, because the wall must consist of magnetic material in which the directions of the electron spins in neighbouring atoms must change continuously as the wall is traversed from one domain to the other. We know that the energy of interaction between two neighbouring electrons whose spin vectors make a small angle ϕ with one another is given by the expression $E_0S^2\phi^2$ where E_0 is the exchange integral. Therefore it is easy to see that a gradual change in direction of magnetization throughout a long line of atoms requires less energy than that required for the same change in direction of magnetization over a small number of atoms.

But the wall cannot have an infinite thickness, because the energy of magnetic anisotropy plays a part. It is well known that we have to supply different quantities of energy per unit volume to magnetize a crystal of a ferromagnetic metal in different directions, as one can see from a glance at the (I, H) curves for a single crystal of iron. Now, the majority of the electron spins contained within a Bloch wall must be directed away from the directions of easy magnetization, and so the wall must possess magnetic anisotropy energy approximately proportional to the thickness of the wall. We therefore see that the thickness of a wall is settled by the conflicting claims of the exchange energy between the electrons within it and their magnetic anisotropy energy. In the case of iron it is calculated that a wall between two antiparallel domains is about 10^{-5} cm thick, or consists of about 300 atoms in one line.

But I have been talking as if it were always necessary that the domains should have their magnetic vectors directed antiparallel or in opposite directions on the two sides of a domain boundary. This picture is indeed correct for the case of a single crystal of cobalt and also for a single crystal of the compound MnBi. A moment's reflection will show that this cannot be the normal arrangement for single crystals of iron or of nickel. We know that in the body-centred cubic iron crystal there are six directions of easy magnetization, viz. the [100] directions, along the cube edges. In the face-centred cubic crystal of nickel at room temperatures the eight easy directions of magnetization are along the cube diagonals, the [111] directions. Yet, the idea that there must be no free surface magnetization on the faces of a domain wall is all-important and leads us to new concepts both of the nature of the domain structure of a demagnetized iron crystal, for example, and of the way in which that structure changes when a magnetic field is applied.

Thus, the old familiar simple picture, fig. 1 (*a*), of a demagnetized iron crystal as made up of little cubes, each magnetized parallel to a cube edge and arranged anyhow within the crystal, must be abandoned and replaced by a picture of the kind shown in fig. 1 (*b*). In the new picture it is obvious that the specimen is magnetically neutral and that the intensity of magnetization is continuous across every domain boundary, a feature which I shall be at pains to emphasize in many of the diagrams and photographs which will be shown today. Figure 1 presupposes that the crystal surface is an exact crystal plane; but we shall see later that when the surface is inclined at a very small angle to a true crystal plane, the main domain boundaries shown by experiment are usually somewhat complicated and often very beautiful. In addition, of course, we have to take into account the closure domains which are found at the edges and sides of a crystal.

Let us therefore consider how domain boundaries may be rendered visible. This may be done by what is known as the Bitter figure technique. We place a small quantity of a finely divided ferromagnetic powder, or a drop of a colloidal solution of magnetite, upon the surface of the crystal. In such experiments the particles of powder etc. simply replace the iron filings which we used in our schooldays. It is easy to understand that on a crystal surface where there is no free surface magnetization the line or narrow region in which a domain boundary intersects the surface must be manifest by a stray magnetic field. Consequently, the finely divided and permanently magnetized particles will be acted upon by such stray fields and form deposits in the manner discussed by Kittel (1949 a, b) and Mee (1950).

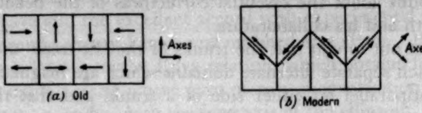

(*a*) Old (*b*) Modern

Fig. 1. Diagrammatic representation of the domain structure of a demagnetized iron crystal.

Of course, it is imperative that the crystal surface shall be most carefully polished and free of surface strain, so that after preliminary polishing with emery down to the finest grade, it is usual to polish the surface electrolytically; for this purpose a useful bridge circuit has been devised (Bates and Mee 1950). Finally, if necessary, the sample is annealed *in vacuo* at 900° c.

Perhaps a word about electrolytic polishing will not be out of place here. The specimen is mounted in a polystyrene mould with its edges well protected with polystyrene glue. It is then mounted on a wheel which can be rotated at a chosen rate to cause the surface to be uniformly polished. I imagine that most of you know that electrolytic polishing is caused by a film of high resistance which covers the anode. Above any tiny surface projections the film will be less thick than above flat regions of the surface, and therefore the protuberances are more vigorously attacked. As it is essential that the viscosity of the solution used in the polishing bath should be everywhere the same so that ionic mobilities may be constant, we now rotate both anode and cathode on a common spindle (Bates 1952), and we use the special bridge circuit already mentioned to maintain the polishing current at the optimum value.

The well-prepared crystal surface is then mounted horizontally in a horizontal or a vertical magnetic field and observed through a metallurgical microscope.

A drop of the colloidal solution is placed on the surface and a microscope cover glass placed on it, when the Bitter figures quickly form. If one uses a vertical field one measures its intensity by means of a flat search coil, but in the case of a horizontal field one uses a small magnetic potentiometer.

I shall now review, very briefly, a few of the patterns which one obtains by this technique. If one obtains a maze pattern, it is generally because the surface is not strain-free, and it must be repolished and annealed. It is easy to prove, however, even by the use of imperfectly prepared specimens that the main or principal domains are definitely situated below the crystal surface.

A very distinctive feature of the Bitter figures on a well-polished surface of an iron single crystal which is almost parallel to a true crystal plane is the appearance for the demagnetized state of a 'fir-tree' pattern. Such 'fir-tree' patterns have been examined and explained by Bozorth, Williams and Shockley. Their explanation can readily be found in at least two modern treatises on magnetism (Bates 1951, Bozorth 1951), but it may help you if I place their interesting diagrams on the screen. If the crystal surface were ideally a true crystal plane we should get few, if any, Bitter figures upon it, but the further the surface departs from the true crystal plane the heavier become the Bitter figure deposits. There is no doubt about the essential correctness of the beautiful explanation given by Bozorth and his collaborators.

Let me point out to you that the trunks of the 'fir-trees' are formed by the Bloch walls which separate alternate domains which are magnetized respectively parallel and antiparallel on either side of a trunk, and that the branches are formed by closure domains, magnetized in a direction roughly perpendicular to the trunks, whose function is to take care of a great quantity of magnetic flux which would otherwise emerge from the crystal surface. Indeed, from the changes in appearance of the 'fir-trees' from place to place over the crystal surface we can now deduce exactly how that surface is shaped, and it almost seems as if Bitter figures, or rather absence thereof, is the best evidence of a truly ground and annealed iron (100) surface that we can possibly supply, for the branches always point downhill.

There are at least three separate methods by which it can be conclusively ascertained how the principal and closure domains are magnetized. We may scratch the surface with a fine glass fibre and note the deposits in the stray field at the scratch, we may use a tiny probe of permanently magnetized metal, or we may note the way in which deposits form on the sides of any little depressions in the surface because of the free poles on the sides of the depressions.

I want later to deal with some quantitative aspects of powder figures, but first I should like to consider the application of the newer domain concepts to one or two well-known problems of the magnetic properties of iron single crystals. Let us follow Néel's description of magnetization processes. He considers that in the demagnetized iron crystal each domain vector is aligned parallel to one of the six directions represented by three cube edges and their extensions in the negative direction, and he designates this condition a state of six-phase magnetization, or Mode I magnetization.

If we now apply a small external field to the crystal, supposing the latter for clarity to be of ellipsoidal shape, then before it can produce an effective field inside the crystal three magnetization phases must disappear, as they are entirely contrary to the direction of the external field. When they have completely disappeared we have left three-phase or Mode II magnetization. It is now possible by further increasing the applied field to produce an effective field within the crystal itself and thus cause one of the phases to be so much less favoured than the others that it disappears, when we are left with two-phase or Mode III magnetization. Eventually, on further increasing the field only single-phase or Mode IV magnetization can persist.

If the single crystal of iron is shaped as an oblate spheroid whose equatorial plane is a (100) crystal plane and we apply an external field H_e in this plane at any angle θ to the nearest [100] direction, we can deduce by a commonsense argument that the resultant of H_e and the demagnetization field of the spheroid must lie symmetrically between the two nearest [100] directions, i.e. the resultant field must lie along the [110] direction in the equatorial plane. But what must then be the shape of the domains? They must be leaf-shaped (French, feuillet) with their boundaries perpendicular to the [110] direction.

I need not deal further with this problem; it has been considered *in extenso* by Néel and also by Lawton and Stewart. I will merely place on the screen one or two slides which illustrate how completely the components of magnetization of the ellipsoidal specimen parallel and normal to the applied field should theoretically behave and the excellent accord with experimental results obtained many years before the theory I have just outlined was given. But I should like to refer to what is known as the Kaya relation, which obtains for a long rod or ellipsoidal iron single crystal whose axes of easy magnetization make angles of direction cosines α_1, α_2 and α_3 with the long axis of the ellipsoid. Obviously, the component of magnetization normal to an applied field will now always be very small, and a commonsense argument shows that when a very small field eventually acts inside the specimen, Mode II magnetization must reign and each of the domain vectors be directed parallel to one of the three directions of easy magnetization. Consequently, we must have the parallel component of magnetization equal to $I_s/(\alpha_1+\alpha_2+\alpha_3)$, a relation which Kaya deduced for the retentivity of such a specimen.

The time has now come for me to deal with quantitative experiments on powder figures, and I must first mention an exceedingly fundamental experiment made by Williams and Shockley who cut a single crystal of silicon–iron in the shape of a picture frame. They were able to cause a 180° boundary to form approximately along the middle of the sides of the picture frame, and to cause it to move by applying a magnetizing field by means of a coil wound around one side of the frame. They thus made some very striking quantitative measurements of the sideways displacement of the boundary as a function of the magnetization.

While I am dealing with picture frame measurements, I should like to mention those of Stewart (1951) who examined the velocity V of the displacement of the 180° wall and found that it obeyed the relation, first given by Sixtus and Tonks, $V=A(H-H_0)$; here H is the applied field and H_0 is a field analogous to, if not actually equal to, the coercivity of the material. But, in these experiments A was found over 1 000 times smaller than the values usually found with polycrystalline materials. The suggested explanation is the enormous braking effect of eddy currents in the single crystal case. In the course of this work it was found that the downward sweep of the hysteresis curve in the demagnetization quadrant was re-entrant, and the two phenomena are possibly linked together.

The effect of eddy currents was the explanation advanced by Snoek to account for the fact that the virgin magnetization curve often lies partly outside the closed hysteresis loop when measurements are made on rod or strip specimens on open magnetic circuit. It is supposed that eddy currents prevent the magnetization from rising rapidly to its proper value when the field is changed, so that the true field acting on the outside of the specimen is not $H-DI$ but $H-DI'$, where $I>I'$, whereupon the effective field as it were 'overshoots', and the outer portions of the specimen assume an intensity of magnetization greater than they ought, particularly on the steeply ascending portions of the loop. Incidentally, Kayser has shown that even if we use an anchor ring specimen with no free poles we may get the same Snoek phenomenon if the material of the ring possesses strong magnetic anisotropy.

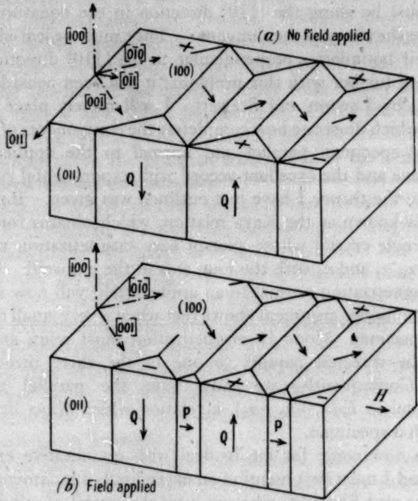

Fig. 2. Domain structure proposed by Néel.

In Nottingham we have made a series of quantitative experiments to test the correctness of certain magnetization processes put forward by Néel. Although the most complete results were only very recently published in our ***Proceedings*** (Bates and Mee 1952 a, b) I should like to show you some of them today together with many pictures which could not be published because of space (and cost). In fig. 2 we have domain structures which Néel showed to be appropriate to a long single crystal strip of iron, with its main upper and lower surfaces very nearly parallel to true (100) crystal planes, and the [011] direction running down the middle as depicted on the upper surface of the strip. When a very weak, indeed practically zero, field acts upon the strip parallel to this [011] direction, the principal domains form slices magnetized as shown in fig. 2(*a*) with their boundaries perpendicular to the [011] direction. When the field is increased we get marked changes in the closure domains as in fig. 2(*b*). Now, Néel has given a formula which allows us to calculate the period *d* of the domains, which is equal to the total thickness of two successive domains, in terms of the true field acting on the specimen. His calculation of the period is based on the particular arrangement of the principal domains and their closure domains as given in fig. 2(*b*). I might mention that we are here dealing with a transition from Mode II to Mode III magnetization.

We have made many measurements of the period *d* both on the (100) surface and on the (110) planes formed by the sides of the specimen. I now place some of them on the screen, together with graphs showing the variation of *d* with *H*, and you will see that there is no doubt whatever about the essential correctness of Néel's ideas, although more profound study of the experimental results shows that these ideas need to be modified in some particulars. For example, we feel fairly certain that we do get some free pole distributions on the (110) faces of our specimens. Again, recent work with single crystals of very pure iron cut in the manner described seems to show that the boundaries on the (110) faces are not vertical as drawn, but are definitely inclined at an angle of about 15° to the vertical. In any case, it is a very strange thought that the period of a principal domain structure, which is in effect the whole state of magnetization of a specimen, can be so markedly influenced by what occurs in a set of closure domains on the sides of the specimen! This is a feature to which I shall return later.

Perhaps this is a convenient point at which the effects of impurities or inclusions in the crystal may be introduced. We all instinctively feel that if we had a perfect crystal it would be possible to magnetize it to technical saturation in an extremely small field, and the obvious mode of increase of magnetization in a particular direction is by boundary displacements. So we at once seize upon the idea that the coercive field is a limiting field which must be overcome before the boundary will move from one stable position to another. It also seems reasonable to suppose that the initial permeability μ_1 is a measure of the internal restoring forces which act upon a domain boundary subjected to small reversible displacements only, the coercive force then being the maximum restoring force which a boundary can stand.

Now, it is well known that Kersten put forward an explanation of coercivity in terms of the movement of a domain boundary from one set of inclusions to another. But Néel showed that this theory was incorrect because no account was taken of the huge quantities of magnetostatic energy which would be associated with a wall passing across or through an inclusion; indeed, he showed that a factor of about 100 was omitted, and he thinks that the real effect of inclusions is to produce large fluctuations in the intensity of magnetization or its direction inside the domains themselves.

Let us look for a few moments at some pictures of the Bitter figures which were recorded in the neighbourhood of inclusions (Bates and Mee 1952b). In many of these pictures you see that a complicated closure domain structure exists round an inclusion. In fig. 3 are given some of the types predicted by Néel, and these are fully confirmed in many of the photographs which I now project on the screen.

I should like to complete this somewhat minor incursion into the realms of coercivity by reference to an important piece of work by Stoner and Wohlfarth. It seems obvious to me that for some time three sets of people, Koenigsberger in Germany, Néel in France, and Stoner and Wohlfarth in Leeds, were grappling with the same question. This question may be put in the following way. If we have a particle of a ferromagnetic element so small that it never contains more than one single domain, how does it behave in a magnetic field; and what field would be required to reverse its direction of magnetization?

The most complete picture of what may happen was given by Stoner and Wohlfarth and I am sorry that I can only give a brief outline of it here. Neglecting any energy of magnetic anisotropy or of internal strain, the total energy of an ellipsoid of revolution, with longitudinal and transverse demagnetization coefficients D_L and D_S respectively, is given by $\frac{1}{2}(D_L - D_S)I_s^2 V\alpha^2$, where V is the volume of the ellipsoid and α is the angle which I_s makes with the long axis. When fields are applied parallel to the long axis, we obtain a rectangular hysteresis loop with the coercivity $H_c = (D_L - D_S)I_s$. A graphical method of calculation shows that for an assembly of such ellipsoids which do not interact with one another the average coercivity is about 0·96 of this value; and, if the ratio of the long and short axes is $1+\epsilon$, where ϵ is small, then $(D_L - D_S) = 8\pi\epsilon/5$, so that $\overline{H}_c = 4\,100\epsilon$ in the case of iron.

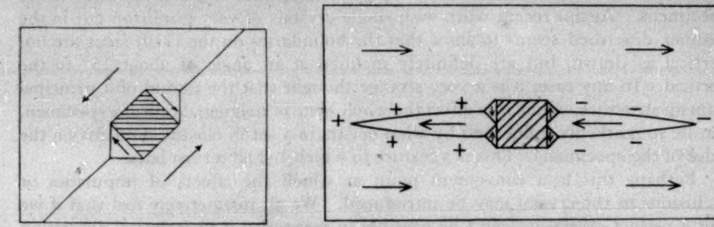

Fig. 3. Closure domains around an inclusion (after Néel).

Let us apply these ideas to the case of a magnet made of compressed finely powdered iron, where we must take account of mutual interactions between domains. Assuming that a number of cavities of relative volume v are uniformly distributed in 1 cm³ of uniformly magnetized material, then the energy of the whole is $\frac{2}{3}\pi(1-v)vI_s^2$, which is $1-v$ times the energy which would be possessed by the material without cavities. H_c is therefore correspondingly decreased. Taking the case of simple cylindrical particles for which the difference in the two demagnetization coefficients is 2π, and assuming that these particles of density d_0 are compressed together to form a structure of density d, we find $\overline{H}_c = 0{\cdot}26\pi(1 - d/d_0)I_s$, giving a value of about 500 oersteds for iron. Now, Weil investigated powder magnets made of 70% iron and 30% cobalt and proved that H_c is proportional to $1-v$, a result in complete agreement with these views.

We have just seen how important a cavity or an inclusion in the surface of a metal can be; it is also of interest to discuss the effects of what might be lightly termed an exclusion. In fig. 4 (*b*) is shown a part of the (100) surface of a single crystal of pure iron. The lowest corner of the crystal has been cut off along a (111) plane as shown. We know that if the crystal had not been thus maltreated, the main and closure domains for the demagnetized state would follow the pattern of fig. 4 (*c*). What was actually photographed by Mr. D. H. Martin at Nottingham is reproduced in fig. 4 (*a*). A partial interpretation of this somewhat beautiful pattern is given in fig. 4 (*b*) where the dotted square indicates the extent of the area photographed in fig. 4 (*a*); the word partial is used to suggest that the closure domain system which must exist at the lowest edge of the (100) surface shown in fig. 4 (*b*) has not yet been photographed or examined. The tree patterns found in the photograph do not particularly interest us at this stage; they are only the outward sign that the surface is not ideally cut parallel to the (100) plane. But what does interest us is the injection of a new domain system cutting across the simple parallel set of boundaries which would exist if the corner of the crystal had not been removed. The somewhat startling idea, to which I referred earlier, that according to Néel's theory the magnetization of a strip is determined by what happens at its edges, is now supported by this direct experiment.

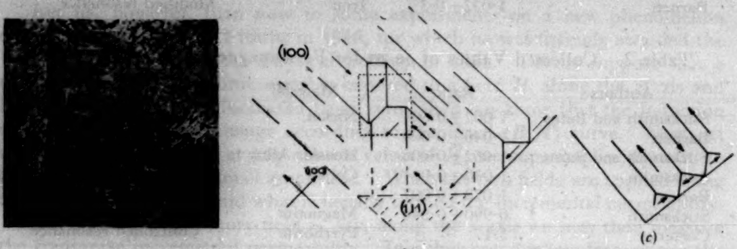

(*a*) (*b*) (*c*)

Fig. 4. The effect of an exclusion from a surface on domain structure.

I said earlier on that we had to abandon the old cubic block picture of domains shown in fig. 1 (*a*). But this statement may not be entirely correct, for I now show you some pictures, taken in my laboratory a few days ago by Mr. D. H. Martin, which indicate that two neighbouring domains in a silicon–iron crystal can have their vectors directed head-on to one another, and you see that the boundary between them is a very tortuous one.

To conclude this portion of my address, I should like to show you a film of the formation of domains on the surface of a single crystal of cobalt which is particularly simple from a magnetic point of view because it possesses only two directions of easy magnetization parallel to the hexagonal axis. As a prelude to the film we will first examine a series of slides of many of the features which will appear in the film (Bates 1951).

§ 3. GYROMAGNETIC MEASUREMENTS

In 1922 there appeared the first of a series of researches on the measurement of the gyromagnetic ratio for ferromagnetic metals which culminated in the brilliant measurement of the gyromagnetic ratios for paramagnetic ions of the iron and rare earth groups by Sucksmith; I should like to spend a little time in dealing with the present state of our knowledge of the value of the ratio for the ferromagnetic elements. You all know that when such an element is magnetized there is a change in the measured intensity of magnetization which is accompanied by a corresponding change in angular momentum, and experiments have been designed either to measure the change in angular momentum which accompanies magnetization or the change in magnetic moment which accompanies a change in rotation of a ferromagnetic specimen.

The results obtained in England and America prior to 1939 are summarized in the following tables.

Table 1. Collected Values of $\rho\mathbf{e}/\mathbf{m}$ for Iron

Authors	Ratio	Material	Method
Chattock and Bates	1·00 ± 1%	Iron	Direct rotation by magnetization
Sucksmith and Bates	1·00 ± 1%	Iron	Modified resonance
Coeterier	1·00 ± (1%?)	Iron	Controlled resonance
Ray-Chaudhuri	1·00 ± 1%	Iron oxides	Resonance
Barnett	1·038 ± 1%	Iron	Magnetization by rotation
Barnett	1·032 ± 0·3%	Iron	Modified resonance

Table 2. Collected Values of $\rho\mathbf{e}/\mathbf{m}$ for Ferromagnetics other than Iron

Authors	Ratio	Material	Method
Sucksmith and Bates	1·002 ± 0·004	Nickel	Modified resonance
Barnett	1·046 ± 0·004		Modified resonance
Sucksmith and Bates	1·002 ± 0·006	Heusler Alloy	Modified resonance
Sucksmith	1·030 ± 0·064	Cobalt	Modified resonance
Barnett	1·078 ± 0·007		Modified resonance
Sucksmith	0·990 ± 0·048	Magnetite	Modified resonance
Coeterier	3·17	Pyrrhotite	Controlled resonance

In these tables the results are expressed in terms of the gyromagnetic ratio; it is defined by $\rho =$ (change in angular momentum)/change in magnetic moment) $= U/\mu$. If the magnetic carrier is an electron without spin describing a plane orbit we should have $\rho = 2\mathbf{m}/\mathbf{e}$, if the carrier is a spinning electron we should have $\rho = \mathbf{m}/\mathbf{e}$, while for the general case in which the carrier is an electron system for which the Landé splitting factor is g, we should have $\rho = 2\mathbf{m}/g\mathbf{e}$. From the tables it follows that g is very nearly equal to 2, so that we deduce that the elementary magnetic particle owes its magnetic properties almost entirely, if not entirely, to electron spin alone.

But, it is clear from the tables that some differences exist between the several determinations with any given element, and these are important, because if the higher values of ρ are correct then g must be slightly less than 2, from which it follows that orbital motion of the electron must play a small but definite part. Naturally, one would like this question to be cleared up completely. Unfortunately, we have had only two determinations of the ratio since the last war.

The first was by Meyer, of Strasbourg, who used the controlled resonance method and made measurements with iron and nickel and with the alloys FeNi, (FeNi)Co, FeCo and Fe$_3$Ni. He paid careful attention to the width of the slit in front of the photoelectric cell whose activation caused a magnetizing field to be reversed. The average value of g which he obtained for the metals and alloys was 2·001 ± 0·005. The work appears to me to have been done with extreme care.

Thus far so good; but we have a second method by Scott (1951) based on the method, and using much of the apparatus, which was so successfully used in a determination of the value of the specific charge of the electron by Kettering and Scott in 1944. The method was a kind of controlled resonance method, in which changes in amplitude were caused by periodic, synchronized reversals of the magnetizing current in a coil wound directly on the specimen; these changes were measured, together with the corresponding changes in the magnetic moment of the specimen. The final result for the gyromagnetic ratio for iron was $(1{\cdot}0278 \pm 0{\cdot}0014)\boldsymbol{m}/\boldsymbol{e}$ or $g = 1{\cdot}946$. Again, the work appears to me to have been very thoroughly carried out.

So we still have differences in the values for g; and perhaps the truth of the matter is that while we can make *relative* measurements of changes in magnetization and in angular momentum with great accuracy, we cannot yet make *absolute* measurements with the necessary degree of certainty.

§ 4. FERROMAGNETIC RESONANCE

Let us, however, turn now to some experiments on a new phenomenon discovered by J. H. E. Griffiths in 1946, for which he was fittingly awarded the Vernon Boys Prize by the Physical Society in 1951. Let us suppose that a demagnetized ferromagnetic metal is exposed to a field H_z along the z axis and that this field is slowly increased from zero; then we know that the induction of the specimen must change according to the usual (B, H) curve. Now, let us further suppose that at any chosen value of H_z we superimpose upon it an oscillating field of very small amplitude. When the two fields are applied along the z axis we may thus find what is usually termed the incremental permeability.

.A
5
2

But when the oscillatory field is, say, along the x axis we may then measure the transverse incremental permeability. In either case for low frequencies the incremental permeability falls from a value greater than unity for low values of the steady field to unity when the latter is high enough to cause saturation. When, however, the frequency of the oscillating field is very high, e.g. in the microwave region, a resonance effect is observed and the incremental permeability, instead of decreasing to unity as would be expected, actually rises from a low value for a small steady field to pass through a maximum and then decrease towards unity as the steady field H_z is increased to a very high value. In other words, when μ_r is plotted against H_z we get a kind of broad resonance curve, as shown in the slide (Standley 1949).

We may explain this resonance effect in the following way. The ferromagnetic carriers may be considered as under the influence of an effective field H', so that they perform Larmor precessions of frequency

$$\nu = g(\boldsymbol{e}/4\pi\boldsymbol{mc})H'. \qquad \ldots\ldots(1)$$

When the Larmor frequency is equal to that of the oscillating field, resonance is set up and energy absorbed at a maximum rate from the oscillating field. Alternatively, we may suppose that the absorption may occur between a series of Zeeman levels in the ferromagnetic material, so that $\boldsymbol{h}\nu = g\mu_B H'$, where μ_B is the Bohr magneton and g is the Landé splitting factor. Writing $\omega = 2\pi\nu$, we have $\omega = g(\boldsymbol{e}/2\boldsymbol{mc})H' = \gamma H'$ where γ is defined as the magneto-mechanical ratio. It is a pity that this term has extensively crept into the literature in place of the term gyromagnetic ratio coined by O. W. Richardson in 1908 and used extensively in England for over a quarter of a century.

Using a semi-classical model Kittel showed that the general resonance equation for an ellipsoidal specimen with axes x, y, z might be written as

$$\omega^2 = \gamma^2[H_z + (N_y - N_z)M_z][H_z + (N_x - N_z)M_z], \qquad \ldots\ldots(2)$$

where M_z is the saturation magnetization of the material along the direction of H_z and N_x, N_y, and N_z are the demagnetization coefficients along the three axes. Two cases are frequently met in practice: firstly, the case of a sphere, where we find $\omega = \gamma H_z$, and secondly a very thin sheet parallel to the xz plane, where we have $\omega = \gamma(B_z H_z)^{1/2}$, a statement derived by both Kittel and Luttinger (1948) and Van Vleck (1950) by quantum theory treatment of the problem.

We therefore see that from such ferromagnetic resonance measurements we may obtain γ and hence calculate g. Let us for a moment consider the usual experimental arrangements. The specimen usually forms part or the whole of one wall of a cavity tuned to resonate at a fixed microwave frequency ν, which is often about 24 000 Mc/s, and the Q or circuit magnification of the cavity is measured for a series of values of H_z. It is reasonable to assume that when H_z is changed only the losses in the ferromagnetic specimen itself are affected, and so we may calculate from the Q measurements the quantity $(\mu_R \rho_e)^{1/2}$, where μ_R is the permeability of the specimen determined by resistive measurements of this kind and ρ_e is its electrical resistivity. If however we retune the cavity as H_z is varied, we thereby measure μ_L the inductive or dispersive permeability.

Now, at high frequencies we must obviously treat the permeability as a complex quantity. Writing $\mu = \mu_1 - j\mu_2$ we can show that $\mu_R = (\mu_1{}^2 + \mu_2{}^2)^{1/2} + \mu_2$, $\mu_L = (\mu_1{}^2 + \mu_2{}^2)^{1/2} - \mu_2$. Hence, from simultaneous measurements of μ_R and μ_L the two quantities μ_1 and μ_2 may be found.

Such experiments have so far been made on about a dozen different ferromagnetic materials, and it is significant that the values of g so obtained generally lie between 2·0 and 2·3, although in Nottingham a value greater than 3 has been found for manganese arsenide. Unfortunately, in my opinion, it is customary among workers in this field to refer to their values of what is in effect the magneto-mechanical ratio factor as g values, and to describe the corresponding values obtained from the older direct measurements of the gyromagnetic ratio as g' values. (It seems obvious to me that g_R (Richardson) for gyromagnetic data and g_G (Griffiths) for ferromagnetic resonance data would have been more appropriate, but the unfortunate terminology now seems rather firmly established.)

A few values are given in the following table, using the objectionable symbols under protest:

Table 3

Specimens	g	g'	
		(1)	(2)
Ni	2·2	1·92	2·00
Co	2·22	1·87	1·94
Fe	2·12—2·17	1·93	2·00 (1·95)*
Magnetite	2·20	1·93	2·02
Permalloy	2·07—2·14	1·91	—

(1) Measurements by Barnett.
(2) Measurements by other workers. * Scott's value.

It has been shown by Kittel (1949 b) and by Van Vleck (1950) that although g and g' are both defined by $\boldsymbol{ge/2mc} = \Delta M/J$, where ΔM is the change in magnetic moment and ΔJ is the corresponding change in angular momentum, it may be suggested that they do in fact refer to different quantities. For, when we determine the gyromagnetic ratio, because angular momentum is conserved the change ΔJ_{total} for the whole system is zero. But in the ferromagnetic resonance experiments $\Delta J_{\text{total}} = \boldsymbol{h}/2\pi$.

Again it has been shown that

$$g'\boldsymbol{e}/2\boldsymbol{mc} = \frac{M_{\text{spin}} + M_{\text{orbit}}}{J_{\text{spin}} + J_{\text{orbit}}}, \quad \text{while} \quad g\boldsymbol{e}/2\boldsymbol{mc} = \frac{M_{\text{spin}} + M_{\text{orbit}}}{J_{\text{spin}}},$$

so that when the orbital contribution is much smaller than that due to spin, we have

$$2 - g' = g - 2. \qquad \ldots\ldots(3)$$

The last equation is only approximate and is based on a simple model, and while the results in the above table may appear to indicate that $g' < 2$ and $g > 2$, it is clear that the equality is not satisfied. It may be pertinent to add that eqn. (2) for ω^2 holds for zero or small damping.

The experimental results for certain manganese ferrites, manganese nitride (Mn_4N) and Heusler alloys show that g is equal to 2·00 within the limits of experimental error of about 2%. In other cases, g is greater than 2·0 and in the case of MnAs, mentioned above, is greater than 3. The simple relation between g and g' cannot account for such cases. Moreover, in the cases of nickel and permalloy no changes in the g values are observed when the specimens are raised from room temperature to above the Curie point; changes have however been recorded by some Japanese workers (Okamura, Torizuka and Kojima 1951) in the case of cobalt ferrite as the temperature approaches the Curie point, and Standley and Adam (unpublished) have found a similar behaviour with MnSb.

In order to explain the broad resonance bands which are observed Stevens has suggested that electrons may fluctuate from one lattice site to another, e.g. from d^9 to d^{10} sites in the case of nickel; if the lifetime in a given site is short compared with the Larmor precession a very broad resonance would be expected.

§ 5. PARAMAGNETIC RESONANCE

I have said so much about ferromagnetic resonance that it may have escaped notice that it is in reality only a special case of electron resonance, and that, in general, we ought to expect similar resonances in non-ferromagnetic materials. However, we do not find such resonances in the majority of substances, for instance, we do not find them with pure water. The reason for this failure of the electrons to resonate in such cases is that they behave as if they are coupled together in pairs with the two spins directed antiparallel to one another. Consequently, each coupled pair forms a non-magnetic system on which the constant and oscillating fields have no effect.

But in the case of the strongly paramagnetic salts we have uncoupled electrons available and electron resonance according to eqn. (1) must take place. Absorption lines are found whenever the separation of the energy levels of a paramagnetic ion is equal to the quantum of energy corresponding to the radio frequency. This experimental procedure is very important, for it enables us to make a detailed examination of these energy levels without the necessity of making corrections for diamagnetism, to measure the relevant g values or splitting factors directly, to measure directly small splittings of the order of 1 cm^{-1} produced by crystalline fields and also to measure very short spin–lattice relaxation times of the order of 10^{-10} sec.

The paramagnetic absorption spectrum of a salt may be very complicated and difficult to interpret, for unless the ion is perfectly free of residual spin–orbit coupling, the paramagnetic crystal may for example be magnetically anisotropic and the spin levels in a magnetic field will then depend on the orientation of the magnetic field to the axes of the crystalline field. Again, it is possible for the unit cell of the crystal to contain two or more paramagnetic ions, each exposed to a differently orientated though otherwise identical crystalline field, so that the paramagnetic resonance spectrum of each ion will be different for an arbitrary setting of the crystal.

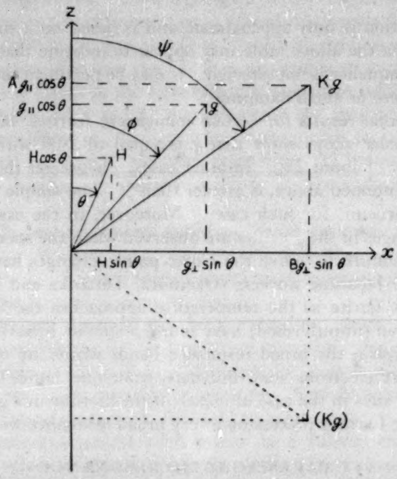

Fig. 5. Orientation of magnetic field H, electron spin g, and nuclear spin Kg when anisotropy is present. The figure is drawn for $g_{\perp} > g_{\parallel}$ and $B > A$. The dotted vector Kg refers to the case where the coefficient giving the interaction between the nuclear magnetic moment and the magnetic field of the unfilled electron shell is negative.

I cannot here go into the wealth of information obtained for example by Bagguley, Bleaney, Griffiths, Penrose and Plumpton, in detailed experiments on over one hundred salts of the iron group, which were published in our *Proceedings*, but I should like to refer to the brilliant discovery of the hyperfine structure of paramagnetic resonances by R. P. Penrose, whose untimely death we all regret. In a flight of genius he realized that with a combination of low temperature and magnetically dilute ions, great resolution of the absorption lines could be expected. He found that at low temperatures in the microwave absorption band of a dilute Tutton salt, in which 95% of the magnesium had been replaced by copper, with $\lambda = 3{\cdot}2$ cm, with H_z about 3 000 oersteds along the K_1 axis, four resonance lines were observed with field separations of about 93 oersteds, as found by adjustment of H_z. These lines corresponded to the four possible orientations in the field H_z of the copper nucleus, for which $I = 3/2$ units of spin. The overall structure of the lines varied with the orientation of H_z in the crystallographic *ac* plane, being a minimum along the K_1 axis, for which the electronic *g* factor is a maximum, and a minimum near the K_2 axis for which the electronic *g* factor is a minimum.

Incidentally, a kind of physical explanation of these different *g* factors has recently been given by Bleaney (1951) and by Garrett (1950). Referring to fig. 5, taken from Bleaney's paper, we may see that a magnetic field *H* applied at an angle θ to an axis of crystalline symmetry has components $H \cos\theta$ and $H \sin\theta$ respectively along the normal to this axis as shown. The components of the magnetic moment must accordingly be proportional to $g_{\parallel} H \cos\theta$ and $g_{\perp} H \sin\theta$, where *g* is proportional to the length of the vector, making an angle ϕ with the *z* axis, which is formed by compounding the two components. The vector *g* is parallel to the resultant magnetic moment of the electrons, but it is not parallel to *H*. Consequently, the factors $g_{\parallel}/g$ and $g_{\perp}/g$ enter into the equations for $\boldsymbol{h}\nu$ as multiplying factors of $\cos\theta$ and $\sin\theta$ respectively.

§6. NUCLEAR RESONANCE

To those of our Society who are concerned with nuclear physics, perhaps the most interesting use of magnetic resonance techniques is in the determination of nuclear magnetic moments. For this purpose we use eqn. (1) in the form $\nu = 2\mu H/\boldsymbol{h}$ where μ now stands for the magnetic moment of the nucleus in which we are interested. As a special case we may consider the measurement of the magnetic moment of the proton itself, when we have $\nu = 2\mu_p H/h$. Let us in this case picture a sample containing protons, e.g. a tube of water, placed upright in a strong, constant, horizontal magnetic field H_z, whose value may conveniently be fixed at 10 000 oersteds. Around this tube let us wind a coil to be supplied with alternating current of a radio frequency of the order of tens of megacycles per second. Measurements of the impedance of this coil show us when absorption corresponding to proton resonance occurs, for this is manifested by an extremely sharp peak on the curve of absorption plotted against frequency. This experiment is in constant use in our teaching laboratories at Nottingham. The apparatus as set up by Dr. R. Street is shown diagrammatically in fig. 6.

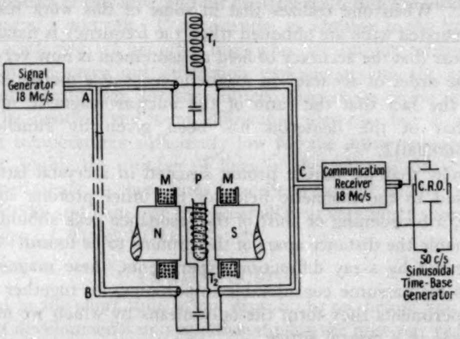
T₁
Signal Generator 18 Mc/s
A
C
Communication Receiver 18 Mc/s
C.R.O.
M
P
M
N
S
T₂
B
50 c/s Sinusoidal Time-Base Generator

Fig. 6. Block schematic diagram for determination of magnetic moment of a proton.

The coils MM are supplied with 50 c/s a.c. to modulate the field in the gap between the pole-pieces NS of the electromagnet. The specimen tube P contains a weak solution of cobalt nitrate. AB is a length of cable which produces a phase shift of 180°. When the circuits T_1 and T_2 are very nearly identical the signal derived from the point C is almost zero because the introduction of a 180° phase shift by means of AB results in feeding T_1 and T_2 in antiphase. The circuit thus behaves as a kind of bridge with out-of-balance voltage derived from C. When the modulated field in the gap between the pole-pieces NS passes through the value required to make the precessional frequency of protons equal to the frequency of the h.f. currents in the coil surrounding the specimen, both the inductance and the associated resistance of the coil change. Therefore at a critical value of field which occurs in general at two epochs of the modulating field the bridge exhibits a slight out-of-balance voltage at C which is amplified by the communication receiver and presented visually as a cathode-ray tube display. It is primarily the ferromagnetic uniformity of pole-piece material which determines the homogeneity of field acting in the specimen, and hence the sharpness of the resonance signals.

The apparatus is assembled easily from components generally available in the laboratory, and is convenient for use as an experiment for advanced students and also as a method of producing very accurately known magnetic field intensities, for the calibration of search coils etc. For a signal generator frequency of 18 Mc/s the field in the gap required to produce proton resonance is 4 000 oersteds approximately.

The importance of proton resonance is that it provides an excellent method of measuring a magnetic field. For, if we use a fixed field of 10 000 oersteds in this experiment, then the sharp proton resonance occurs at a frequency $\nu = 42{\cdot}6$ Mc/s. When one realizes that in some of this work resonance peaks less than 0·2 oersted wide are obtained when the frequency is fixed and the field varied, it is clear that the accuracy of field measurement is now very high indeed. An idea of the order of accuracy in magnetic resonance measurements may be gained from the fact that the ratio of the nuclear magnetic moment of the proton to that of the deuteron has been given by Smaller (1951) as $3{\cdot}2571999 \pm 0{\cdot}0000012$.

Suppose now that we have a proton situated in a crystal lattice. Then it will be exposed to the magnetic fields of the other protons surrounding it. Consequently, a broadening or shift of the resonance peak should be observed, and should enable the distance apart of the protons to be found. Since protons cannot be located by x-ray diffraction experiments, these magnetic resonance measurements may assume considerable importance, for together with neutron diffraction experiments they form the only means by which we may determine proton positions in a crystal lattice.

Now, we are used in physics to being able to repeat our experiments *ad libitum*. In the case of these resonance peaks, however, the height of the peak may vary with time. This is because every time a radio-frequency quantum is absorbed a proton is turned from the parallel setting into the antiparallel setting, and it takes time to come back. This effect has now been found experimentally, and an application of Boltzmann's law shows us how small is the relative difference in the number of protons directed parallel and antiparallel respectively to the applied field. For example (Darrow 1951) if we have 2 000 000 protons in thermal equilibrium at room temperature, the whole effect is occasioned by 1 000 007 set parallel and 999 993 set antiparallel, a difference of only 14.

§ 7. NEUTRON DIFFRACTION EXPERIMENTS

The mention of neutron diffraction reminds me that I have not dealt today with another outstanding feature of magnetic research during the last ten years, namely the intensive study of antiferromagnetism and ferrimagnetism. I should normally have dealt in some detail with these phenomena, but I have good reason to believe that this year's Holweck Prizeman, Professor L. Néel, will devote a large part of his Holweck Lecture to their consideration.

If we now assume that between the metal ions and the oxygen ions in substances like CoO, MnO or NiO there are forces, of what is called a superexchange type, which cause the metal ions represented by the red spheres in the model before you to have their spin vectors directed towards you, while the ions represented by the blue spheres have their spin vectors directed away from you, then it follows that the whole system is almost magnetically neutral. We should, of course, expect the system to show a complicated variation of susceptibility with rise in temperature, and an anomaly in its specific heat analogous to that found with a ferromagnetic metal, and these are characteristic of the typical antiferromagnetic substances which I have just mentioned.

From the point of view of x-ray diffraction measurements the model represents two unit cells because the scattering of x-rays does not depend markedly upon the direction of electron spin. But, suppose we have a radiation whose scattering does depend upon the directions of the magnetic spin vectors in the individual ions. Then the two kinds of metal ions represented by the two kinds of circles are not equivalent as far as this radiation is concerned, and the unit cell of metal ions is doubled linearly for this radiation. Now a beam of neutrons may be regarded as radiation of this type, and for neutron scattering the model represents only one quarter of a unit cell. Consequently, in addition to the lines which we get with x-ray scattering, we get other lines when we employ neutron scattering. Alternatively, if we carry out diffraction experiments on the material at a temperature sufficiently high for the antiferromagnetism to be absent we get similarity of the neutron and x-ray diffraction patterns, but if we make the experiments at temperatures sufficiently low for the antiferromagnetism to be present we get double the number of lines in the neutron diffraction pattern. Conclusive experiments on these lines have been carried out by Shull and his collaborators (1951), and I am sure that we shall hear very much more about them in the near future (cf. Street 1951).

§ 8. CONCLUSION

I have tried in the short time at my disposal to set before you some of the more important developments in magnetism during the post-war years. I realize that I have left untouched many important pieces of work and I can only hope that what you have heard today may entice you to seek out descriptions of these elsewhere.

REFERENCES

Many references are made in this Address to works which are described in *Modern Magnetism* by L. F. Bates (1951). Such references are therefore not given in the following list.

Bates, L. F., 1951 a, *J. Phys. Radium*, **12**, 323; 1951 b, *Modern Magnetism*, 3rd edn. (Cambridge : University Press); 1952, *Rev. Metall.*, in the press.

Bates, L. F., and Mee, C. D., 1950, *J. Sci. Instrum.*, **27**, 317; 1952 a, *Proc. Phys. Soc.* A, **65**, 129; 1952 b, *Ibid.*, **65**, 140.

BLEANEY, B., 1951, *Phil. Mag.*, **42,** 441.
BOZORTH, R. M., 1951, *Ferromagnetism* (London : Macmillan).
DARROW, K. K., 1951, *Elect. Eng.*, **70,** 401.
GARRETT, C. G. B., 1950, *Proc. Roy. Soc.* A, **203,** 375, 392 ; 1951, *Ibid.*, **206,** 242.
KITTEL, C., 1949 a, *Rev. Mod. Phys.*, **21,** 541 ; 1949 b, *Phys. Rev.*, **76,** 743.
KITTEL, C., and LUTTINGER, J. M., 1948, *Helv. Phys. Acta*, **21,** 480.
LANDAU, L., and LIFSHITZ, E., 1935, *Phys. Z. Sowjet*, **8,** 153.
MEE, C. D., 1950, *Proc. Phys. Soc.* A, **63,** 922.
OKAMURA, T., TORIZUKA, Y., and KOJIMA, Y., 1951, *Phys. Rev.*, **84,** 372.
SCOTT, G. G., 1951, *Phys. Rev.*, **82,** 542.
SHULL, C. G., STRAUSSER, W. A., and WOLLAN, E. O, 1951, *Phys. Rev.*, **83,** 333.
SMALLER, B., 1951, *Phys. Rev.*, **83,** 812.
STANDLEY, K. J., 1949, *Thesis*, Oxford University.
STEWART, K. H., 1951, *Proc. Phys. Soc.* A, **63,** 761.
STREET, R., 1951, *Sci. Prog.*, **39,** 258.
VAN VLECK, J. H., 1950, *Phys. Rev.*, **78,** 266.

Paramagnetic Resonance and Spin–Lattice Relaxation Times in the Copper Tutton Salts

BY D. M. S. BAGGULEY AND J. H. E. GRIFFITHS
The Clarendon Laboratory, Oxford

MS. received 14*th January* 1952

ABSTRACT. Paramagnetic resonance absorption in single crystals of the copper Tutton salts has been investigated at 3·10 cm wavelength between 90° K and room temperature. In salts diluted with zinc Tutton salt the hyperfine lines are clearly resolved at 90° K but broaden and merge into one another as the temperature is raised. From these measurements the spin–lattice relaxation time τ can be estimated and is found to be about 2×10^{-9} sec. It is found that $1/\tau$ varies linearly with temperature between 150° K and 290° K. An investigation of the crystalline field in the Tutton salts shows that for the concentrated salts the field has a strong rhombic component above 150° K, whilst in the salts diluted with zinc to less than 1% copper the crystalline field has tetragonal symmetry at 290° K, but the tetragonal axis lies in a plane perpendicular to that containing the tetragonal axis at 90° K.

§ 1. INTRODUCTION

THE experiments of Gorter and his collaborators (Gorter 1947) have enabled spin–lattice relaxation times to be measured for many salts of the iron group between 1° K and 90° K, and a theory which is in broad agreement with the experimental results has been formulated. At present, however, there are few results with which to compare the theoretical predictions for the temperature range 90° K to 300° K. It is the purpose of this paper to give an estimate for spin–lattice relaxation times in this temperature interval which have been derived from measurements of line widths in the paramagnetic resonance spectra of magnetically dilute copper Tutton salts.

In crystals containing less than 0·1% copper the hyperfine structure is clearly resolved at 90° K, but as the temperature is raised the absorption lines gradually merge into each other until at room temperature only a single broad absorption line is observed. The magnetic interaction between the copper ions is negligible for these dilutions, and it is improbable that the variation in line width can be due to a change in position of the neighbouring protons since the minimum line width measured at 90° K is in good agreement with theoretical estimates based on X-ray measurements made at room temperature. The broadening of the hyperfine absorption lines is interpreted therefore in terms of a variation in spin–lattice relaxation time when the temperature is raised from 90° K to room temperature.

With such broad lines and dilute samples the resonance absorption at room temperature is very weak, and so the experimental technique is difficult. The measurements are further complicated by a change in the crystalline field so that the interpretation involves assumptions about both the hyperfine splitting and the line shape. However, it does not seem possible to fit our experimental curves if the relaxation time decreases more rapidly than $1/T$ between 150° K and 300° K, and we believe that the magnitudes we have estimated are sufficiently accurate to provide a reasonable check on any theory of relaxation times in this temperature range.

The crystalline electric field in the Tutton salts was determined, in so far as was necessary, by measurements at a wavelength of 3·10 cm for temperatures between 90° K and room temperature. For the concentrated salts our results are in good agreement with the susceptibility measurements of Krishnan and Mookherji (1938), but indicate that the crystalline field has a component of rhombic symmetry at all temperatures. In crystals diluted with the corresponding zinc Tutton salt the crystalline field appears to be very nearly tetragonal at room temperature, but the axis lies in a plane perpendicular to that containing the tetragonal axis at 90° K. For intermediate temperatures the crystalline field has rhombic symmetry. These measurements are discussed further in § 4 (ii).

§ 2. EXPERIMENTAL ARRANGEMENT

In order to observe paramagnetic resonance it is usual to place the sample in a cavity resonator situated between the poles of a magnet and measure the change in Q of the resonator as the applied magnetic field is varied, the incident frequency meanwhile remaining constant. A change in Q of less than 1% cannot easily be detected by the direct method of measuring the power transmitted through the resonator using a silicon tungsten crystal detector (Bagguley and Griffiths 1950), and for improved sensitivity one of two other methods is usually employed. When the absorption lines are sufficiently narrow it is convenient to extend the technique of field modulation employed in nuclear resonance experiments and to sweep the magnetic field completely through the line or to measure its differential. To apply this method to broad lines, requiring a field sweep of a few hundred gauss, is difficult and not easily achieved at a frequency which will pass through an a.c. amplifier. Alternatively a 'magic tee' or a hybrid ring circuit may be used (England and Schneider 1950). We have found it more convenient to use a bridge circuit in which the steady signal transmitted by the resonator when no absorption takes place is balanced by a similar signal from a reference resonator. The reflector voltage of the 3 cm klystron is modulated at 1 Mc/s and the resulting frequency modulation traverses the response curves of the resonators once in each half cycle of the impressed voltage. The power transmitted by each resonator therefore has a 2 Mc/s amplitude modulation, and after detection by silicon tungsten crystals the signals are fed in antiphase to a balanced transformer tuned to this frequency. The system is balanced when there is no paramagnetic absorption, and the unbalance within an absorption line is amplified using a narrow-band 2 Mc/s amplifier and displayed on a cathode-ray oscilloscope.

With two resonators in such a bridge circuit it was hoped to balance out frequency and amplitude fluctuations due to the reflex klystron, and by detecting a 2 Mc/s signal a reduction in crystal noise was expected so that a considerable increase in sensitivity might be obtained. In fact the sensitivity has been improved by a factor of about one thousand compared with the simple crystal detector and galvanometer method, but it appears that the method has limitations which prevent it from attaining sensitivities which should in principle be available to microwave spectroscopy. The balanced arrangement is perfect only when the resonators have the same Q value, and this cannot be achieved when the resonator containing the paramagnetic sample is cooled through a temperature range in which the dielectric loss of the sample undergoes a considerable change. Further, the use of two crystal detectors introduces additional noise voltages, and it seems that at 2 Mc/s this is still a serious factor. The method is, however, extremely flexible and, being independent of ring circuits and 'magic tee' junctions, can be used continuously over a wide range of wavelengths. In addition only one reflex klystron is required for the spectroscope described in this paper, so that if too high a sensitivity is not required the method may be of considerable value in microwave research.

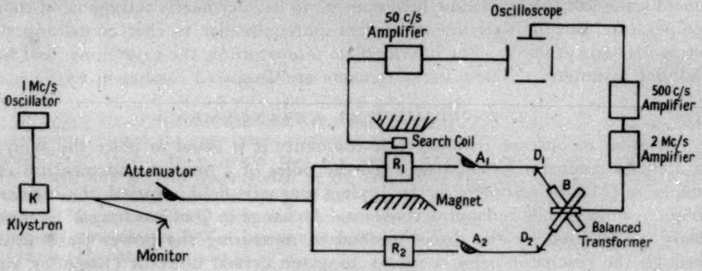

Fig. 1. Block diagram of apparatus.

A block diagram of the apparatus is shown in fig. 1. The reflex klystron K (C.V. 223) was operated at 3·10 cm and produced about 50 mw power. Sufficient stability could only be obtained by supplying all the potentials of the klystron from batteries. The reflector voltage was modulated with an amplitude of 40 v at 1 Mc/s from a quartz crystal controlled oscillator (Montgomery 1947). Power from the klystron was fed into the resonators R_1 and R_2 via a 'T' junction. Each resonator was excited in the H_{11} mode, R_1 was coupled to the waveguide by coaxial line and probe, and R_2 was directly coupled by an iris $\frac{1}{4}$ in. in diameter. The Q of each resonator was about 5 000 at 3·10 cm. The power transmitted by each resonator could be varied independently by the attenuators A_1 and A_2 and, after detection by the silicon tungsten crystals D_1 and D_2, the resulting 2 Mc/s signals were fed in antiphase to the mutually perpendicular windings of the balanced transformer B. The crystals were matched to the transformer by a tapping and the input and output circuits were tuned. The output from the transformer was amplified by a narrow-band crystal amplifier tuned to 2 Mc/s with a gain of about 120 db. During an experiment the bridge was balanced initially using the attenuators A_1 and A_2 for amplitude adjustment, and phase changes were controlled from the tuned circuits of the transformer. It was possible to balance to better than 1 part in 10^4. Paramagnetic absorption decreased the power through R_1 and the out of balance signal was amplified by the 2 Mc/s amplifier. The output from this amplifier was detected and fed through a low-pass filter with a cut-off at about 100 c/s and operated a diode switch which impressed the absorption curve on a 500 c/s sine wave. After further amplification this signal was detected and applied to the Y plates of the oscilloscope. A 50 v bias was applied to the 500 c/s switch so that no signal was visible until a 50 v unbalance was registered at the output of the 2 Mc/s amplifier. This was effective in removing the residual unbalance of the bridge and enabled the magnitudes of the two signals to be so adjusted that paramagnetic absorption further increased the output voltage applied to the oscilloscope.

The magnet was excited from the 100 v d.c. mains and produced a maximum field of 6 500 gauss. By means of a motor-driven rheostat a periodic field sweep was obtained having an amplitude variable between zero and 4 000 gauss and a period variable between 10 and 20 seconds. The field was calibrated using a fluxmeter and standardized search coils to an accuracy of within about 1%. A rotating search coil with slip rings and carbon brushes provided a voltage proportional to the magnetic field. The coil rotated at 3 000 r.p.m. and the output voltage after amplification and detection was applied to the X plates of the oscilloscope. The absorption lines were photographed using Kodak recording paper R.P.30.

§ 3. CRYSTALLOGRAPHY

A detailed discussion of the crystallography of the copper Tutton salts in relation to paramagnetic resonance has been given previously (Bleaney, Penrose and Plumpton 1949) and we shall use the notation and designation of magnetic axes given by these authors. The crystals are monoclinic, the dimensions of unit cell for the potassium salt being $a, b, c = 9{\cdot}1$ Å, 12·2 Å, 6·1 Å, whilst for other salts the axial lengths are slightly greater, corresponding to the increase in ionic volume. Unit cell contains two inequivalent Cu^{2+} ions, the one at $(\frac{1}{2}, \frac{1}{2}, 0)$ being obtained from that at $(0, 0, 0)$ by translation followed by reflection in the $(0, 1, 0)$ plane. Each ion is surrounded by six water molecules situated at the corners of a distorted octahedron, the mean Cu–H_2O distance being about 2 Å.

Single crystals of the potassium, ammonium and rubidium Tutton salts were grown by slow cooling of a saturated solution. These were diluted with varying amounts of the corresponding zinc salt so that mixed crystals having between 1% and 0·05% of the copper salt could be used. For the determination of the crystalline field symmetry and the g values, plane sections were cut, 1 or 2 mm in thickness and about 0·5 cm² in area, containing the magnetic axes, i.e. the planes K_1K_2, K_1K_3, K_2K_3.

§ 4. RESULTS AND DISCUSSION

(i) *Introduction*

Measurements were made at 3·1 cm wavelength at temperatures between 90° K and room temperature. From the values of magnetic field H at which resonance absorption occurred, the g values were determined using the relation

$h\nu = g\beta H$ where ν is the frequency and β the Bohr magneton. The results of the measurements at 290° K are summarized in table 1. The g values are in agreement with those derived from the susceptibility measurements on the concentrated salts made by Krishnan *et al.* (1933, 1938) at room temperature. The appropriate diamagnetic correction to the susceptibility measurements was calculated and found to be -200×10^{-6} c.g.s. e.m.u. per gram mol. The accuracy of the g values is between 1% and 2%.

Table 1

Salt	Crystalline field	ψ	α	g_1	g_2	g_3
$K_2Cu(SO_4)_2.6H_2O$	Rhombic	105°	—	2·31	2·07	2·25
		(102°)		(2·33)	(2·06)	(2·28)
$(NH_4)_2Cu(SO_4)_2.6H_2O$	Rhombic	77°	—	2·32	2·09	2·25
		(77°)		(2·32)	(2·09)	(2·28)
$Rb_2Cu(SO_4)_2.6H_2O$	Rhombic	105°	—	2·28	—	2·24
		(105°)		(2·31)	(2·06)	(2·23)
$K_2(Zn+Cu)(SO_4)_2.6H_2O$*	Tetragonal	15°	32°	2·26	2·06	2·24
$(NH_4)_2(Zn+Cu)(SO_4)_2.6H_2O$*	Tetragonal	167°	32°	2·28	2·09	2·24
$Rb_2(Zn+Cu)(SO_4)_2.6H_2O$*	Tetragonal	15°	33°	2·25	2·09	2·25

* These salts were diluted with zinc Tutton salt to less than 1% copper.
The figures in brackets are derived from Krishnan *et al.* (1933, 1938).
The angles ψ, α are as defined by Bleaney, Penrose and Plumpton (1949).

Table 2

	$(Cu+Zn)K_2(SO_4)_2.6H_2O$				$(Cu+Zn)(NH_4)_2(SO_4)_2.6H_2O$				$(Cu+Zn)Rb_2(SO_4)_2.6H_2O$			
T (°K)	(1)	(2)	(3)	(4)	(1)	(2)	(3)	(4)	(1)	(2)	(3)	(4)
90	220				230				210			
125									200	18	12	4·2
163									180	23	17	3·0
170	195	25	19	2·7								
173									180	26	20	2·5
210					195	26	20	2·5				
215									180	29	23	2·2
240	180	30	24	2·1								
290	150	36	30	1·7	150	33	27	1·9	150	33	27	1·9
	Half width of complete line observed at 290° K is 100 gauss.				Half width of complete line observed at 290° K is 90 gauss.				Half width of complete line observed at 290° K is 90 gauss.			

(1) Hyperfine splitting (gauss); (2) half width of individual lines (gauss); (3) ΔH_s (gauss); (4) τ (sec $\times 10^{-9}$).

Typical photographs of the absorption spectrum of the potassium and rubidium salts containing less than 0·1% Cu are given in fig. 2 (Plate). These show the variation in width of the hyperfine lines as the temperature is raised from 90° K to room temperature. It can be seen that the absorption lines which are clearly resolved at 90° K merge into one another as the temperature increases. Measurements were made with the magnetic field normal to an (0, 1, 0) plane since this direction must remain a principal magnetic axis independent of crystalline field changes, and hence the spectrum can contain only four hyperfine lines. In table 2 the hyperfine splitting and line widths obtained from such photographs of the absorption spectrum are given together with the derived values of spin–lattice relaxation time.

(ii) *Crystalline Field*

It has been reported previously (Bleaney, Penrose and Plumpton 1949) that at 90° K for concentrated copper Tutton salts the crystalline field is predominantly of cubic symmetry with an additional tetragonal and smaller rhombic component. We have observed two absorption lines in both the K_1K_3 and K_2K_3 planes of the K_2, $(NH_4)_2$ and Rb_2 concentrated copper Tutton salts at room temperature. If the crystalline field had tetragonal symmetry we should have observed a single absorption line for all orientations in one of these planes, namely, that in which the magnetic field direction made equal angles with the tetragonal axes of the two ions, and the fact that we could resolve two lines in each plane indicates that a large rhombic component of crystalline field must be present.*

In fig. 3 (Plate) we give typical absorption curves for the concentrated potassium salt at 45° to K_3 in the K_1K_3 and K_2K_3 planes. The maximum and minimum g values in these planes are (for the potassium salt): K_1K_3, $g_{\max}=2{\cdot}40$, $g_{\min}=2{\cdot}14$; K_2K_3, $g_{\max}=2{\cdot}32$, $g_{\min}=2{\cdot}04$.

For crystals diluted with zinc Tutton salt to less than 1% copper the crystalline field is very nearly tetragonal at 290° K. The absorption line at room temperature has a half width of about 100 gauss, so that the measurements are not extremely sensitive to small departures from tetragonal symmetry, but only a single absorption line is observed at 45° to K_3 in the K_1K_3 plane (a direction in which any rhombic field would produce maximum separation of the absorption lines), and also there is very good agreement between the values of $g_\perp$ measured in the K_2K_3 plane and along K_1. These values are given in table 3.

Table 3

	K_2K_3 plane		K_1
Salt	$g_\parallel$	$g_\perp$	$g_\perp$
$(Zn+Cu)K_2(SO_4)_2.6H_2O$	2·05	2·25	2·26
$(Zn+Cu)(NH_4)_2(SO_4)_2.6H_2O$	2·04	2·26	2·28
$(Zn+Cu)Rb_2(SO_4)_2.6H_2O$	2·08	2·27	2·25

The tetragonal axis, at room temperature, lies in the K_2K_3 plane at an angle of about 30° to K_2 (see table 1). This is approximately at 70° to the direction of the tetragonal axis at 90° K, which is in the K_1K_3 plane inclined to K_1 at an angle of about 40°. There is a considerable change in crystalline field, therefore, as the crystal is cooled down to 90° K, but this does not result in a pure cubic field at any temperature, there being a strong rhombic component present at intermediate temperatures.

Polder (1942) has given a theoretical account of the magnetism of the copper ion in the Tutton salts assuming the crystalline field to be of cubic symmetry with a small tetragonal perturbation. He remarked that the susceptibility measurements (Krishnan *et al.* 1933, 1938, Hupse 1942) did not distinguish between two possible orientations of the tetragonal axis, and he arbitrarily chose that orientation which gave reasonable values for the splitting of the orbital levels and the susceptibility of the individual Cu^{2+} ions when the tetragonal field had a positive sign. He showed that the g values parallel and perpendicular to a tetragonal axis were given by

---

* Arnold and Kip (1949) have reported measurements on $CuK_2(SO_4)_2.6H_2O$ at 290° K and conclude that the crystalline field is tetragonal. These authors, however, examined the K_1K_3 plane only, and this is insufficient to exclude the possibility of a rhombic crystalline field.

$$g_{\parallel}=2\left(1-\frac{4\lambda}{F_4-F_3}\right),\quad g_{\perp}=2\left(1-\frac{\lambda}{F_5-F_3}\right).$$

Here λ is the spin–orbit coupling coefficient; F_1, F_3, F_4, F_5 are the levels into which the ^{2}D state is split by the crystalline electric field, and of these F_3 is the ground state whilst F_4, F_5 are components of the triplet in a cubic electric field. Polder assumed that the tetragonal axis was in the K_1K_3 plane inclined at 40° to K_1 and obtained good agreement between theory and experiment using the values $g_{\parallel}=2{\cdot}44$, $g_{\perp}=2{\cdot}05$, $\lambda=-852\ \mathrm{cm}^{-1}$, $F_4-F_3=15\,400\ \mathrm{cm}^{-1}$, $F_5-F_3=26\,600\ \mathrm{cm}^{-1}$. The experiments reported in this paper, however, show that whilst Polder's assumption is valid at 90° K it is not correct at room temperature. Using the values for $g_{\parallel}$ and $g_{\perp}$ derived from the paramagnetic resonance experiments at 290° K, i.e. $g_{\parallel}=2{\cdot}05$, $g_{\perp}=2{\cdot}26$, the values for F_4-F_3 and F_5-F_3 are found to be $135\,000\ \mathrm{cm}^{-1}$ and $6\,500\ \mathrm{cm}^{-1}$ respectively, so that, on Polder's theory, F_5 lies below F_4 and the splittings are of widely differing magnitude. It is usually assumed that the crystalline field arises from the octahedron of water molecules surrounding the copper ion, and under these circumstances we should expect the values of F_4-F_3 and F_5-F_3 each to be about $20\,000\ \mathrm{cm}^{-1}$. These values are confirmed by optical measurements on solutions of cupric salts which show a broad absorption band at about $12\,300\ \mathrm{cm}^{-1}$ and no further absorption below $32\,000\ \mathrm{cm}^{-1}$ (Abragam and Pryce 1951 b). A splitting of this order of magnitude can give rise to the observed g values if tetragonal terms opposite in sign to those given by Polder are used (Polder 1942, Abragam and Pryce 1951 a). We then obtain $g_{\parallel}=2{\cdot}0$, $g_{\perp}=2-6\lambda/\Delta E$, where ΔE is the splitting of the ^{2}D state in a cubic field and hence, for $g_{\perp}=2{\cdot}26\ \mathrm{cm}^{-1}$ and $\lambda=-828\ \mathrm{cm}^{-1}$ (Abragam and Pryce 1951 b) we obtain $\Delta E=19\,000\ \mathrm{cm}^{-1}$. The agreement between experiment and theory is now much more satisfactory; the splitting ΔE is of the expected order of magnitude, and the value for $g_{\parallel}=2{\cdot}0$ approaches the experimental result of 2·05. The small difference may be due to a weak rhombic component of the electric field. We conclude therefore that, in crystals of the copper Tutton salts diluted with zinc to less than 1% copper, the crystalline field at 290° K is, to a good approximation, tetragonal, but with a negative sign, and the tetragonal axis lies in the K_2K_3 plane making an angle of about 30° with K_2.

(iii) *Hyperfine Structure*

Abragam and Pryce (1951 a) have given a theoretical interpretation of the hyperfine structure for a Cu^{2+} ion in a crystalline electric field of tetragonal symmetry. The Hamiltonian (in their notation) is

$$W=g_{\parallel}\beta H_zS_z+g_{\perp}\beta(H_xS_x+H_yS_y)+AS_zI_z+B(S_xI_x+S_yI_y)$$
$$+Q\{I_z^2-\tfrac{1}{3}I(I+1)\}-\gamma\beta_N\mathbf{H}\,.\,\mathbf{I}.$$

In this equation the last two terms are small and may be neglected for this discussion. When the steady magnetic field is directed parallel and perpendicular to the tetragonal axis the overall separation of the hyperfine lines is $3A$ and $3B$ respectively, whilst for any arbitrary orientation of the crystal the separation will not be less than the smaller of these values. For a tetragonal field the constants A and B are given by

$$A=\frac{2\gamma\beta\beta_N}{r^3}(\mp\tfrac{4}{7}-\kappa+g_{\parallel}-2),\quad B=\frac{2\gamma\beta\beta_N}{r^3}(\pm\tfrac{2}{7}-\kappa+g_{\perp}-2)$$

in which the notation is again that of Abragam and Pryce (1951 a). For the dilute copper Tutton salts, in which the tetragonal component is negative, the lower sign is to be taken so that, writing $2\gamma\beta\beta_N/r^3=0{\cdot}025$, $\kappa=0{\cdot}28$, $g_{\parallel}=2{\cdot}05$, $g_{\perp}=2{\cdot}26$, we obtain $|A|=85\times10^{-4}\,\mathrm{cm}^{-1}$, $|B|=78\times10^{-4}\,\mathrm{cm}^{-1}$, from which the overall splitting of the hyperfine lines corresponding to $3|A|$ is 270 gauss, and that corresponding to $3|B|$ is 220 gauss. The hyperfine structure is therefore almost isotropic, and in fact the calculated value of the hyperfine splitting when the magnetic field is along the b axis of the crystal is 225 gauss.

It will be seen from table 2 that we have given the value for the overall hyperfine splitting along the b axis at room temperature as 150 gauss, and this is considerably less than the theoretical estimate of 225 gauss. It is necessary therefore to indicate how the experimental value has been obtained. When constructing the absorption spectrum theoretically the line shape was first determined (see § 4 (iv) below) and the line width and hyperfine splitting then adjusted to give the best fit with the experimental curves. Below 250° K it is possible to distinguish the peaks of the individual absorption lines; the hyperfine splitting is therefore known fairly accurately and the width of the lines is adjusted to reproduce the observed spectrum. At room temperature, however, the absorption lines are completely merged together so that the choice of hyperfine splitting is somewhat arbitrary. We have chosen a value which gives results most consistent with measurements at the lower temperatures both for the hyperfine splitting and the line width. In any case it seems unlikely that the hyperfine splitting can be as great as 225 gauss at room temperature since the total width of the absorption line at half power is only about 200 gauss. If the splitting were to be as great as 225 gauss the separate peaks would be resolved unless there has been a considerable broadening of the absorption lines, and such a broadening would of course further increase the width of the absorption band beyond 225 gauss. It may be that the term $2\gamma\beta\beta_N/r^3$ or κ has changed, but these are not expected to be temperature dependent and are taken from the accurate measurements of the hyperfine structure described by Bleaney, Bowers and Ingram (1951).

(iv) *Line Widths*

In the copper Tutton salts diluted with zinc to less than 1% copper the contribution to the line width from dipolar coupling between the Cu^{2+} ions is negligible, and so the line width arises from spin–lattice coupling and the magnetic interaction of the Cu^{2+} ions with the protons in the neighbouring water molecules. It is usual to assume that the complete width is given by simple addition of these two contributions so that 6 gauss, representing the proton contribution, must be subtracted from the measured line width in order to derive the effect of spin–lattice interaction. The line shape should be a combination of the gaussian and damped harmonic oscillator equations, but we have found sufficient agreement by replacing this bell-shaped curve by that for a damped harmonic oscillator alone. In order to construct the spectrum we assumed, therefore, a line shape of the form $I = I_0(1+x^2)^{-1}$, in which x is the distance from resonance measured in units of half the width between the half-power points, i.e. in units of the half width of the absorption line.

From the half widths of the absorption lines so constructed as to give best fit with the experimental curves the spin–lattice relaxation time was derived using the relation $\tau = 1{\cdot}14 \times 10^{-7}/g\Delta H_s$. Here g is given by $h\nu = g\beta H$ at the centre of an absorption line, ΔH_s is half the line width between half-power points minus the 6 gauss mentioned above, and τ is the relaxation constant as defined by Van Vleck (1940). The relaxation times for the different copper salts are plotted in fig. 4. It can be seen that they lie on a single curve and extrapolate back reasonably well to the point at 90° K which is taken from the measurements of Bleaney, Bowers and Ingram (1951). Above 150° K the points on the $(1/\tau, T)$ curve lie approximately on a straight line, so that in this temperature interval the relaxation time does not appear to be changing more rapidly than $1/T$.

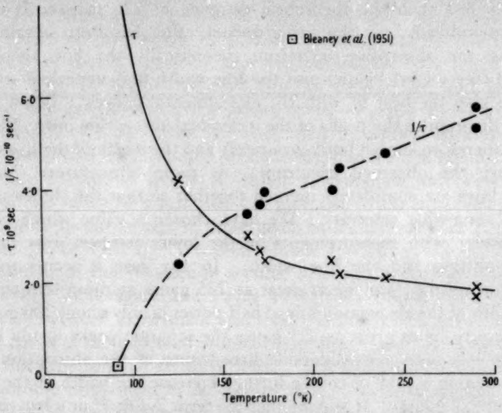

Fig. 4. Spin–lattice relaxation time as a function of temperature.

The theory of spin–lattice interaction distinguishes two coupling mechanisms. The 'direct' process, in which a magnetic ion can interchange energy with the lattice vibrations only by a simple quantum exchange, gives rise to a relaxation time proportional to $1/T$, whereas if Raman scattering of lattice waves can take place, the relaxation time should be proportional to $1/T^7 (T<\theta)$ or $1/T^2 (T>\theta)$ where θ is the Debye temperature (Kronig 1939, Van Vleck 1940).

At liquid helium temperatures the relaxation times for the concentrated copper Tutton salts vary more slowly than $1/T^2$ (Cooke, private communication), so that the 'direct' process appears to predominate below 4° K. The value of τ at 4·015° K for $CuK_2(SO_4)_2.6H_2O$ is about $9{\cdot}5 \times 10^{-3}$ sec in a field of 675 gauss (Bijl 1950). Measurements at 77° K and 90° K have been reported by Broer and Klemperman (1947) for $CuK_2(SO_4)_2.6H_2O$ and $Cu(NH_4)_2(SO_4)_2.6H_2O$ in a field of 2400 gauss, which is comparable with the field strength used in a paramagnetic resonance experiment. The values of τ obtained from these authors are

	77° K	90° K
$Cu(NH_4)_2(SO_4)_2 . 6H_2O$	$10 \cdot 7 \times 10^{-8}$ sec	$6 \cdot 4 \times 10^{-8}$ sec
$CuK_2(SO_4)_2 . 6H_2O$	$14 \cdot 3 \times 10^{-8}$ sec	$8 \cdot 6 \times 10^{-8}$ sec

Another estimate of the spin–lattice relaxation time, derived from the width of hyperfine lines in paramagnetic resonance, has been given by Bleaney, Bowers and Ingram (1951). At 90° K the relaxation time is reported to be about 5×10^{-8} sec, in good agreement with the dispersion measurements on the concentrated salts. Thus the relaxation time is varying rapidly with temperature between 4° K and 90° K, and it is thought that the Raman process is predominant in this temperature interval. Our measurements indicate that a striking change occurs about 150° K. In the 140° interval between this temperature and 290° K the relaxation time decreases only by a factor of two, whereas in the 60° interval above 90° K the relaxation time has changed by a factor of twenty. It seems unlikely that the linear variation of $1/\tau$ with T above 150° K can be adequately described by the present theory of Raman scattering, which gives a relaxation time changing at least as rapidly as $1/T^2$.

ACKNOWLEDGMENTS

Our thanks are due to Professor Lord Cherwell for extending to us the facilities of the Laboratory, to many of our colleagues for very helpful discussion, in particular Dr. B. Bleaney and Dr. K. W. H. Stevens, and to the Board of Admiralty for apparatus and other assistance in carrying out this work.

REFERENCES

Abragam, A., and Pryce, M. H. L., 1951 a, *Proc. Roy. Soc.* A, **205**, 135; 1951 b, *Ibid.*, **206**, 164.

Arnold, R. D., and Kip, A. F., 1949, *Phys. Rev.*, **75**, 1199.

Bagguley, D. M. S., and Griffiths, J. H. E., 1950, *Proc. Roy. Soc.* A, **204**, 188.

Bijl, D., 1950, *Thesis*: Leiden.

Bleaney, B., Penrose, R. P., and Plumpton, B. I., 1949, *Proc. Roy. Soc.* A, **198**, 406.

Bleaney, B., Bowers, K. D., and Ingram, D. J. E., 1951, *Proc. Phys. Soc.* A, **64**, 758.

Broer, L. J. F., and Klemperman, J., 1947, *Physica*, **13**, 465.

England, T. S., and Schneider, E. E., 1950, *Nature, Lond.*, **166**, 437.

Gorter, C. J., 1947, *Paramagnetic Relaxation* (New York: Elsevier Publ. Co.).

Hupse, J. C., 1942, *Physica*, **9**, 633.

Krishnan, K. S., Chakravorty, N. C., and Banerjee, S., 1933, *Phil. Trans. Roy. Soc.* A, **232**, 99.

Krishnan, K. S., and Mookherji, A., 1938, *Phil. Trans. Roy. Soc.* A, **237**, 135.

Kronig, R., 1939, *Physica*, **6**, 33.

Montgomery, C. G., 1947, *Technique of Microwave Measurements* (New York: McGraw-Hill).

Polder, D., 1942, *Physica*, **9**, 709.

Van Vleck, J. H., 1940, *Phys. Rev.*, **57**, 426.

A Note on the Theory of Semiconductors

By P. T. LANDSBERG
Department of Natural Philosophy, University of Aberdeen

MS. received 19*th March* 1952

ABSTRACT. One obtains two different theories of semiconductors, depending on whether the free energy due to the spin of electrons in donor (or acceptor) centres is taken into account (approach A) or not (approach B). It is shown (i) that the former approach can be carried through for a degenerate semiconductor, (ii) that it applies *formally* to the case when the interaction between impurity centres and conduction electrons is taken into account, provided one of the symbols is reinterpreted, and (iii) that it is to be preferred. Approach B has, however, been used almost universally. It is shown that it corresponds to the unlikely situation in which fifty per cent of the electrons from each impurity level come from paired states, and the remaining fifty per cent from unpaired states having the same activation energy.

---

§ 1. INTRODUCTION

It does not seem to be realized that two models are in use in current semiconductor theory. The first is essentially due to Mott and Gurney (1948, p. 157) and depends on minimizing the free energy. It will be referred to as A. It has not so far been formulated so as to take the Fermi–Dirac distribution of current carriers in the conduction band into account rigorously, and has, therefore, not yet been applied to degenerate semiconductors. The second approach, to be referred to as B, is essentially Wilson's original approach (Wilson 1931, Seitz 1940, p. 186). It is known to hold also for degenerate semiconductors, but it cannot take into account the contribution to the free energy due to the unpaired electrons which remain behind in impurity centres at any given temperature.

We shall show that approach A can be extended to degenerate semiconductors, and that the equations obtained differ markedly from those obtained by approach B. *The present form of approach A is always to be preferred to approach B.*

§ 2. EXTENSION OF APPROACH A

The simple generalization of Mott and Gurney's argument for approach A is as follows. Consider a crystal of an excess semiconductor having donor impurity levels at the energies $E_j (j=1, 2, \ldots)$, which are generally negative if the zero of the energy scale is taken at the bottom of the conduction band. The free energy is

$$A = -\Sigma_j n_j E_j + (\Sigma_j n_j)\boldsymbol{k}T\eta^* - \tfrac{2}{3}\boldsymbol{k}T\eta_0 F_{3/2}(\eta^*) - \boldsymbol{k}T \log P - g, \quad \ldots\ldots(1)$$

where n_j is the number of electrons donated by the jth level; and the summations are over all impurity levels. The first term represents the energy to bring electrons into the conduction band. The next two terms come from the theory of a gas of n electrons, according to which its free energy is

$$\boldsymbol{k}T[n\eta^* - \tfrac{2}{3}n_0 F_{3/2}(\eta^*)], \text{ where } n_0 = \frac{4\pi}{\boldsymbol{h}^3}(2m^*\boldsymbol{k}T)^{3/2} \text{ and}$$

$$F_c(\eta^*) = \int_0^\infty \frac{x^c\,dx}{1+\exp(x-\eta^*)}. \quad \ldots\ldots(2)$$

η^* is the Fermi level ζ divided by $\boldsymbol{k}T$, m^* is the effective electron mass. The last term but one gives the free energy of the vacant places from which electrons have been removed. Let N_{ej} be the number of available donor electrons and $N_j - N_{ej}$ the number of electron vacancies in the jth energy level at the absolute zero of temperature. Then there will be $N_j - N_{ej} + n_j$ electron vacancies at higher temperatures. P is the number of ways in which $N_1 - N_{e1} + n_1$ vacant places can be distributed among N_1 sites, $N_2 - N_{e2} + n_2$ places among N_2 sites, etc. Thus, using Stirling's approximation,

$$\frac{\partial \log P}{\partial n_k} \sim \log \frac{N_{ek} - n_k}{N_k - N_{ek} + n_k} \, (k = 1, 2, \ldots .). \qquad \ldots\ldots(3)$$

The last term of (1) is some function of the N_j's, N_{ej}'s and n_j's which is to take account formally of the contribution of the spins of the electrons to the free energy, of the effect of interactions among the electrons and impurity centres and of any other terms which have not been included explicitly. For equilibrium $(\partial A/\partial n_r)_T = 0$, so that by (1) to (3)

$$-E_r + \zeta + \boldsymbol{k}T \log \frac{N_r - N_{er} + n_r}{N_{er} - n_r} - \frac{\partial g}{\partial n_r} = 0, \quad r = 1, 2, \ldots \qquad \ldots\ldots(4)$$

Here we have used the results

$$\frac{dF_c(\eta^*)}{d\eta^*} = cF_{c-1}(\eta^*) \, (c > 0) \quad \text{and} \quad \Sigma_j n_j = n_0 F_{1/2}(\eta^*).$$

Hence the number of electrons in the level E_r at temperature T is

$$N_{er} - n_r = \frac{N_r}{1 + \beta_r \exp(\eta_r - \eta^*)}, \qquad \ldots\ldots(5)$$

where

$$\beta_r = \exp\left[\frac{1}{\boldsymbol{k}T} \frac{\partial g}{\partial n_r}\right] \qquad \ldots\ldots(6)$$

and $\eta_r = E_r/\boldsymbol{k}T$. The Fermi level is determined by

$$\Sigma_r \left[N_{er} - \frac{N_r}{1 + \beta_r \exp(\eta_r - \eta^*)}\right] = n_0 F_{1/2}(\eta^*). \qquad \ldots\ldots(7)$$

If g takes account only of the spin contribution to the free energy then any quantity β_r has the value $\frac{1}{2}$ if none of the N_r sites of the rth energy level has paired electrons (two electrons of opposite spin) at the absolute zero, while it has the value 2 if all N_r sites have paired electrons, since the argument follows then exactly along the lines laid down by Mott and Gurney. (More generally, it may readily be shown that if a fraction f_r of the n_r electrons donated by the level E_r comes from paired sites, then $\beta_r = 2^{2f_r - 1}$.) Approach B is obtained if $\beta_r = 1$ (for all r). This corresponds to the case in which fifty per cent of the electrons which come from the rth level come at all temperatures from paired states, and fifty per cent from unpaired states. This situation is most unlikely as electrons in paired states have in general a lower activation energy than electrons in corresponding unpaired states. *It follows that approach B is less satisfactory than approach A.*

The value of β_r has an important effect on the relation between the parameters of the theory. We merely show (in the figure) the degree of ionization of a single impurity level at room temperatures as a function of the impurity concentration for $\beta_1 = \frac{1}{2}, 1, 2$. The figure shows incidentally that, for a fixed activation energy, impurity centres with paired electrons are more readily ionized than impurity centres with unpaired electrons. This is entirely due to the effect which the spin of the electrons left behind in the impurity centres has on the minimum of the free energy. A wrong choice of β_r in the analysis of experiments can lead to an incorrect activation energy. In particular, if E_r is independent of temperature, *a wrong value of β_r may lead one to infer an incorrect and temperature-dependent activation energy*, which would agree with the true activation energy only at the absolute zero of temperature.

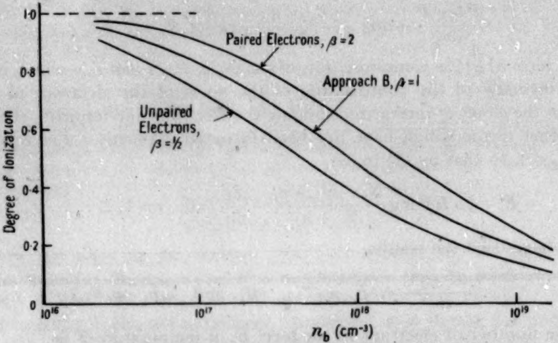

The effect of the two different approaches on the degree of ionization of the impurity centres. A simple excess semiconductor at room temperature is assumed, having a donor level 0·1 ev below the conduction band and having $N_1 = N_{e1}$.

§ 3. SPECIAL CASES

The above results can be extended to take the full band and acceptors into account. We shall, however, merely indicate the modifications brought about by approach A in the usual formulae for some important special cases. Suppose only one impurity level is present. The mass action law for the 'reaction':

excess electron + ionized donor = neutral donor

is easily seen to be

$$\frac{n_1(N_1 - N_{e1} + n_1)}{N_{e1} - n_1} = K = \beta_1 n_0 F_{1/2}(\eta^*) \exp(\eta_1 - \eta^*), \qquad \ldots\ldots(8)$$

K being the reaction constant. Using the classical approximation

$$F_{1/2}(\eta^*) \sim \tfrac{1}{2}\sqrt{\pi} \exp \eta^* \qquad \ldots\ldots(9)$$

and putting $N_1 = N_{e1}$, $\beta_1 = \frac{1}{2}$, one obtains from (8) a formula which has been used by Pearson and Bardeen (1949)† in the analysis of their experimental results, which is therefore based on approach A. *Most other work on semiconductors is, however, based on approach B.*

If $N_{e1} = N_1$, (7) can be written in the form

$$N_1 = [1 + \beta_1^{-1} \exp(\eta^* - \eta_1)] n_0 F_{1/2}(\eta^*). \qquad \ldots\ldots(10)$$

---

† When comparing their equation with (8), their value of N_A must be put equal to zero, as the possibility of having acceptors present has here been excluded.

If β_1 is replaced by unity, (10) yields a result which is well known in theories based on B. From (10) follows for given E_1 a relation between the maximum, $\eta_0{}^*$, say, of η^* and the temperature for which it is reached:

$$\eta_0{}^* = \beta_1\eta_1 - \log\left(-\tfrac{2}{3}\beta_1\eta_1 - 1\right). \qquad \ldots\ldots(11)$$

For $\beta_1 = 1$ one obtains a result first given by Shifrin (1944)†, using approach B. From (10) there also follows the well-known approximate expression for the Fermi level, provided (9) can be used and $\exp(\eta^* - \eta_1) \gg 1$:

$$\eta^* = \tfrac{1}{2}\eta_1 + \tfrac{1}{2}\log\frac{2\beta_1 N_1}{\sqrt{\pi}n_0}.\ddagger \qquad \ldots\ldots(12)$$

These modifications must be borne in mind in the usual expression for the electrical conductivity and the various coefficients which arise in second-order effects (Hall effect, thermoelectric power, etc.: for a list of formulae, see R. W. Wright 1951, approach B) wherever the formulae involve the Fermi level or the impurity level. The reason is that the former is affected by the value of β_1 and the latter occurs usually in the improved approach A multiplied by β_1 (cf. the equations of § 2). We merely note here that if the mean free path l is independent of the energy and inversely proportional to the temperature, and we put $l = l_0/\boldsymbol{k}T$, then the electrical conductivity is given by (Shifrin 1944)

$$\sigma = \sigma_0 \log(1 + \exp\eta^*), \quad \sigma_0 = 16\pi m^* \boldsymbol{e}^2 l_0/3\boldsymbol{h}^3. \qquad \ldots\ldots(13)$$

At low temperatures (12) and (13) lead to

$$\log(\sigma T^{3/4}) = \log\left[\frac{\sigma_0}{2\pi}\frac{(2N_1\boldsymbol{h}^3)^{1/2}}{(2m^*\boldsymbol{k})^{3/4}}\right] + \frac{E_1 + \partial g/\partial n_1}{\boldsymbol{k}T}. \qquad \ldots\ldots(14)$$

If the term g is due only to the spin of the electrons in the impurity levels, then $(\partial g/\partial n_1)/\boldsymbol{k}T$ is independent of temperature. Thus, if the activation energy has been determined from a plot of $\log(\sigma T^{3/4})$ against $1/T$, the value obtained will be independent of β_1, and will therefore be the same whether the analysis is based on approach A or approach B. If g takes into account interactions, and so becomes a function of N_1 and n_1, (14) shows that the experimentally determined activation energy must also be expected to depend on these quantities, as observed for silicon alloys containing boron (Pearson and Bardeen 1949, Castellan and Seitz 1951), cuprous iodide in equilibrium with iodine vapour (Vine and Maurer 1951, using approach B), and the oxides of titanium, iron, nickel and zinc (Mitchell 1952, using approach B).

ACKNOWLEDGMENT

The author is indebted to Miss L. S. Souter of the Research Laboratories of the General Electric Company Ltd., Wembley, Middlesex, for some stimulating discussions concerning the paper by Pearson and Bardeen. It is to these that this note owes its origin.

---

† An analytical proof is also known (Landsberg, Mackay and McRonald 1951, approach B) and is readily generalized to deduce (11).

‡ There is some confusion in the literature with respect to this equation. It should be noted that in Mott and Gurney's book (1948) the '(2)' refers to the case of paired electrons on p. 158 and to the case of unpaired electrons on p. 175. In Wright's book (1950, p. 51) on the other hand, '(2)' should be replaced by '2' on the right-hand sides of eqns. (26) and (27). The term in the logarithm of eqn. (28) will then be found to be multiplied by the additional factor (2)/2, and this is in agreement with our eqn. (12).

REFERENCES

Castellan, G. W., and Seitz, F., 1951, *Semi-Conducting Materials*, ed. H. K. Henisch (London : Butterworths Scientific Publications), p. 8.

Landsberg, P. T., Mackay, R. W., and McRonald, A. D., 1951, *Proc. Phys. Soc.* A, **64,** 476.

Mitchell, E. W. J., 1952, *Proc. Phys. Soc.* B, **65,** 154.

Mott, N. F., and Gurney, R. W., 1948, *Electronic Processes in Ionic Crystals*, 2nd ed. (Oxford : University Press).

Pearson, G. L., and Bardeen, J., 1949, *Phys. Rev.*, **75,** 865.

Seitz, F., 1940, *Modern Theory of Solids* (London : McGraw-Hill).

Shifrin, K., 1944, *J. Phys., U.S.S.R.*, **8,** 242.

Vine, B. H., and Maurer, R. J., 1951, *Z. phys. Chem.*, **198,** 147.

Wilson, A. H., 1931, *Proc. Roy. Soc.* A, **133,** 458, **134,** 277.

Wright, D. A., 1950, *Semi-Conductors* (London : Methuen).

Wright, R. W., 1951, *Proc. Phys. Soc.* A, **64,** 984.

Quantization of Einstein's Gravitational Field: General Treatment

By SURAJ N. GUPTA

I.C.I. Research Fellow, University of Manchester

Communicated by L. Rosenfeld; MS. received 27th December 1951

ABSTRACT. The quantization of the complete gravitational field is carried out by extending the work of an earlier paper. The main obstacles in the quantization of Einstein's field are overcome by expressing the field quantities in the Riemannian space as expansions in the flat space, and then splitting the gravitational field into the linear and the non-linear parts. The linear part of the gravitational field is regarded as the free gravitational field, while the non-linearity is treated as a direct interaction between the gravitons. This treatment is quite general, but it suffers from the usual limitations of the perturbation method.

The gravitational self-energies of the photon and the electron are also investigated by using the linear approximation of the gravitational field. It is found that the photon self-energy vanishes unambiguously, while the electron self-energy is quadratically divergent.

§ 1. INTRODUCTION

THE quantization of the approximate linear form of Einstein's gravitational field has been carried out in an earlier paper (Gupta 1952). We shall now consider the quantization of the exact non-linear field. Einstein's gravitational field differs from other fields in two respects: it involves the use of the Riemannian space, and it is non-linear. We shall overcome these two obstacles in the following way.

As usual, we shall put $\mathfrak{g}^{\mu\nu}=\epsilon^{\mu\nu}-\kappa\gamma^{\mu\nu}$, where $\epsilon^{\mu\nu}$ is the Minkowskian metrical tensor given by

$$\epsilon^{\mu\nu}=\begin{bmatrix} -1 & 0 & 0 & 0 \\ 0 & -1 & 0 & 0 \\ 0 & 0 & -1 & 0 \\ 0 & 0 & 0 & +1 \end{bmatrix}$$

and κ is a constant. Then we can regard the Minkowskian space as the zero-th order approximation to the Riemannian space. Moreover, by expanding all the field quantities in powers of κ, it is possible to express them as expansions in the Minkowskian space. This procedure does not involve any departure from Einstein's ideas. However, we shall differ slightly from Einstein in the choice of the coordinate conditions, and use those given by De Donder (1921), Fock (1939) and Papapetrou (1948).

After passing over from the Riemannian space to the Minkowskian space, we shall split the gravitational field into the linear and the non-linear parts. Then we shall treat the linear part as a 'free' gravitational field, while the non-linearity will be treated as a direct interaction between the gravitons. It will also be shown in the next section that the splitting of the gravitational field into the linear and the non-linear parts may be given a simple physical interpretation.

The present treatment is quite general, although it suffers from the usual limitations of the perturbation method. However, the treatment of the non-linearity of the gravitational field as a perturbation seems well justified, because we know that the linear approximation of Einstein's theory, which includes Newton's theory of gravitation, accounts for the observed facts up to a very high degree of accuracy. This shows that the non-linearity can only give rise to secondary effects.

Throughout this work we shall refer to the earlier paper (Gupta 1952) as I, and the equations of I will be referred to as (I, 1), (I, 2) etc.

§2. COORDINATE CONDITIONS FOR THE GRAVITATIONAL FIELD EQUATIONS

As mentioned above, we shall use the coordinate conditions of De Donder (1921), which are given by

$$\partial \mathfrak{g}^{\mu\nu}/\partial x^{\nu} = 0. \qquad \ldots\ldots(1)$$

Using (1), Papapetrou (1948) has been able to express the field equations for the gravitational field in an extremely simple form. In this section we shall give a brief account of his work and discuss its physical implications.

The Lagrangian density for Einstein's gravitational field may be taken as

$$\mathfrak{L} = -\kappa^{-2}\mathfrak{g}^{\mu\nu}\left(\begin{Bmatrix}\alpha\\ \mu\beta\end{Bmatrix}\begin{Bmatrix}\beta\\ \nu\alpha\end{Bmatrix} - \begin{Bmatrix}\alpha\\ \mu\nu\end{Bmatrix}\begin{Bmatrix}\beta\\ \alpha\beta\end{Bmatrix}\right). \qquad \ldots\ldots(2)$$

Regarding $\mathfrak{L}$ as a function of $\mathfrak{g}^{\alpha\beta}$ and $\mathfrak{g}^{\alpha\beta}_{\mu} = \partial\mathfrak{g}^{\alpha\beta}/\partial x^{\mu}$, we get for the canonical energy momentum pseudo-tensor density of the gravitational field

$$\mathfrak{t}^{\mu}_{\nu} = \frac{\partial\mathfrak{L}}{\partial\mathfrak{g}^{\alpha\beta}_{\mu}}\mathfrak{g}^{\alpha\beta}_{\nu} - \delta^{\mu}_{\nu}\mathfrak{L}. \qquad \ldots\ldots(3)$$

We can further obtain the symmetrical energy momentum density by Belinfante's method, as we have done in §5 of I. We consider an infinitesimal linear transformation

$$\delta x^{\mu} = -\epsilon^{\mu\lambda}\delta\omega_{\lambda\nu}x^{\nu} \text{ with } \delta\omega_{\lambda\nu} = -\delta\omega_{\nu\lambda}, \qquad \ldots\ldots(4)$$

and define a quantity $\mathfrak{f}^{\mu\nu,\varrho}$, given by

$$\begin{aligned}\mathfrak{f}^{\mu\nu,\varrho} &\equiv -\frac{\delta\mathfrak{g}^{\alpha\beta}}{\delta\omega_{\mu\nu}}\frac{\partial\mathfrak{L}}{\partial\mathfrak{g}^{\alpha\beta}_{\varrho}}\\ &= 2\frac{\partial\mathfrak{L}}{\partial\mathfrak{g}^{\alpha\beta}_{\varrho}}(\epsilon^{\alpha\mu}\mathfrak{g}^{\beta\nu} - \epsilon^{\alpha\nu}\mathfrak{g}^{\beta\mu}). \qquad \ldots\ldots(5)\end{aligned}$$

Then the symmetrical energy momentum density $\theta^{\mu\nu}$ will be

$$\theta^{\mu\nu}=\epsilon^{\mu\lambda}\mathfrak{t}^{\nu}_{\lambda}-\frac{1}{2}\frac{\partial}{\partial x^{\varrho}}(\mathfrak{f}^{\mu\nu,\varrho}+\mathfrak{f}^{\varrho\mu,\nu}+\mathfrak{f}^{\varrho\nu,\mu}), \qquad \ldots\ldots(6)$$

and the angular momentum density is given by

$$\begin{aligned}\mathfrak{M}^{\mu\nu,\varrho}&=x^{\mu}\theta^{\nu\varrho}-x^{\nu}\theta^{\mu\varrho}\\&=x^{\mu}\epsilon^{\nu\lambda}\mathfrak{t}^{\varrho}_{\lambda}-x^{\nu}\epsilon^{\mu\lambda}\mathfrak{t}^{\varrho}_{\lambda}+\mathfrak{f}^{\mu\nu,\varrho}. \qquad \ldots\ldots(7)\end{aligned}$$

Adding the symmetrical energy momentum tensor density of the matter field $\epsilon^{\mu\lambda}\mathfrak{T}^{\nu}_{\lambda}$ to (5), we obtain for the total energy momentum density $\Theta^{\mu\nu}$ of the system

$$\Theta^{\mu\nu}=\epsilon^{\mu\lambda}(\mathfrak{T}^{\nu}_{\lambda}+\mathfrak{t}^{\nu}_{\lambda})-\frac{1}{2}\frac{\partial}{\partial x^{\varrho}}(\mathfrak{f}^{\mu\nu,\varrho}+\mathfrak{f}^{\varrho\mu,\nu}+\mathfrak{f}^{\varrho\nu,\mu}). \qquad \ldots\ldots(8)$$

In order to simplify (8), we note that (Tolman 1930)

$$\mathfrak{T}^{\mu}_{\nu}+\mathfrak{t}^{\mu}_{\nu}=2\frac{\partial}{\partial x^{\lambda}}\mathfrak{R}^{\lambda\mu}_{\nu} \qquad \ldots\ldots(9)$$

with

$$\mathfrak{R}^{\lambda\mu}_{\nu}=\frac{\partial\mathfrak{L}}{\partial\mathfrak{g}^{\nu\varrho}_{\lambda}}\mathfrak{g}^{\mu\varrho}-\tfrac{1}{2}\delta^{\mu}_{\nu}\frac{\partial\mathfrak{L}}{\partial\mathfrak{g}^{\varrho\sigma}_{\lambda}}\mathfrak{g}^{\varrho\sigma}. \qquad \ldots\ldots(10)$$

Moreover, according to (5) and (10), we have

$$\mathfrak{f}^{\mu\nu,\varrho}=-2(\mathfrak{R}^{\varrho\mu}_{\lambda}\epsilon^{\nu\lambda}-\mathfrak{R}^{\varrho\nu}_{\lambda}\epsilon^{\mu\lambda}). \qquad \ldots\ldots(11)$$

Using (9) and (11), we can write (8) as

$$\Theta^{\mu\nu}=\frac{\partial}{\partial x^{\alpha}}[\epsilon^{\mu\beta}(\mathfrak{R}^{\alpha\nu}_{\beta}+\mathfrak{R}^{\nu\alpha}_{\beta})+\epsilon^{\nu\beta}(\mathfrak{R}^{\alpha\mu}_{\beta}+\mathfrak{R}^{\mu\alpha}_{\beta})-\epsilon^{\alpha\beta}(\mathfrak{R}^{\mu\nu}_{\beta}+\mathfrak{R}^{\nu\mu}_{\beta})]. \qquad \ldots\ldots(12)$$

Evaluating $\mathfrak{R}^{\lambda\mu}_{\nu}$ from (2) and (10), and substituting in (12), we find

$$\kappa^{2}\Theta^{\mu\nu}=\frac{\partial^{2}}{\partial x^{\alpha}\partial x^{\beta}}(\mathfrak{g}^{\mu\nu}\epsilon^{\alpha\beta}-\mathfrak{g}^{\mu\alpha}\epsilon^{\nu\beta}+\mathfrak{g}^{\alpha\beta}\epsilon^{\mu\nu}-\mathfrak{g}^{\alpha\nu}\epsilon^{\mu\beta}). \qquad \ldots\ldots(13)$$

If we now use the supplementary conditions (1), we get the simple result

$$\epsilon^{\alpha\beta}\frac{\partial^{2}\mathfrak{g}^{\mu\nu}}{\partial x^{\alpha}\partial x^{\beta}}=\kappa^{2}\Theta^{\mu\nu}. \qquad \ldots\ldots(14)$$

Since the supplementary conditions (1) lead to the simple field equations (14), and also reduce to Einstein's supplementary conditions (I, 12) in linear approximation, it is reasonable to expect that they are the appropriate conditions.

The field equations (14), obtained by using (1), are similar to those for an electromagnetic field, the only difference being that, instead of the four-vectors A_{μ} and j_{μ} we now have the symmetrical quantities $\mathfrak{g}^{\mu\nu}$ and $\Theta^{\mu\nu}$ respectively. Thus we may take the field equations for a 'free' gravitational field as

$$\epsilon^{\alpha\beta}\frac{\partial^{2}\mathfrak{g}^{\mu\nu}}{\partial x^{\alpha}\partial x^{\beta}}=0, \qquad \ldots\ldots(15)$$

and regard the entire interaction as caused by $\Theta^{\mu\nu}$, which represents the energy momentum density of the whole system, including the gravitational field itself. This shows that the choice of the linear field (15) as the free gravitational field simply means that we are putting the interaction of the gravitational field with its own energy momentum pseudo-tensor on the same footing as its interaction with the energy momentum tensor of the matter field.

It was pointed out in I that the supplementary conditions (I, 12) are only approximately compatible with the field equations (I, 11). But here, on account of the conservation equation

$$\partial \Theta^{\mu\nu}/\partial x^{\mu} = 0, \qquad \ldots\ldots(16)$$

(1) and (14) are exactly compatible.

§ 3. FLAT SPACE EXPANSION FOR THE GRAVITATIONAL LAGRANGIAN DENSITY

We shall now expand the Lagrangian density for Einstein's gravitational field in powers of the coupling constant κ, and show that this expansion can be regarded as an infinite series in flat space. For this, as already explained, we put

$$\mathfrak{g}^{\mu\nu} = \epsilon^{\mu\nu} - \kappa\gamma^{\mu\nu}. \qquad \ldots\ldots(17)$$

Then, on account of the relation

$$|\mathfrak{g}^{\mu\nu}| = (\sqrt{-g})^4 |g^{\mu\nu}| = \frac{(\sqrt{-g})^4}{g} = g, \qquad \ldots\ldots(18)$$

we get

$$g = -1 + \kappa\epsilon_{\mu\nu}\gamma^{\mu\nu} + \frac{\kappa^2}{2}(\epsilon_{\mu\varrho}\epsilon_{\nu\lambda} - \epsilon_{\mu\nu}\epsilon_{\lambda\varrho})\gamma^{\mu\nu}\gamma^{\lambda\varrho} + O(\kappa^3), \qquad \ldots\ldots(19)$$

and

$$\begin{aligned} g^{\mu\nu} &= (-g)^{-1/2}\mathfrak{g}^{\mu\nu} \\ &= \epsilon^{\mu\nu} - \kappa\gamma^{\mu\nu} + \tfrac{1}{2}\kappa\epsilon^{\mu\nu}\epsilon_{\alpha\beta}\gamma^{\alpha\beta} - \tfrac{1}{2}\kappa^2\epsilon_{\alpha\beta}\gamma^{\alpha\beta}\gamma^{\mu\nu} \\ &\quad + \tfrac{1}{4}\kappa^2\epsilon^{\mu\nu}\epsilon_{\alpha\varrho}\epsilon_{\beta\lambda}\gamma^{\alpha\beta}\gamma^{\lambda\varrho} + \tfrac{1}{8}\kappa^2\epsilon^{\mu\nu}\epsilon_{\alpha\beta}\epsilon_{\lambda\varrho}\gamma^{\alpha\beta}\gamma^{\lambda\varrho} + O(\kappa^3), \end{aligned} \qquad \ldots\ldots(20)$$

where the tensor $\epsilon_{\mu\nu}$ is reciprocal to $\epsilon^{\mu\nu}$. In order to obtain the expansion for $g_{\mu\nu}$ we note that

$$g_{\mu\nu} = \frac{\text{minor}(g^{\mu\nu})}{|g^{\mu\nu}|} = -(-g)^{-1/2}\,\text{minor}\,(\mathfrak{g}^{\mu\nu}). \qquad \ldots\ldots(21)$$

But we easily find that

$$\begin{aligned} \text{minor}\,(\mathfrak{g}^{\mu\nu}) &= -\epsilon_{\mu\nu} + \kappa\epsilon_{\mu\nu}\epsilon_{\alpha\beta}\gamma^{\alpha\beta} - \kappa\epsilon_{\mu\alpha}\epsilon_{\nu\beta}\gamma^{\alpha\beta} \\ &\quad - \kappa^2\epsilon_{\alpha\mu}\epsilon_{\lambda\nu}\epsilon_{\beta\varrho}\gamma^{\alpha\beta}\gamma^{\lambda\varrho} + \kappa^2\epsilon_{\alpha\mu}\epsilon_{\beta\nu}\epsilon_{\lambda\varrho}\gamma^{\alpha\beta}\gamma^{\lambda\varrho} \\ &\quad - \tfrac{1}{2}\kappa^2\epsilon_{\mu\nu}\epsilon_{\alpha\beta}\epsilon_{\lambda\varrho}\gamma^{\alpha\beta}\gamma^{\lambda\varrho} + \tfrac{1}{2}\kappa^2\epsilon_{\mu\nu}\epsilon_{\alpha\lambda}\epsilon_{\beta\varrho}\gamma^{\alpha\beta}\gamma^{\lambda\varrho} + O(\kappa^3). \end{aligned} \qquad \ldots\ldots(22)$$

Hence we get

$$\begin{aligned} g_{\mu\nu} &= \epsilon_{\mu\nu} - \tfrac{1}{2}\kappa\epsilon_{\mu\nu}\epsilon_{\alpha\beta}\gamma^{\alpha\beta} + \kappa\epsilon_{\mu\alpha}\epsilon_{\nu\beta}\gamma^{\alpha\beta} \\ &\quad + \kappa^2\epsilon_{\alpha\mu}\epsilon_{\lambda\nu}\epsilon_{\beta\varrho}\gamma^{\alpha\beta}\gamma^{\lambda\varrho} - \tfrac{1}{2}\kappa^2\epsilon_{\alpha\mu}\epsilon_{\beta\nu}\epsilon_{\lambda\varrho}\gamma^{\alpha\beta}\gamma^{\lambda\varrho} \\ &\quad + \tfrac{1}{8}\kappa^2\epsilon_{\mu\nu}\epsilon_{\alpha\beta}\epsilon_{\lambda\varrho}\gamma^{\alpha\beta}\gamma^{\lambda\varrho} - \tfrac{1}{4}\kappa^2\epsilon_{\mu\nu}\epsilon_{\alpha\lambda}\epsilon_{\beta\varrho}\gamma^{\alpha\beta}\gamma^{\lambda\varrho} + O(\kappa^3). \end{aligned} \qquad \ldots\ldots(23)$$

Now, in order to expand the Lagrangian density (2), we use the relation

$$\left\{ {\alpha \atop \mu\nu} \right\} = \tfrac{1}{2}g^{\alpha\lambda}\left(\frac{\partial g_{\mu\lambda}}{\partial x^{\nu}} + \frac{\partial g_{\nu\lambda}}{\partial x^{\mu}} - \frac{\partial g_{\mu\nu}}{\partial x^{\lambda}}\right), \qquad \ldots\ldots(24)$$

and get, after some simplification,

$$\begin{aligned} \mathfrak{L} = -\frac{1}{4\kappa^2}\mathfrak{g}^{\mu\nu}g^{\alpha\lambda}g^{\beta\varrho}\Big[& 2\frac{\partial g_{\mu\lambda}}{\partial x^{\beta}}\frac{\partial g_{\nu\varrho}}{\partial x^{\alpha}} - 2\frac{\partial g_{\mu\nu}}{\partial x^{\alpha}}\frac{\partial g_{\varrho\lambda}}{\partial x^{\beta}} \\ & - \frac{\partial g_{\beta\lambda}}{\partial x^{\mu}}\frac{\partial g_{\alpha\varrho}}{\partial x^{\nu}} + \frac{\partial g_{\beta\varrho}}{\partial x^{\mu}}\frac{\partial g_{\alpha\lambda}}{\partial x^{\nu}}\Big]. \end{aligned} \qquad \ldots\ldots(25)$$

Using the expansions (17), (20) and (23), we find

$$\mathfrak{L} = -\frac{1}{4}\Big[2\epsilon_{\alpha\beta}\frac{\partial\gamma^{\beta\mu}}{\partial x^{\nu}}\frac{\partial\gamma^{\alpha\nu}}{\partial x^{\mu}} - \epsilon^{\mu\nu}\epsilon_{\varrho\alpha}\epsilon_{\lambda\beta}\frac{\partial\gamma^{\lambda\alpha}}{\partial x^{\nu}}\frac{\partial\gamma^{\varrho\beta}}{\partial x^{\mu}} + \tfrac{1}{2}\epsilon^{\mu\nu}\epsilon_{\lambda\varrho}\epsilon_{\alpha\beta}\frac{\partial\gamma^{\lambda\varrho}}{\partial x^{\mu}}\frac{\partial\gamma^{\alpha\beta}}{\partial x^{\nu}}$$

$$+\kappa\epsilon_{\varrho\alpha}\epsilon_{\lambda\beta}\gamma^{\mu\nu}\frac{\partial\gamma^{\lambda\alpha}}{\partial x^{\nu}}\frac{\partial\gamma^{\varrho\beta}}{\partial x^{\mu}} - \tfrac{1}{2}\kappa\epsilon_{\lambda\varrho}\epsilon_{\alpha\beta}\gamma^{\mu\nu}\frac{\partial\gamma^{\lambda\varrho}}{\partial x^{\mu}}\frac{\partial\gamma^{\alpha\beta}}{\partial x^{\nu}} + 2\kappa\epsilon_{\alpha\lambda}\epsilon_{\beta\varrho}\gamma^{\alpha\beta}\frac{\partial\gamma^{\lambda\mu}}{\partial x^{\nu}}\frac{\partial\gamma^{\varrho\nu}}{\partial x^{\mu}}$$

$$+\kappa\epsilon^{\mu\nu}\epsilon_{\alpha\beta}\epsilon_{\sigma\lambda}\epsilon_{\eta\varrho}\gamma^{\lambda\varrho}\frac{\partial\gamma^{\alpha\beta}}{\partial x^{\mu}}\frac{\partial\gamma^{\sigma\eta}}{\partial x^{\nu}} - 2\kappa\epsilon^{\mu\nu}\epsilon_{\varrho\eta}\epsilon_{\alpha\lambda}\epsilon_{\beta\sigma}\gamma^{\alpha\beta}\frac{\partial\gamma^{\lambda\eta}}{\partial x^{\nu}}\frac{\partial\gamma^{\sigma\varrho}}{\partial x^{\mu}} + O(\kappa^2)\Big]. \quad ..(26)$$

According to (1) and (17) the supplementary conditions will now be given by

$$\partial\gamma^{\mu\nu}/\partial x^{\nu} = 0, \qquad ......(27)$$

which enables us to simplify (26). For, the first term in (26) may be written as

$$-\tfrac{1}{2}\epsilon_{\alpha\beta}\frac{\partial\gamma^{\beta\mu}}{\partial x^{\nu}}\frac{\partial\gamma^{\alpha\nu}}{\partial x^{\mu}} = -\frac{\partial}{\partial x^{\nu}}\left(\tfrac{1}{2}\epsilon_{\alpha\beta}\gamma^{\beta\mu}\frac{\partial\gamma^{\alpha\nu}}{\partial x^{\mu}}\right) + \tfrac{1}{2}\epsilon_{\alpha\beta}\gamma^{\beta\mu}\frac{\partial}{\partial x^{\mu}}\left(\frac{\partial\gamma^{\alpha\nu}}{\partial x^{\nu}}\right). \qquad ......(28)$$

Since the first term on the right-hand side of (28) is a divergence and the second term vanishes on account of (27), we can drop the first term in (26).

We can write the above results in a more compact form if we use the usual flat space notation, i.e. we allow the Greek indices to take the values 1, 2, 3, 4, instead of 1, 2, 3, 0, where $x_4 = ix_0$. Then it becomes unnecessary to introduce the Minkowskian metrical tensors $\epsilon^{\mu\nu}$ and $\epsilon_{\mu\nu}$, and all the indices may be written as lower indices. Thus, using the flat space notation and dropping the first term in (26), as explained above, we may write (26) and (27) as

$$\mathfrak{L} = -\frac{1}{4}\Big[\frac{\partial\gamma_{\mu\nu}}{\partial x_{\lambda}}\frac{\partial\gamma_{\mu\nu}}{\partial x_{\lambda}} - \frac{1}{2}\frac{\partial\gamma_{\alpha\alpha}}{\partial x_{\lambda}}\frac{\partial\gamma_{\beta\beta}}{\partial x_{\lambda}} + \kappa\gamma_{\mu\nu}\frac{\partial\gamma_{\alpha\beta}}{\partial x_{\mu}}\frac{\partial\gamma_{\alpha\beta}}{\partial x_{\nu}} - \frac{\kappa}{2}\gamma_{\mu\nu}\frac{\partial\gamma_{\alpha\alpha}}{\partial x_{\mu}}\frac{\partial\gamma_{\beta\beta}}{\partial x_{\nu}}$$

$$+2\kappa\gamma_{\mu\nu}\frac{\partial\gamma_{\mu\alpha}}{\partial x_{\beta}}\frac{\partial\gamma_{\nu\beta}}{\partial x_{\alpha}} + \kappa\gamma_{\mu\nu}\frac{\partial\gamma_{\beta\beta}}{\partial x_{\alpha}}\frac{\partial\gamma_{\mu\nu}}{\partial x_{\alpha}} - 2\kappa\gamma_{\mu\nu}\frac{\partial\gamma_{\mu\beta}}{\partial x_{\alpha}}\frac{\partial\gamma_{\nu\beta}}{\partial x_{\alpha}} + O(\kappa^2)\Big], \qquad ......(29)$$

$$\partial\gamma_{\mu\nu}/\partial x_{\nu} = 0. \qquad ......(30)$$

It may be noted that the terms independent of κ in (29) are identical with the Lagrangian density (I, 16).

§ 4. INTERACTION OF GRAVITATIONAL AND ELECTROMAGNETIC FIELDS

In order to show how to deal with the interaction of the gravitational field with other fields, we shall here consider the interaction of the gravitational and the electromagnetic fields.

In the presence of the gravitational field, the field equations for the electromagnetic field are given by (see Tolman 1934)

$$F_{\mu\nu} = \frac{\partial A_{\nu}}{\partial x^{\mu}} - \frac{\partial A_{\mu}}{\partial x^{\nu}}, \qquad F^{\mu\nu} = g^{\mu\lambda}g^{\nu\varrho}F_{\lambda\varrho}, \qquad ......(31)$$

$$\frac{\partial\mathfrak{F}^{\mu\nu}}{\partial x^{\nu}} = -\mathfrak{J}^{\mu}, \qquad \frac{\partial\mathfrak{A}^{\mu}}{\partial x^{\mu}} = 0, \qquad ......(32)$$

where $\mathfrak{F}^{\mu\nu} = \sqrt{-g}\,F^{\mu\nu}, \quad \mathfrak{A}^{\mu} = \sqrt{-g}\,A^{\mu}, \quad \mathfrak{J}^{\mu} = \sqrt{-g}\,J^{\mu}. \qquad ......(33)$

The total Lagrangian density for the gravitational and the electromagnetic fields may be taken as

$$\mathfrak{L}_{\text{total}} = \mathfrak{L} + \mathfrak{L}_{\mathrm{R}}, \qquad ......(34)$$

where $\mathfrak{L}$ is given by (2), and

$$\mathfrak{L}_{\mathrm{R}} = -\tfrac{1}{4}\sqrt{-g}\,F^{\mu\nu}F_{\mu\nu} = -\tfrac{1}{4}\sqrt{-g}\,g^{\mu\lambda}g^{\nu\varrho}F_{\lambda\varrho}F_{\mu\nu}. \qquad \ldots\ldots(35)$$

Now we have

$$\begin{aligned} A_{\nu} &= (-g)^{-1/2}g_{\nu\sigma}\mathfrak{A}^{\sigma} \\ &= \epsilon_{\nu\sigma}\mathfrak{A}^{\sigma} + \kappa\epsilon_{\sigma\alpha}\epsilon_{\nu\beta}\gamma^{\alpha\beta}\mathfrak{A}^{\sigma} + \mathrm{O}(\kappa^2), \qquad \ldots\ldots(36) \end{aligned}$$

so that

$$\begin{aligned} F_{\mu\nu} = \epsilon_{\nu\sigma}\frac{\partial\mathfrak{A}^{\sigma}}{\partial x^{\mu}} - \epsilon_{\mu\sigma}\frac{\partial\mathfrak{A}^{\sigma}}{\partial x^{\nu}} &+ \kappa\epsilon_{\sigma\alpha}\epsilon_{\nu\beta}\frac{\partial}{\partial x^{\mu}}(\gamma^{\alpha\beta}\mathfrak{A}^{\sigma}) \\ &- \kappa\epsilon_{\sigma\alpha}\epsilon_{\mu\beta}\frac{\partial}{\partial x^{\nu}}(\gamma^{\alpha\beta}\mathfrak{A}^{\sigma}) + \mathrm{O}(\kappa^2). \qquad \ldots\ldots(37) \end{aligned}$$

Using (17), (20) and (37), we may expand (35) as

$$\begin{aligned} \mathfrak{L}_{\mathrm{R}} = -\tfrac{1}{4}&(\epsilon^{\lambda\mu}\epsilon^{\varrho\nu} - \kappa\epsilon^{\lambda\mu}\gamma^{\varrho\nu} - \kappa\epsilon^{\varrho\nu}\gamma^{\lambda\mu} + \tfrac{1}{2}\kappa\epsilon^{\lambda\mu}\epsilon^{\varrho\nu}\epsilon_{\alpha\beta}\gamma^{\alpha\beta}) \\ &\times\left(\frac{\partial\mathfrak{A}^{\alpha}}{\partial x^{\mu}}\epsilon_{\alpha\nu} - \frac{\partial\mathfrak{A}^{\alpha}}{\partial x^{\nu}}\epsilon_{\alpha\mu}\right)\left(\frac{\partial\mathfrak{A}^{\beta}}{\partial x^{\lambda}}\epsilon_{\beta\varrho} - \frac{\partial\mathfrak{A}^{\beta}}{\partial x^{\varrho}}\epsilon_{\beta\lambda}\right) \\ &+ \left[\kappa\frac{\partial\mathfrak{A}^{\alpha}}{\partial x^{\mu}}\frac{\partial}{\partial x^{\alpha}}(\mathfrak{A}^{\beta}\gamma^{\mu\nu})\epsilon_{\beta\nu} - \kappa\frac{\partial\mathfrak{A}^{\alpha}}{\partial x^{\mu}}\frac{\partial}{\partial x^{\nu}}(\mathfrak{A}^{\beta}\gamma^{\lambda\varrho})\epsilon^{\mu\nu}\epsilon_{\beta\varrho}\epsilon_{\alpha\lambda}\right] + \mathrm{O}(\kappa^2). \quad \ldots(38) \end{aligned}$$

The terms within the square brackets in (38) may be written as

$$-\kappa\frac{\partial}{\partial x^{\mu}}\left(\frac{\partial\mathfrak{A}^{\alpha}}{\partial x^{\alpha}}\right)\mathfrak{A}^{\beta}\gamma^{\mu\nu}\epsilon_{\beta\nu} + \kappa\left(\epsilon^{\mu\nu}\frac{\partial^2\mathfrak{A}^{\alpha}}{\partial x^{\mu}\partial x^{\nu}}\right)\mathfrak{A}^{\beta}\gamma^{\lambda\varrho}\epsilon_{\beta\varrho}\epsilon_{\alpha\lambda} + \text{divergence terms.} \quad .(39)$$

The first term in (39) vanishes on account of the Lorentz condition $\partial\mathfrak{A}^{\alpha}/\partial x^{\alpha} = 0$, while the second term may be absorbed in $\mathrm{O}(\kappa^2)$, because $\epsilon^{\mu\nu}\partial^2\mathfrak{A}^{\alpha}/\partial x^{\mu}\partial x^{\nu} = \mathrm{O}(\kappa)$. Thus (38) may be reduced to the simpler form

$$\begin{aligned} \mathfrak{L}_{\mathrm{R}} = -\tfrac{1}{4}&(\epsilon^{\lambda\mu}\epsilon^{\varrho\nu} - \kappa\epsilon^{\lambda\mu}\gamma^{\varrho\nu} - \kappa\epsilon^{\varrho\nu}\gamma^{\lambda\mu} + \tfrac{1}{2}\kappa\epsilon^{\lambda\mu}\epsilon^{\varrho\nu}\epsilon_{\alpha\beta}\gamma^{\alpha\beta}) \\ &\left(\frac{\partial\mathfrak{A}^{\alpha}}{\partial x^{\mu}}\epsilon_{\alpha\nu} - \frac{\partial\mathfrak{A}^{\alpha}}{\partial x^{\nu}}\epsilon_{\alpha\mu}\right)\left(\frac{\partial\mathfrak{A}^{\beta}}{\partial x^{\lambda}}\epsilon_{\beta\varrho} - \frac{\partial\mathfrak{A}^{\beta}}{\partial x^{\varrho}}\epsilon_{\beta\lambda}\right) + \mathrm{O}(\kappa^2). \qquad \ldots\ldots(40) \end{aligned}$$

Using the flat space notation, as we have done in the last section, we may write (40) as

$$\mathfrak{L}_{\mathrm{R}} = -\tfrac{1}{4}F_{\mu\nu}F_{\mu\nu} - \tfrac{1}{2}\kappa\gamma_{\alpha\beta}(F_{\alpha\mu}F_{\beta\mu} - \tfrac{1}{4}\delta_{\alpha\beta}F_{\mu\nu}{}^2) + \mathrm{O}(\kappa^2), \qquad \ldots\ldots(41)$$

where, according to our flat space notation, $F_{\mu\nu} = \partial\mathfrak{A}_{\nu}/\partial x_{\mu} - \partial\mathfrak{A}_{\mu}/\partial x_{\nu}$. We notice that the first order interaction term in (41) is given by $-\tfrac{1}{2}\kappa\gamma_{\mu\nu}T_{\mu\nu}$, where $T_{\mu\nu}$ is the usual flat space energy-momentum tensor of the electromagnetic field. This result agrees with (I, 54) when we take into account the fact that the trace of $T_{\mu\nu}$ vanishes.

§ 5. QUANTIZATION OF THE COMPLETE GRAVITATIONAL FIELD

As already explained we may regard the linear part of the gravitational field as the 'free' gravitational field, while the non-linear terms may be treated as a direct interaction between the gravitons. Thus, by putting $\kappa = 0$ in (29) we obtain the Lagrangian density for the free gravitational field, which is precisely the same as that given by (I, 16). It follows that the entire treatment of quantization described in I still holds for the free gravitational field. Among other results we can still use the vacuum conditions (I, 40), the commutation relations (I, 23) and (I, 24), and the vacuum expectation values (I, 58).

For the treatment of the complete gravitational field we have to use the complete Lagrangian density (29). Then we can pass over to the interaction representation in the usual way by treating the linear part as the uncoupled gravitational field and the non-linear part as the interaction. In the interaction representation we can again make use of the commutation relations (I, 23) and (I, 24) and the vacuum expectation values (I, 58). Similarly, we can deal with the interaction of the gravitational and the electromagnetic fields by adding the Lagrangian density (41) to (29) and treating all the non-linear terms as interaction.

It may also be noted that the supplementary conditions for the complete gravitational field in the Heisenberg representation are still given by (I, 56). For, according to the field equations (14), $\partial\gamma_{\mu\nu}/\partial x_\nu$ always satisfies the wave equation for plane waves

$$\Box^2 \frac{\partial\gamma_{\mu\nu}}{\partial x_\nu} = \kappa \frac{\partial\Theta_{\mu\nu}}{\partial x_\nu} = 0.$$

Therefore $\partial\gamma_{\mu\nu}/\partial x_\nu$ can always be split into the positive and the negative frequency parts, and the supplementary conditions (I, 56) are maintained in course of time. In the interaction representation the supplementary conditions can be obtained in the usual way.

We conclude this investigation with some applications of the present method of quantizing the gravitational field. We have seen that according to the above method it is possible to treat the complete gravitational field up to any desired order of approximation. However, for simplicity we shall use only the linear approximation of the gravitational field in the applications to be discussed in the following two sections. A more complete account of the applications of the present treatment will be given in a separate paper, where the influence of the non-linear terms will also be taken into consideration.

§ 6. SELF-ENERGY OF THE PHOTON

We shall first consider the problem of the gravitational self-energy of the photon, because the corresponding problem in quantum electrodynamics has attracted much attention. As already remarked, for simplicity we shall here use only the linear approximation of the gravitational field.

According to (I, 54) or (41), the Lagrangian density for an electromagnetic field interacting with the linear gravitational field is given by

$$L = -\tfrac{1}{4}F_{\mu\nu}{}^2 - \frac{1}{2}\left(\frac{\partial A_\mu}{\partial x_\mu}\right)^2 - \frac{1}{4}\left(\frac{\partial\gamma_{\mu\nu}}{\partial x_\lambda}\frac{\partial\gamma_{\mu\nu}}{\partial x_\lambda} - \frac{1}{2}\frac{\partial\gamma}{\partial x_\lambda}\frac{\partial\gamma}{\partial x_\lambda}\right) - \tfrac{1}{2}\kappa\gamma_{\alpha\beta}(F_{\alpha\mu}F_{\beta\mu} - \tfrac{1}{4}\delta_{\alpha\beta}F_{\mu\nu}{}^2). \qquad \ldots\ldots(42)$$

Denoting the canonical conjugates of $\gamma_{\mu\nu}$, γ and A_μ by $\pi_{\mu\nu}$, π and π_μ respectively, we have

$$\pi_{\mu\nu} = \frac{1}{2}\frac{\partial\gamma_{\mu\nu}}{\partial t}, \qquad \pi = -\frac{1}{4}\frac{\partial\gamma}{\partial t}, \qquad \ldots\ldots(43)$$

$$\left.\begin{aligned} \pi_i &= -iF_{i4} + i\kappa\gamma_{4j}F_{ji} - i\kappa\gamma_{ij}F_{j4} + \tfrac{1}{2}i\kappa(\gamma_{\alpha\alpha} - 2\gamma_{44})F_{i4}, \\ \pi_4 &= i\partial A_\nu/\partial x_\nu. \end{aligned}\right\} \qquad \ldots\ldots(44)$$

Obtaining the Hamiltonian density from (42) in the usual way, and expressing it in terms of the field variables, their space derivatives and the canonical conjugates, we get $H = H_G + H_R + H_{int}$, where H_G and H_R are the Hamiltonian densities for the gravitational and the radiation fields respectively, and H_{int} is the interaction energy density given by

$$\begin{aligned} H_{\text{int}} = & -\tfrac{1}{8}\kappa\gamma_{\alpha\alpha}F_{ij}^2+\tfrac{1}{2}\kappa\gamma_{jk}F_{ij}F_{ik}-i\kappa\gamma_{4j}\pi_i F_{ji} \\ & +\tfrac{1}{4}\kappa(\gamma_{\alpha\alpha}-2\gamma_{44})\pi_i^2-\tfrac{1}{2}\kappa\gamma_{ki}\pi_i\pi_k+\tfrac{1}{8}\kappa^2(\gamma_{\alpha\alpha}-2\gamma_{44})^2\pi_i^2 \\ & -\tfrac{1}{2}\kappa^2\gamma_{ij}(\gamma_{\alpha\alpha}-2\gamma_{44})\pi_i\pi_j+\tfrac{1}{2}\kappa^2\gamma_{ij}\gamma_{ki}\pi_k\pi_j-\tfrac{1}{2}i\kappa^2\gamma_{4j}(\gamma_{\alpha\alpha}-2\gamma_{44})\pi_i F_{ji} \\ & +i\kappa^2\gamma_{4j}\gamma_{ki}\pi_k F_{ji}-\tfrac{1}{2}\kappa^2\gamma_{4j}\gamma_{4k}F_{ji}F_{ki}+O(\kappa^3). \qquad \ldots\ldots(45) \end{aligned}$$

The above equation gives the interaction energy density in the Heisenberg representation. In the interaction representation the interaction energy density will have the same form as (45), but with the difference that now the field variables and their canonical conjugates will refer to free fields. Thus, passing over to the interaction representation and expressing the canonical conjugates in terms of the field variables, we get*

$$\begin{aligned} H_{\text{int}} = & \tfrac{1}{2}\kappa\gamma_{\alpha\beta}(F_{\alpha\mu}F_{\beta\mu}-\tfrac{1}{4}\delta_{\alpha\beta}F_{\mu\nu}^2) \\ & -\tfrac{1}{8}\kappa^2\gamma_{\alpha\alpha}\gamma_{\beta\beta}F_{4\nu}F_{4\nu}-\tfrac{1}{2}\kappa^2\gamma_{\alpha\nu}\gamma_{\beta\nu}F_{4\alpha}F_{4\beta}+\tfrac{1}{2}\kappa^2\gamma_{\alpha\nu}\gamma_{\beta\beta}F_{4\alpha}F_{4\nu} \\ & -\tfrac{1}{2}\kappa^2\gamma_{\alpha 4}\gamma_{\beta 4}F_{\mu\alpha}F_{\mu\beta}+\tfrac{1}{2}\kappa^2\gamma_{\alpha 4}\gamma_{\beta\beta}F_{\mu\alpha}F_{\mu 4}+\kappa^2\gamma_{\alpha\mu}\gamma_{\beta 4}F_{4\alpha}F_{\mu\beta}+O(\kappa^3). \qquad \ldots\ldots(46) \end{aligned}$$

Now according to Dyson (1949) the *S*-matrix for the interaction of the gravitons and the photons will be given by

$$S=1+(-i)\int_{-\infty}^{\infty}dx\,H_{\text{int}}(x)+\tfrac{1}{2}(-i)^2\int_{-\infty}^{\infty}dx'\int_{-\infty}^{\infty}dx'\,P\{H_{\text{int}}(x),H_{\text{int}}(x')\}+\ldots \qquad \ldots\ldots(47)$$

The terms in the *S*-matrix contributing to the second-order self-energy of the photon are

$$S_{\text{photon}}=-i\int_{-\infty}^{\infty}dx\,H_2(x)-\tfrac{1}{2}\int_{-\infty}^{\infty}dx\int_{-\infty}^{\infty}dx'\,P\{H_1(x),H_1(x')\} \qquad \ldots\ldots(48)$$

where H_1 and H_2 denote the terms involving the first and the second powers of κ in (46). In order to evaluate the *P*-bracket in (48) we have to find the vacuum expectation values of *P*-brackets containing a pair of $\gamma_{\mu\nu}$'s or a pair of $F_{\mu\nu}$'s. It follows from (I, 23) and (I, 58) that

$$\langle P(\gamma_{\mu\nu}(x),\gamma_{\lambda\varrho}(x'))\rangle_0=\tfrac{1}{2}(\delta_{\mu\lambda}\delta_{\nu\varrho}+\delta_{\mu\varrho}\delta_{\nu\lambda})D_F'(x-x'), \qquad \ldots\ldots(49)$$

where $D_F'(x-x')$ is Feynman's singular function for the gravitational field. Also, we have for the radiation field

$$\begin{aligned} \left\langle P\left(\frac{\partial A_\nu(x)}{\partial x_\mu},\frac{\partial A_\varrho(x')}{\partial x'_\lambda}\right)\right\rangle_0 &= \frac{\partial^2}{\partial x_\mu\partial x'_\lambda}\langle P(A_\nu(x),A_\varrho(x'))\rangle_0+i\delta_{\nu\varrho}\delta_{\mu 4}\delta_{\lambda 4}\delta(x-x') \\ &= \tfrac{1}{2}\delta_{\nu\varrho}\frac{\partial^2 D_F(x-x')}{\partial x_\mu\partial x'_\lambda}+i\delta_{\nu\varrho}\delta_{\mu 4}\delta_{\lambda 4}\delta(x-x'), \end{aligned}$$

which gives

$$\begin{aligned} \langle P(F_{\mu\nu}(x),F_{\lambda\varrho}(x'))\rangle_0 = & \tfrac{1}{2}\delta_{\nu\varrho}\frac{\partial^2 D_F(x-x')}{\partial x_\mu\partial x'_\lambda}+\tfrac{1}{2}\delta_{\mu\lambda}\frac{\partial^2 D_F(x-x')}{\partial x_\nu\partial x'_\varrho} \\ & -\tfrac{1}{2}\delta_{\nu\lambda}\frac{\partial^2 D_F(x-x')}{\partial x_\mu\partial x'_\varrho}-\tfrac{1}{2}\delta_{\mu\varrho}\frac{\partial^2 D_F(x-x')}{\partial x_\nu\partial x'_\lambda} \\ & +i\delta_{\nu\varrho}\delta_{\mu 4}\delta_{\lambda 4}\delta(x-x')+i\delta_{\mu\lambda}\delta_{\nu 4}\delta_{\varrho 4}\delta(x-x') \\ & -i\delta_{\nu\lambda}\delta_{\mu 4}\delta_{\varrho 4}\delta(x-x')-i\delta_{\mu\varrho}\delta_{\nu 4}\delta_{\lambda 4}\delta(x-x'). \qquad \ldots\ldots(50) \end{aligned}$$

---

* It should be remembered that for simplicity we are using the same symbols for the corresponding quantities in the Heisenberg and the interaction representations.

It can now be easily verified that the terms involving the δ-function in (50) give rise to a contribution (48) which exactly cancels the contribution of H_2. In fact it is well known that such a cancellation always occurs. Thus, instead of (48) we may take

$$S_{\text{photon}} = -\tfrac{1}{2}\int_{-\infty}^{\infty} dx \int_{-\infty}^{\infty} dx'\, P\{H_1(x),\, H_1(x')\}, \qquad \ldots\ldots(51)$$

provided we also take effectively

$$\langle P(F_{\mu\nu}(x),\, F_{\lambda\varrho}(x'))\rangle_0 = \tfrac{1}{2}\left(\delta_{\nu\varrho}\frac{\partial^2 D_{\mathrm{F}}(x-x')}{\partial x_\mu \partial x'_\lambda} + \delta_{\mu\lambda}\frac{\partial^2 D_{\mathrm{F}}(x-x')}{\partial x_\nu \partial x'_\varrho} - \delta_{\nu\lambda}\frac{\partial^2 D_{\mathrm{F}}(x-x')}{\partial x_\mu \partial x'_\varrho} - \delta_{\mu\varrho}\frac{\partial^2 D_{\mathrm{F}}(x-x')}{\partial x_\nu \partial x'_\lambda}\right). \qquad \ldots\ldots(52)$$

Substituting the value of H_1 from (46) in (51), we get

$$S_{\text{photon}} = -\tfrac{1}{8}\kappa^2 \int_{-\infty}^{\infty} dx \int_{-\infty}^{\infty} dx'\, P\{(\gamma_{\alpha\nu}(x)F_{\mu\alpha}(x)F_{\mu\nu}(x) - \tfrac{1}{4}\gamma_{\alpha\alpha}(x)F_{\mu\nu}(x)F_{\mu\nu}(x)),\ (\gamma_{\beta\varrho}(x')F_{\lambda\beta}(x')F_{\lambda\varrho}(x') - \tfrac{1}{4}\gamma_{\beta\beta}(x')F_{\lambda\varrho}(x')F_{\lambda\varrho}(x'))\}. \qquad \ldots\ldots(53)$$

Extracting the photon self-energy contribution from (53), we get, after some simplification,

$$S_{\text{photon}} = -\tfrac{1}{4}\kappa^2 \int_{-\infty}^{\infty} dx \int_{-\infty}^{\infty} dx'\, F_{\mu\lambda}(x)\left(\frac{\partial^2 D_{\mathrm{F}}(x-x')}{\partial x_\mu \partial x'_\nu} + \tfrac{1}{2}\delta_{\mu\nu}\frac{\partial^2 D_{\mathrm{F}}(x-x')}{\partial x_\alpha \partial x'_\alpha}\right) \times D'_{\mathrm{F}}(x-x')F_{\nu\lambda}(x'). \qquad \ldots\ldots(54)$$

We now pass over to the momentum-energy representation by putting

$$F_{\nu\lambda}(x') = F_{\nu\lambda}(p)\exp(ipx')$$

$$D_{\mathrm{F}}(x-x') = \frac{-2i}{(2\pi)^4}\int dk(k^2+\lambda^2)^{-1}\exp\{ik(x-x')\}$$

$$D'_{\mathrm{F}}(x-x') = \frac{-2i}{(2\pi)^4}\int dk'(k'^2+\rho^2)^{-1}\exp\{ik'(x-x')\}$$

where, following Feynman (1949), the photons and the gravitons have been assumed to have small masses λ and ρ respectively, which have to be put equal to zero ultimately. Then, we get

$$S_{\text{photon}} = \frac{\kappa^2}{(2\pi)^4}\int_{-\infty}^{\infty} dx\, F_{\mu\lambda}(x)F_{\nu\lambda}(p)\, e^{ipx}\int dk\,\frac{k_\mu k_\nu + \tfrac{1}{2}\delta_{\mu\nu}k_\alpha{}^2}{(k^2+\lambda^2)[(k-p)^2+\rho^2]}$$

$$= -i\int_{-\infty}^{\infty} dx\, F_{\mu\lambda}(x)F_{\nu\lambda}(p)\, e^{ipx}\, J_{\mu\nu}(p), \qquad \ldots\ldots(55)$$

where

$$J_{\mu\nu}(p) = \frac{i\kappa^2}{(2\pi)^4}\int dk\,\frac{k_\mu k_\nu + \tfrac{1}{2}\delta_{\mu\nu}k_\alpha{}^2}{(k^2+\lambda^2)[(k-p)^2+\rho^2]}. \qquad \ldots\ldots(56)$$

Since the photon self-energy density W_{photon} is connected with S_{photon} by the relation

$$S_{\text{photon}} = -i\int_{-\infty}^{\infty} dx\, W_{\text{photon}},$$

eqn. (55) shows that W_{photon} involves only the electromagnetic field strengths. It follows that our result is gauge-invariant, and therefore the photon self-energy vanishes unambiguously. This situation is much simpler than the corresponding situation in quantum electrodynamics, where the photon self-energy is found to be ambiguous.

Though we have seen that the self-energy of a free photon vanishes, it will be interesting to see what divergencies are involved in an internal photon self-energy 'graph'. For this we have to evaluate the integral (56), which may be easily carried out by regularization and using familiar devices of integration. Thus we find

$$J_{\mu\nu}(p) = -\frac{\kappa^2}{16\pi^2}\int_0^1 dx\,[\tfrac{3}{2}\delta_{\mu\nu}\{2x\xi^2 \log 2 - \Delta \log(x\xi^2) + \Delta \log(2\Delta) - \Delta\}$$
$$+ x^2(p_\mu p_\nu + \tfrac{1}{2}\delta_{\mu\nu}p^2)\{\log(x\xi^2) - \log(2\Delta)\}], \qquad \ldots\ldots(57)$$

where $\Delta = x(p^2+\rho^2) + (1-x)\lambda^2 - p^2x^2$, and the parameter ξ, which has the dimensions of mass, tends to infinity. We may write (57) as

$$J_{\mu\nu}(p) = -\frac{3\kappa^2}{32\pi^2}\log 2\,\delta_{\mu\nu}\xi^2 - \frac{\kappa^2}{24\pi^2}(p_\mu p_\nu - \tfrac{1}{4}\delta_{\mu\nu}p^2)\log \xi + \text{finite terms.} \qquad \ldots\ldots(58)$$

The quadratically divergent term in (58) may be absorbed by a renormalization of the electromagnetic field strengths (Gupta 1951), but the remaining logarithmically divergent term remains a source of difficulty.

§7. SELF-ENERGY OF THE ELECTRON

According to (I, 54), the Lagrangian density for the electron field interacting with the linear gravitational field is given by

$$L = -\frac{1}{2}\left(\bar{\psi}\gamma_\mu\frac{\partial\psi}{\partial x_\mu} - \frac{\partial\bar{\psi}}{\partial x_\mu}\gamma_\mu\psi + 2m\bar{\psi}\psi\right) - \frac{1}{4}\left(\frac{\partial\gamma_{\mu\nu}}{\partial x_\lambda}\frac{\partial\gamma_{\mu\nu}}{\partial x_\lambda} - \frac{1}{2}\frac{\partial\gamma}{\partial x_\lambda}\frac{\partial\gamma}{\partial x_\lambda}\right)$$
$$-\tfrac{1}{8}\kappa(\gamma_{\mu\nu} - \tfrac{1}{2}\delta_{\mu\nu}\gamma)\left\{\left(\bar{\psi}\gamma_\mu\frac{\partial\psi}{\partial x_\nu} - \frac{\partial\bar{\psi}}{\partial x_\nu}\gamma_\mu\psi\right) + \left(\bar{\psi}\gamma_\nu\frac{\partial\psi}{\partial x_\mu} - \frac{\partial\bar{\psi}}{\partial x_\mu}\gamma_\nu\psi\right)\right\}.$$
$$\ldots\ldots(59)$$

As in the case of the electromagnetic field, we may take the interaction energy density in the interaction representation as

$$H(x) = \tfrac{1}{8}\kappa(\gamma_{\mu\nu} - \tfrac{1}{2}\delta_{\mu\nu}\gamma)\left\{\left(\bar{\psi}\gamma_\mu\frac{\partial\psi}{\partial x_\nu} - \frac{\partial\bar{\psi}}{\partial x_\nu}\gamma_\mu\psi\right) + \left(\bar{\psi}\gamma_\nu\frac{\partial\psi}{\partial x_\mu} - \frac{\partial\bar{\psi}}{\partial x_\mu}\gamma_\nu\psi\right)\right\}, \qquad \ldots\ldots(60)$$

provided we also take effectively

$$\epsilon(t,t')\left\langle P\left(\frac{\partial\psi(x)}{\partial x_\mu},\ \bar{\psi}(x')\right)\right\rangle_0 = \frac{\partial}{\partial x_\mu}[\epsilon(t,t')\langle P(\psi(x),\ \bar{\psi}(x'))\rangle_0]$$
$$\epsilon(t,t')\left\langle P\left(\frac{\partial\psi(x)}{\partial x_\mu},\ \frac{\partial\bar{\psi}(x')}{\partial x'_\nu}\right)\right\rangle_0 = \frac{\partial^2}{\partial x_\mu \partial x'_\nu}[\epsilon(t,t')\langle P(\psi(x),\ \bar{\psi}(x'))\rangle_0],$$

in addition to the usual result

$$\epsilon(t,t')\langle P(\psi(x),\ \bar{\psi}(x'))\rangle_0 = -\tfrac{1}{2}S_F(x-x'). \qquad \ldots\ldots(61)$$

It will also be convenient to put

$$\gamma_{\mu\nu} - \tfrac{1}{2}\delta_{\mu\nu}\gamma = h_{\mu\nu} \qquad \ldots\ldots(62)$$

and we easily find that

$$\langle P(h_{\mu\nu}(x),\ h_{\lambda\varrho}(x'))\rangle_0 = \tfrac{1}{2}(\delta_{\mu\lambda}\delta_{\nu\varrho} + \delta_{\mu\varrho}\delta_{\nu\lambda} - \delta_{\mu\nu}\delta_{\lambda\varrho})D'_F(x-x'). \qquad \ldots\ldots(63)$$

Using (62), and remembering that $h_{\mu\nu} = h_{\nu\mu}$, we may write (60) in the simpler form

$$H(x) = \tfrac{1}{4}\kappa h_{\mu\nu}\left(\bar{\psi}\gamma_\mu\frac{\partial\psi}{\partial x_\gamma} - \frac{\partial\bar{\psi}}{\partial x_\nu}\gamma_\mu\psi\right). \qquad \ldots\ldots(64)$$

Now the second-order contribution of the S-matrix for the interaction of electrons and gravitatons is given by

$$\begin{aligned} S &= -\tfrac{1}{2}\int_{-\infty}^{\infty} dx \int_{-\infty}^{\infty} dx' P\{H(x),\, H(x')\} \\ &= -\frac{\kappa^2}{32}\int_{-\infty}^{\infty} dx \int_{-\infty}^{\infty} dx' P\left\{h_{\mu\nu}(x)\left(\overline{\psi}(x)\gamma_\mu \frac{\partial\psi(x)}{\partial x_\nu} - \frac{\partial\overline{\psi}(x)}{\partial x_\nu}\gamma_\mu\psi(x)\right),\right. \\ &\qquad \left. h_{\lambda\varrho}(x')\left(\overline{\psi}(x')\gamma_\lambda \frac{\partial\psi(x')}{\partial x'_\varrho} - \frac{\partial\overline{\psi}(x')}{\partial x'_\varrho}\gamma_\lambda\psi(x')\right)\right\}. \end{aligned} \qquad \ldots\ldots(65)$$

Extracting the electron self-energy part from (65), we get

$$\begin{aligned} S_{\text{electron}} &= -\frac{\kappa^2}{64}\int_{-\infty}^{\infty} dx \int_{-\infty}^{\infty} dx' \,(\delta_{\mu\lambda}\delta_{\nu\varrho} + \delta_{\mu\varrho}\delta_{\nu\lambda} - \delta_{\mu\nu}\delta_{\lambda\varrho}) D'_{\mathrm{F}}(x-x') \\ &\quad \times \left[-\overline{\psi}(x)\gamma_\mu \frac{\partial}{\partial x_\nu} S_{\mathrm{F}}(x-x')\gamma_\lambda \frac{\partial\psi(x')}{\partial x'_\varrho} + \frac{\partial\overline{\psi}(x)}{\partial x_\nu}\gamma_\mu \frac{\partial}{\partial x_\varrho} S_{\mathrm{F}}(x-x')\gamma_\lambda\psi(x') \right. \\ &\quad \left. + \frac{\partial\overline{\psi}(x)}{\partial x_\nu}\gamma_\mu S_{\mathrm{F}}(x-x')\gamma_\lambda \frac{\partial\psi(x')}{\partial x'_\varrho} - \overline{\psi}(x)\gamma_\mu \frac{\partial^2}{\partial x_\nu \partial x_\varrho} S_{\mathrm{F}}(x-x')\gamma_\lambda\psi(x') \right]. \end{aligned} \qquad \ldots\ldots(66)$$

Putting

$$\psi(x') = \psi(p)\exp(ipx')$$

$$D'_{\mathrm{F}}(x-x') = \frac{-2i}{(2\pi)^4}\int dk' \,(k'^2+\rho^2)^{-1}\exp\{ik'(x-x')\}$$

$$S_{\mathrm{F}}(x-x') = \frac{-2i}{(2\pi)^4}\int dk \,\frac{ik\gamma - m}{k^2+m^2}\exp\{ik(x-x')\},$$

we find in the momentum energy representation

$$S_{\text{electron}} = -i\int_{-\infty}^{\infty} dx\, \overline{\psi}(x) I(p)\psi(p)\exp(ipx) \qquad \ldots\ldots(67)$$

where

$$\begin{aligned} I(p) &= -\frac{\kappa^2}{16(2\pi)^4}\int dk\,(\delta_{\mu\lambda}\delta_{\nu\varrho} + \delta_{\mu\varrho}\delta_{\nu\lambda} - \delta_{\mu\nu}\delta_{\lambda\varrho}) \\ &\quad \times \frac{\gamma_\mu(k_\nu k_\varrho + p_\varrho k_\nu + p_\nu k_\varrho + p_\nu p_\varrho)(k\gamma + im)\gamma_\lambda}{(k^2+m^2)[(k-p)^2+\rho^2]}. \end{aligned} \qquad \ldots\ldots(68)$$

Using familiar devices of integration with regularization, we find

$$\begin{aligned} I(p) &= \frac{\kappa^2}{128\pi^2}\int_0^1 dx \left[\{2im(1+x)^2p^2 - x(1+x)^2p^2(p\gamma)\} \right. \\ &\quad \times \left\{ \log\frac{\xi^2}{m^2} + \log\frac{3xm^2}{8} - \log\Lambda \right\} + \{4im - (1+3x)(p\gamma)\} \\ &\quad \left. \times \left\{ 3x\log\left(\tfrac{4}{3}\right)\xi^2 - \Lambda\left(\log\frac{\xi^2}{m^2} + \log\frac{3xm^2}{8} - \log\Lambda + 1 \right) \right\} \right], \end{aligned} \qquad \ldots\ldots(69)$$

where the parameter ξ, which is of the dimensions of mass, tends to infinity, and $\Lambda = (p^2+\rho^2)x + m^2(1-x) - x^2p^2$.

Since for the free electron

$$p^2 + m^2 = 0, \quad (ip\gamma + m)\psi(p) = 0, \qquad \ldots\ldots(70)$$

we obtain from (69)

$$I(p) = \frac{\kappa^2 m^3}{128\pi^2}\left(\frac{3}{2}\log\left(\frac{4}{3}\right)\frac{\xi^2}{m^2} - 4\log\frac{3\xi^2}{8m^2} - \frac{13}{3} \right), \qquad \ldots\ldots(71)$$

which is simply the gravitational self-mass of the electron.

In order to find all the divergencies in an internal electron self-energy graph we have to evaluate (69) without using (70). Then it is found that $I(p)$ is of the form

$$I(p) = A + B(ip\gamma + m) + C(ip\gamma + m)^2 + D(ip\gamma + m)^3 + \text{finite terms}, \qquad \ldots\ldots(72)$$

where A and B are quadratically divergent and C and D are logarithmically divergent. This situation is much worse than the corresponding situation in quantum electrodynamics, where the electron self-energy graph involves only two divergencies.

According to our investigation of the 'graphs' for the gravitational self-energies of the photon and the electron, the gravitational field involves many more divergencies besides those occurring in quantum electrodynamics. This suggests that it is not possible to remove all divergencies from the gravitational field by mass and charge renormalizations. However, it must be noted that in our calculations we have not taken into account the contributions of the non-linear terms to the self-energy graphs. In order to see whether the renormalization theory really breaks down for the gravitational field, it would be necessary to carry out more involved calculations by including the non-linear terms. This problem will be fully discussed in a subsequent paper.

ACKNOWLEDGMENT

I would like to thank Professor L. Rosenfeld for valuable comments.

REFERENCES

De Donder, T., 1921, *La Gravifique Einsteinienne* (Paris : Gauthiers-Villars).
Dyson, F. J., 1949, *Phys. Rev.*, **75**, 486.
Feynman, R. P., 1949, *Phys. Rev.*, **76**, 769.
Fock, V. A., 1939, *J. Phys. U.S.S.R.*, **1**, 81.
Gupta, S. N., 1951, *Proc. Phys. Soc.* A, **64**, 426 ; 1952, *Ibid.*, **65**, 161.
Papapetrou, A., 1948, *Proc. Roy. Irish Acad.* A, **52**, 11.
Tolman, R. C., 1930, *Phys. Rev.*, **35**, 875; 1934, *Relativity Thermodynamics and Cosmology* (Oxford : University Press), Chap. VIII.

A New Theory of Liquid Helium

By H. N. V. TEMPERLEY
King's College, Cambridge

MS. received 8*th February* 1952

ABSTRACT. A model of liquid helium is described, which incorporates the main features of the Landau (1941) and London (1939) theories, making use also of Mayer's concept of clusters. The ordinary process of liquefaction is associated with the formation of clusters in coordinate space, while the λ-transition is probably associated with the formation of small clusters in momentum space. The latter process is probably prevented, or greatly modified, in helium 3.

Possible reasons for the appearance of superfluid effects are given, and it is suggested that the unique properties of helium II may be traced to the fact that the interactions between two atoms is of about the strength needed to form a molecule.

§ 1. INTRODUCTION

In a previous paper (1952), referred to as I, a comparison was made between the two most successful theories of liquid helium II, usually known as the Landau (1941) and London (1939) theories. The following model incorporates some of the most successful features of the two theories, and was put forward in I as a natural synthesis of them. It was supposed that one might think of liquid helium II as a Debye lattice of helium atoms in statistical equilibrium with helium atoms in states of zero or small energy, and it was shown that such states would be appreciably occupied only below a certain transition temperature whereas, above this transition temperature, any such nearly free atoms would be immediately incorporated into the Debye lattice. The condition determining this transition temperature was found to be

$$(\partial S/\partial N)_{E,V}=0 \quad \text{or} \quad g=0 \qquad \ldots\ldots(1)$$

which, it was pointed out, is equivalent to the accepted criterion for Bose–Einstein condensation in a 'one-particle' type of assembly, but, in this form, could equally well be applied to a many-body assembly.

A discussion of this model showed that it was, in principle, capable of accounting for many of the observed features of liquid helium II, such as the occurrence of a sharp transition temperature, the appearance of a thick film, the fact that the velocity of second sound at low temperatures is given correctly by Landau's (1941) expression, the peculiar behaviour of the 'viscosity of the normal fluid' as a function of temperature and the successes of the phenomenological 'two-fluid' theory in describing second sound and pseudo-heat conduction. There is, however, one experimental fact that shows clearly that the above model is still too specialized. Equation (1) requires that the chemical potential of liquid helium II should be zero or positive, whereas the experimental evidence indicates quite clearly that g is negative and of the order of 10–15 calories per mole. Although this figure is small compared with either the attractive or zero-point energies, it is large compared with $N\boldsymbol{k}T$, and therefore cannot possibly be neglected.

In this paper we shall show that a generalization of the model developed in I is possible, and we now make use of the concept of 'clusters' due to Mayer and Mayer (1940). We shall suggest that the behaviour of liquid helium II can be interpreted in terms of statistical equilibrium between 'large' and 'small' clusters in momentum space, while the ordinary equilibrium between liquid and vapour is interpreted on the lines of Mayer and Mayer's original theory (1940), i.e. in terms of statistical equilibrium between 'large' and 'small' clusters in coordinate space. It will be suggested that the processes of clustering in momentum and coordinate space are of comparable importance in liquid helium II because the interaction energy between two helium atoms is approximately that required to form a bound state. If it were much larger than this, the assembly could probably be described in classical terms, the 'clustering' taking place in coordinate space, i.e. a net gain in energy results if atoms approach one another whereas, if it were much smaller than this, we should have a model resembling the perfect Bose–Einstein gas, the 'clustering' then taking place in momentum space. A 'cluster' in momentum space is to be thought of as a number of atoms having nearly the same momentum, in which case (Mott 1949) a gain in energy can result in certain circumstances. Price (1951) has deduced a very similar result, that a weak interaction can result in a 'potential well' in momentum space.

§2. MAYER'S CONCEPT OF A CLUSTER

If we consider, for the present, a purely classical assembly, in which the interactions are supposed to be between pairs of atoms only and to be independent of their velocities, it is well known that the process of averaging over momentum space can be performed at once, and the evaluation of the equilibrium properties of the assembly could then be carried out completely, if we could evaluate the 'configuration integral'

$$Q(T)=\int\dots\int\exp\left(-\frac{1}{\boldsymbol{k}T}\sum_{i\neq j}\epsilon_{ij}\right)d\tau_i\dots \qquad\dots\dots(2)$$

the integrations being taken over all possible values of the coordinates of all the atoms. Mayer and Mayer (1940) write this in the form

$$Q(T)=\int\dots\int\prod_{ij}(1+f_{ij})\dots d\tau_i\dots \qquad\dots\dots(3)$$

where $f_{ij}=\exp(-\epsilon_{ij}/\boldsymbol{k}T)-1$ which is appreciable only if ϵ_{ij} is significantly different from zero, which, in turn, implies that atoms i and j must be fairly near one another. Mayer proceeds by expanding the product occurring in (3) and attempting to estimate the relative importance of terms of various types, such as $1, f_{ij}, f_{ij}f_{jk}$ etc. after the integrations over the coordinates have been carried out. This product is expressed in terms of the 'cluster integrals' b_l defined as

$$b_l=\frac{1}{l!\,V}\int\dots\int\Sigma'\Pi f_{ij}f_{jk}\dots d\tau_i\dots$$

in which Σ' implies that the summation is to be restricted in the following ways

(*a*) $l\geqslant i>j>k\dots$

(*b*) Each of the terms f_{jk} is to have at least one suffix in common with some other term.

(*c*) Each of the l atoms is linked directly or indirectly with every other.

It is then a simply matter to show that

$$\frac{Q(T)}{N!}=\sum_{m_l}\prod_{l}\frac{(Vb_l)^{m_l}}{m_l!}, \qquad\dots\dots(4)$$

where possible values of m_l are restricted by the condition $\Sigma_l l m_l=N$.

By the familiar technique of searching for the value of m_l which, for each l, gives the maximum term in the sum (4), we may replace (4) by the equivalent result

$$\log\left(\frac{Q(T)}{N!}\right)\sim V\sum_{l}b_lZ^l-N\log Z, \qquad\dots\dots(5)$$

where Z is determined by $V\Sigma_l lb_lZ^l=N$. In these expressions, the method of constructing the cluster integral b_l implies that it is negligibly small unless every one of l molecules is near enough to at least one of the others for the interactions to be appreciable. Because of the nature of partition functions, the higher terms in (3) are a measure of the proportion of time a typical molecule spends in the neighbourhood of others, and the various terms in expression (4) measure the relative probabilities of the presence in the assembly of clusters of various sizes—a gas consisting mainly of single molecules ($l=1$)—while liquefaction occurs when the main contribution to (5) is given by $l\simeq N$, which implies that nearly every molecule is physically near to several others. Thus, all the equilibrium properties of the assembly are known if b_l is known as a function

.A
5
2

of l and T, though the relationship between the cluster integrals and other accepted means of describing an assembly, e.g. by means of a molecular distribution function, may be very complicated. The 'cluster' concept is a very valuable one, easily understood intuitively, but hard to define in precise terms. (It could be made precise for an interaction energy that vanished beyond a certain distance.)

In a quantum mechanical assembly, it is also possible to think of cluster formation in momentum space. Consider, for example, the well-known expression for the partition function of a perfect gas of atoms obeying Bose statistics

$$\log f = V\left(\frac{2\pi \boldsymbol{mk}T}{\boldsymbol{h}^2}\right)^{3/2} \sum_{S=1}^{\infty} \frac{\alpha^s}{s^{5/2}} - \log(1-\alpha), \qquad \text{......(6)}$$

with

$$N = V\left(\frac{2\pi \boldsymbol{mk}T}{\boldsymbol{h}^2}\right)^{3/2} \sum_{S=1}^{\infty} \frac{\alpha^s}{s^{3/2}} + \frac{\alpha}{1-\alpha}.$$

The resemblance of this expression to expressions such as (5) has already been remarked upon by Kahn and Uhlenbeck (1938) and by Mayer and Mayer (1940). Examination of the method of deriving (6) shows that the sth term in the first series is related to configurations in which there are s atoms in the same quantum state in just the same way that the term $b_l Z^l$ in (5) is related to clusters of size l. We find that, as long as the b_l are positive, the probable number of atoms in clusters of size l is proportional to $lb_l Z^l$ while the probable number of groups of s atoms in the same quantum state is proportional to $\alpha^s s^{-3/2}$.

The phenomenon of Bose–Einstein condensation of a perfect gas may be regarded as the simplest case of the formation of a cluster in momentum space, the occupation of the very lowest state, measured by the term $\alpha/(1-\alpha)$ in (6), becoming appreciable below the transition temperature. Mott (1949) has called attention to another process that might accentuate such cluster formation. He considers the gas of Bose atoms with small interactions, and, following a suggestion of Bijl, de Boer and Michels (1941), shows that the application of perturbation theory suggests that the formation of clusters in momentum space, i.e. the multiple occupation of one quantum state, is energetically favourable provided that the interaction between two atoms is *not* great enough to form a molecule. A similar point has very recently been made by Price (1951) but his method fails to give any information if the interactions *are* greater than this. Very recently an attempt has been made (Matsubara 1951) to express the Slater 'sum over states' (for a quantum assembly with interactions between the atoms) in a form similar to (5). However, this can only be done at present by neglecting the lack of commutation between the momentum and the potential energy, which is equivalent to calculating the first term of a series in ascending powers of $\boldsymbol{h}$, so that the validity of the results is doubtful. We shall not attempt a rigorous discussion on these lines, but we first assume the possibility of a development such as (5) or (6) in a quantum assembly, a result made plausible by Kahn and Uhlenbeck's work (1938), and then make certain assumptions about the behaviour of the b_l's in liquid helium. Some of our considerations will be based on the fact that the interaction between two helium atoms is certainly of the order of magnitude required to form a molecule and we need not expect them to apply to other liquids. In particular, we shall introduce a distinction between 'small' and 'large' clusters which can be made only if the interaction is near this critical value.

If the interaction is large compared with the critical value, cluster formation takes place mainly in coordinate space. In this case, the atoms are already prevented by their repulsive fields from approaching one another too closely and the influence of the type of statistics obeyed by the atoms should be quite small (Wergeland 1946). If the interaction is smaller than the critical value, two atoms do not gain any energy by approaching one another (as they would if they behaved classically) because the gain in potential energy is more than offset by the increase in 'zero-point' kinetic energy. On the other hand, we have already noted Mott's (1949) result that, in just this situation, it is energetically profitable to place a number of Bose atoms in one quantum state, and this 'clustering in momentum space' would be prevented, or would take place in an entirely different way, if the atoms obeyed Fermi–Dirac statistics.

§ 3. THE CONCEPT OF 'LARGE' AND 'SMALL' CLUSTERS

Let us assume provisionally that the binding between two He_4 atoms is sufficient to form a stable molecule. We shall then have a system very like the deuteron, namely a molecule with small binding energy and only a single bound level. Similarly, if the interaction is just less than the critical value we can gain only a small amount of energy by assigning two atoms to the same momentum state. As we add more and more atoms to a cluster, there will evidently come a stage where the cluster can have excited levels, and a very large cluster can evidently go into a large number of excited levels without breaking up. We shall describe a cluster as 'small' if it has no excited levels and 'large' otherwise. We shall suppose further that the spectrum of levels of a large cluster is, to a first approximation, the same as that of a Debye lattice, and we shall consider the conditions for equilibrium between the two types of cluster. We shall then show how this first approximation can be improved. The energy of the assembly is made up of various contributions: (*a*) the translational and rotational energies of each cluster; (*b*) the energy gained when one forms free atoms into clusters; (*c*) the energy associated with the internal degrees of freedom of the clusters; (*d*) the intraction energy between clusters.

For a 'small' cluster, contribution (*c*) is absent because there are no excited levels. Contribution (*d*) can probably always be neglected. In a classical assembly Mayer and Mayer's theory (1940) shows that $PV=\boldsymbol{k}T\Sigma_l \boldsymbol{m}_l$, where $\boldsymbol{m}_l$ is the most probable number of clusters of size l, that is the assembly behaves formally as if it were made up of $\Sigma_l \boldsymbol{m}_l$ non-interacting particles, so that the interactions between atoms are completely taken into account by the introduction of clusters without introducing an inter-cluster interaction. It does not follow that a similar result holds strictly for quantum assemblies (for which PV is not equal to $N\boldsymbol{k}T$ even in the absence of interactions, except in the limit of very high temperatures), but it is probably a reasonable first approximation. It holds for the perfect Bose–Einstein gas as well as for a 'classical' gas.

§ 4. EQUILIBRIUM BETWEEN 'SMALL' AND 'LARGE' CLUSTERS

We consider first the condition of statistical equilibrium between 'large' and 'small' clusters when both have zero or small velocities of translation, secondly, the conditions in which they can transfer momentum to one another. For this purpose, it is probably sufficiently accurate to think of p 'small' clusters each containing l atoms, where l is the most probable size of a small cluster, in equilibrium with a large cluster containing $N-N_c$ atoms, where $N_c=lp$. (We measure interaction energies reckoning that of atoms a great distance apart as zero.) The total free energy of the small clusters is simply $N_c E_l$ where $-E_l$ is the mean binding energy per atom in such clusters. The entropy is negligible since such clusters have no excited states. The free energy of the large cluster is

$$(N-N_c)\left[V_0+\frac{9}{8}\boldsymbol{k}\Theta-\frac{\pi^4}{5}(\boldsymbol{k}T)\left(\frac{T}{\Theta}\right)^3\dots\right], \qquad \dots\dots(7)$$

where V_0 is the mean potential energy per atom of the interaction forces, $9\boldsymbol{k}\Theta/8$ is the zero-point energy per atom of the large cluster, treated as a Debye lattice, and the form in T^4 takes account of the entropy and extra energy associated with thermal agitation. The condition for minimum free energy of the assembly is

$$\partial F/\partial N_c=0 \text{ or}$$

$$E_l+N_c\frac{\partial E_l}{\partial N_c}-V_0-\frac{9}{8}\boldsymbol{k}\Theta+\frac{\pi^4}{5}\boldsymbol{k}T\left(\frac{T}{\Theta}\right)^3\dots=0, \qquad \dots\dots(8)$$

if we neglect any changes in V_0 or Θ due to adding another atom to the large cluster. (If the addition took place with the large cluster keeping constant volume, the terms involving $\partial\Theta/\partial N_c$ could not be neglected, but we are keeping the volume of the *whole assembly* constant, so the neglect is probably justified.)

The behaviour of this model evidently depends on that of E_l as a function of l, the mean size of the 'small' clusters, and l in turn depends on N_c, the total number of atoms in the 'small' clusters. As an illustration, consider the result of assuming the total energy of the 'small' clusters to be given by

$$N_c E_l=N_c E_1+AN_c^2. \qquad \dots\dots(9)$$

Assumptions of this kind are often used in discussing co-operative phenomena. Moreover, it is known (see for example Price 1951) that quadratic terms of this nature appear when one treats the quantum mechanical many-body problem by perturbation theory.

Equation (8) now gives

$$2AN_c=E_0-E_1-\frac{\pi^4}{5}\boldsymbol{k}T\left(\frac{T}{\Theta}\right)^3, \qquad \dots\dots(10)$$

where we have written E_0 for $V_0+9\boldsymbol{k}\Theta/8$, the energy per atom in a large cluster at absolute zero. The condition for stability requires A to be positive. If E_0-E_1 is positive, this leads to N_c taking a finite value, not necessarily as great as N, at absolute zero, then gradually diminishing to zero at some transition temperature. Behaviour similar to this was expected in I for N_z, the number of atoms in 'z-states'. Substitution of expression (10) for N_c into (9) leads to an extra term in the specific heat proportional to T^7, which disappears abruptly at the transition temperature at which N_c vanishes. Thus, this first approximation gives a result of the right form, though it is not possible to choose A and E_0-E_1 to fit both the observed transition temperature and the observed height of the specific heat anomaly (the latter coming out about 20 times too small if we choose E_1-E_0 to give a transition temperature of 2·2° K). It has, however, been pointed out in I that, according to Blackman's work (1935), strict concurrence with the Debye law is not to be expected even for a perfect crystal lattice above temperatures of the order of $0{\cdot}01\Theta$ ($\sim$0·3° for liquid helium). If we admit a deviation from the Debye law of the type discussed in I, as suggested by Blackman's work (1935), together with some co-operative effect such as that involving the smaller clusters in (9) and (10) (due to E_l being a function of N_c) it is easily possible to explain the observed specific heat anomaly quantitatively, but we have too many adjustable constants for this fact to be significant by itself. The increase in the number of clusters in the liquid phase as the temperature falls could, by analogy with Mayer and Mayer's theory (1940), imply an increase in pressure at constant volume, that is a negative expansion coefficient, as is observed. For a classical assembly Mayer found that the pressure was strictly proportional to the mean number of 'clusters' present.

So far, we have left open the question whether the small clusters are to be thought of as occurring in coordinate or in momentum space. Either would be consistent with E_l for the small clusters being a fairly rapidly varying function of l, as the data seem to require, and either would be consistent with the interaction between two atoms being near the critical value. However, the following considerations seem to point to the clustering being in momentum space, though, on present knowledge, a third possibility cannot be excluded, viz. clustering partly in coordinate, partly in momentum space, that is in phase space as a whole.

(*a*) The ordinary process of condensation of the vapour involves the sudden appearance of large clusters in coordinate space. It seems unreasonable that the large clusters should begin to break up into smaller ones again as the temperature drops still lower, which is what would have to happen if our 'small clusters' were in coordinate space.

(*b*) The 'small' and 'large' clusters are supposed to be simultaneously present in the liquid. If the clustering were in coordinate space, opalescence would be expected. (In the ordinary liquid–vapour equilibrium, the large clusters form the liquid, the small ones the vapour.)

(*c*) Clustering certainly occurs in momentum space for the perfect Bose gas. It is reasonable, therefore, to expect it in a liquid with weak interactions.

§5. COLLISIONS OF 'SMALL' AND 'LARGE' CLUSTERS

We are thus led to think of helium II as consisting of one or more 'large' clusters, resembling a Debye lattice, in equilibrium with 'small' clusters. On this basis, we can define three distinct 'masses per unit volume' and three distinct 'stream velocities', as follows: (i) ρ_l and v_l the mass and velocity of propagation of the centre of gravity of the Debye lattice or 'large' clusters. (ii) ρ_{ph} and v_{ph} the mass and stream velocity associated with the 'phonons' which describe the excited states of the Debye lattice.

In the Appendix to I, it is shown that, given any assembly of phonons, one can determine, first the total momentum, $\rho_{\mathrm{ph}} v_{\mathrm{ph}}$ per unit volume, that they could transfer to a material body, secondly the apparent stream velocity v_{ph}, this being the velocity of a material body in statistical equilibrium with these phonons, hence the effective phonon density ρ_{ph}, which is found to be identical with Landau's expression (1941). (iii) ρ_c and v_c the mass per unit volume and mean stream velocity of the small clusters. In I it is pointed out that free particles of a mass comparable with that of helium atoms do not behave classically at very low temperatures, their lowest wave functions being extremely sensitive to fields such as that of gravity. This could probably be allowed for by the usual device of introducing effective masses for these clusters, differing from their gravitational masses, but we shall not introduce this refinement in the quantitative treatment. Effective mass in this context is defined not by Landau's method but in the normal quantum mechanical way as (total force)/(rate of change of flux) (Seitz 1940).

We can find a number of relations between these six quantities and the four quantities ρ_n, v_n, ρ_s, v_s used in the phenomenological two-fluid theory. (*a*) $\rho_{ph}=\rho_n$ because the observed velocity of second sound at very low temperatures requires such an assumption, and also because the phonons are the means by which a Debye lattice exchanges energy with its environment, for example, a moving boundary such as an oscillating disc. (*b*) $\rho_l v_l+\rho_c v_c=\rho_n v_n+\rho_s v_s$ because sound waves, in both classical and quantum mechanics, never result in any transfer of matter as long as anharmonic terms are negligible, but v_c and v_l both correspond to actual movement of matter. (*c*) $\rho_c+\rho_l=\rho_n+\rho_s=\rho$ because either of these sums represents the total mass of helium atoms present per unit volume. (*d*) $v_n=v_{ph}$ because it can be shown (Dingle 1951) that the entropy of a Debye lattice is transported with the velocity v_{ph}. These equations are sufficient to determine all four quantities ρ_n, v_n, ρ_s, v_s. Penrose (1951) and Dingle (1952) write $v_{ph}=v_n-v_s$ instead of the last of the above equations, so we shall also examine the physical consequences of this alternative assumption.

On the assumption that $v_n=v_{ph}$ we derive without difficulty the equation

$$v_s-v_n=\frac{\rho_l(v_l-v_{ph})+\rho_c(v_c-v_{ph})}{\rho-\rho_{ph}}. \qquad \text{......(11)}$$

(The absence of 'superfluid' effects means $v_s=v_n$ *not* $v_s=0$.) The two main facts that have to be explained by any theory of liquid helium are: (*a*) that relative flow of superfluid and normal fluid can be initiated and maintained by extremely small pressure or temperature differences; (*b*) that, once initiated, such relative flow is damped out only very slowly (some recent unpublished work by D. V. Osborne suggests that the characteristic time is of the order of seconds). For large values of the relative velocity, stronger dissipative effects do occur.

We are suggesting that both of these facts can be accounted for if we postulate the presence of 'small' clusters in the liquid. Fact (*a*) may be a consequence of their having small effective masses. Equation (11) shows that, in an ordinary liquid, the absence of any 'superfluid' effects seems to require that $v_l=v_{ph}$ even if $\rho_{ph}>\rho$. This is actually the condition for thermodynamic equilibrium in a moving Debye lattice (see Appendix to I). The mechanism that maintains this equilibrium is presumably the Umklapp process of Peierls (1929), which plays an important part in determining the heat conductivity of a crystal, and which may be described roughly as a Bragg reflection of phonons by the lattice, the net result of which is a transfer of momentum between the phonons and the centre of gravity of the lattice. We shall assume that this process is effective in maintaining the equality of v_l and v_{ph} even in helium II. We now have to consider what mechanisms are available for maintaining equilibrium between the 'small' clusters and the Debye lattice that is, equality of v_c and v_l. The Appendix to I shows that a given assembly of phonons cannot be in true statistical equilibrium with a material body moving at any velocity other than v_{ph}, but it does not follow *a priori* that any effective mechanism for maintaining equality between v_c and v_{ph} actually exists. We consider a collision between a 'small' cluster and the Debye lattice at rest. (Collisions between the small clusters themselves lead to no change in $\rho_c v_c$ and can be ignored.)

A collision between a small cluster and the Debye lattice may result either in the transfer of momentum to the centre of gravity (which, by eqn. (11), does not affect $\boldsymbol{v}_n-\boldsymbol{v}_s$ since it leaves $\rho_0 v_0+\rho_l v_l$ constant) or in the creation or disappearance of a phonon or phonons. The latter are the only processes that can result in a change of $v_{ph}-v_c$, and we may consider two possibilities:

(*a*) The lattice is knocked into a higher excited state by the collision. Since the lattice is so much heavier than the cluster, this process becomes possible if the energy of a phonon is less than the kinetic energy of the small cluster, the situation being analogous to that of an electron colliding with an atom, losing some or all of its kinetic energy, and leaving the atom in an excited state. Now, according to the Debye theory, the sound quantum of lowest energy would have a wavelength of about 1 cm in an ordinary vessel, and the corresponding frequency would thus be $\nu\simeq2{\cdot}5\times10^4\,\mathrm{sec}^{-1}$ so that the critical velocity of a 'small' cluster of l atoms would be given by equating its kinetic energy to $\boldsymbol{h}\nu$, the energy of a phonon: $\frac{1}{2}lmv^2=2{\cdot}5\times10^4\,\boldsymbol{h}$ or $v\simeq7/l^{1/2}$ cm/sec for m equal to the mass of a helium atom. This calculated velocity is somewhat smaller than the observed critical velocities, which again suggests that the effective mass of the clusters may be less than their actual mass.

(*b*) A process involving a large number of phonons but a resultant very small change of energy occurs. As an example, one may suppose that the small cluster initially collides with a few atoms in the lattice from which an elastic wave spreads out. In I it is pointed out that a process involving the initial displacement of only a few atoms in the lattice necessarily involves a large number of phonons, and there is therefore no lower limit on the energy required to bring about such a process.

While we certainly cannot say *a priori* that processes such as (*b*) are ineffective, it does seem suggestive that the assumption of the predominance of processes (*a*) does predict critical velocities of the correct order of magnitude. If we accept this idea, it is also possible, because of the variation of the expected critical velocity with size of cluster, to understand why the observed critical velocity is rather indefinite, at least in the bulk liquid, ranging, apparently, from values of the order of 1 cm/sec in an oscillating disc type of experiment, to 100 cm/sec for 'second sound', so that many of the facts can be accounted for by assuming instead a frictional term that increases rapidly with the velocity $\boldsymbol{v}_n-\boldsymbol{v}_s$ (Gorter and Mellink 1949).

We now discuss briefly the consequences of the alternative assumption that $\boldsymbol{v}_{ph}=\boldsymbol{v}_n-\boldsymbol{v}_s$. If we assume this, we have some difficulty in accounting for the non-existence of superfluid effects in other liquids. v_{ph} zero means that on an average every phonon is balanced by another one of equal and opposite momentum, which implies some fairly strong coupling between such phonons. It is hard to see why such coupling should be absent in the one liquid helium II, yet should appear suddenly when the temperature is raised.

§6. CONCLUSIONS

We have arrived at the following tentative picture of liquid helium:

(*a*) The condensation of vapour to form liquid helium I is probably quite normal, and should be describable by the Mayer and Mayer theory (1940) except that we must take account of the zero-point energy, which, in both 'small' and 'large' clusters, is comparable with the attractive energy between atoms.

(*b*) The λ-transition is interpreted as heralding the appearance of 'small' clusters in the liquid itself (probably in momentum space). It is then necessary to assume that the binding energy, per atom in the average 'small' cluster, is numerically greater than that in a 'large' one, and that it varies fairly rapidly with the size of cluster. All this is quite a plausible consequence of the known fact that the interaction between two helium atoms is of about the strength needed to form a molecule.

(*c*) The appearance of 'superfluid' effects is interpreted as a consequence of the fact that the 'small' clusters cannot easily lose their kinetic energy by collision with a 'large' one. It is also possible that their quantum mechanical effective mass is less than their actual mass.

(*d*) The possibility of the formation of clusters in momentum space as well as in coordinate space is probably confined to helium atoms because of the particular strength of the atomic interaction. Clustering in coordinate space is not much affected by the symmetry properties but clustering in momentum space will be quite different for the two helium isotopes (if indeed it occurs for He_3 at all). This seems in agreement with the facts known about He_3.

REFERENCES

Bijl, A., de Boer, J., and Michels, A., 1941, *Physica*, **8,** 655.

Blackman, M., 1935, *Proc. Roy. Soc.* A, **149,** 117.

Dingle, R. B., 1951, *Phil. Mag.*, **42,** 1080; 1952, *Advances in Physics* (*Phil. Mag.* Suppl.), **1,** 111.

Gorter, C. J., and Mellink, J. H., 1949, *Physica*, **15,** 285.

Kahn, B., and Uhlenbeck, G. E., 1938, *Physica*, **5,** 399.

Matsubara, T., 1951, Report on Oxford Conference on Low Temperatures, p. 104.

Mayer, J. E., and Mayer, M. G., 1940, *Statistical Mechanics* (New York : Wiley and Sons), Chaps. 13, 14, and 16.

Mott, N. F., 1949, *Phil. Mag.*, **40,** 61.

Landau, L., 1941, *J. Phys., U.S.S.R.*, **5,** 71.

London, F., 1939, *J. Phys. Chem.*, **43,** 49.

Peierls, R. E., 1929, *Ann. Phys., Lpz.* (Ser. 3), **5,** 1055.

Penrose, O., 1951, Report on Oxford Conference on Low Temperatures, p. 109.

Price, P. J., 1951, Report on Oxford Conference on Low Temperatures, p. 109.

Seitz, F., 1940, *Modern Theory of Solids* (New York : McGraw-Hill).

Temperley, H. N. V., 1952, *Proc. Phys. Soc.* A, in the press.

Wergeland, H., 1946, *Kgl. Norsk. Vidensk. Selsk. Forh.*, **19,** 8.

The Absorption Spectra of Gallium and Indium Monofluorides

By D. WELTI and R. F. BARROW
Physical Chemistry Laboratory, University of Oxford

MS. received 26th February 1952

ABSTRACT. Gaseous GaF and InF are formed when the metals are heated with aluminium trifluoride, and sufficient pressures of the monofluorides for observation of their absorption spectra are obtained at about 1 000° c for GaF and 1 400° c for InF. The three ultra-violet band-systems, $^1\Pi$, $^3\Pi_1$, $^3\Pi_{0+} \leftarrow {}^1\Sigma^+$ expected by analogy with GaCl and InCl have been photographed on spectrographs of moderate dispersion, and vibrational analyses have been carried out. The $^1\Pi$ states converge rapidly to give rather sharp dissociation limits: the products are probably Ga or In, $({}^2P_{3/2})$, $+F({}^2P_{1/2})$. The bearing of the present results upon the interpretation of the electronic levels of TlF and on the dissociation energy of AlF is briefly considered.

§ 1. INTRODUCTION

Our interest in the spectra of GaF and InF arose in the first place because of the possibility of determining their energies of dissociation. It was thought that values for these molecules would probably throw some light upon the very large discrepancy which existed between the results of the spectroscopic and thermochemical determinations of the energy of dissociation of AlF (see § 5). Moreover, if sufficiently precise values were derived, they could be combined with results to be obtained from future equilibrium measurements to provide values for the dissociation energy of fluorine. GaF and InF were also of some interest as, apart from BI, they were the only two molecules of the group stretching from BF to TlI about which there was no spectroscopic information.

The possibility of studying these molecules by a simple absorption technique was suggested by the work of Gross, Campbell, Kent and Levi (1948) on heterogenous equilibria of the type $2Al + AlCl_3 = 3AlCl$. Their results showed that it would be reasonable to attempt to produce small pressures of the gaseous monofluorides of gallium and indium by heating the metals with aluminium trifluoride. This expectation was fulfilled, and sufficient GaF and InF for the examination of their absorption spectra were found to be readily produced in this way.

Three ultra-violet band-systems have been found for each molecule, which correspond closely with those already known for the other gallium and indium halides (Miescher and Wehrli 1934, Wehrli and Miescher 1934). The forbidden systems, A $^3\Pi_{0+} \leftarrow$ X $^1\Sigma^+$ and B $^3\Pi_1 \leftarrow$ X $^1\Sigma^+$, are situated not far from 3 000 Å, and appear with only low intensity: the other systems, C $^1\Pi \leftarrow$ X $^1\Sigma^+$, lie at shorter wavelengths, and seem to be much stronger. The vibrational levels in the states C $^1\Pi$ converge rapidly, and fairly precise dissociation limits have been obtained. Their significance is discussed in a later section.

.A
5
2

§ 2. EXPERIMENTAL

Mixtures of Ga or In metal with AlF_3 were placed in Pythagoras boats in aluminium oxide tubes. The tubes carried water-cooled brass end-pieces with silica windows and were heated in a Globar furnace: the effective column length was about 20 cm. The GaF plates were taken at about 1 000° C, the InF at about 1 400° C.

A hydrogen lamp was used as source of continuum. The absorption spectra were photographed with Hilger Small and Medium quartz prism instruments on Ilford Q1 and Process plates. Cu and Fe arc comparison spectra were used: the wavelengths of the lines were taken from the M.I.T. list (1939).

§ 3. ANALYSES OF THE SPECTRA

(i) *Appearance*

The reproductions in figs. 1 and 2 give a general impression of the absorption spectra. Both molecules show two distinct regions of banded absorption. In GaF, there are weak violet-degraded bands of two kinds, single- and double-headed, in the region 2 900–3 100 Å, and a much stronger system of predominantly red-degraded double-headed bands lying between 2 050 and 2 200 Å. The systems of InF are similar, but shifted slightly to longer wavelengths, at 3 050–3 300 Å and 2 275–2 475 Å respectively.

Apart from some GaCl bands, which appeared on one or two of the GaF plates, no other molecular absorption was observed; in particular the plates were quite free from AlF. Lines of In I appeared strongly, and on the exposures at the highest temperatures, there was strong development of the series $n^2S_{1/2}$, $n^2D_{3/2,\,5/2} - 5^2P_{1/2,\,3/2}$ of In I with limits at 2 145 and 2 252 Å (Garton 1951).

(ii) *Vibrational Analyses*

The vibrational analyses presented no especial difficulties. It is most probable that the far ultra-violet transitions are $^1\Pi - {}^1\Sigma$, as has been demonstrated for the corresponding system of InCl by the rotational analysis of Froslie and Winans (1947). The two heads are thus R and Q, or in the few violet-degraded bands, P and Q. In all the systems, $B' \simeq B''$, and the 0, 0 bands are much the strongest. The 0, 0 band of the C–X system of InF is of unusual type, with two Q heads, an R head and a rather diffuse P head. This kind of band has been encountered in other systems in this group of molecules, for example in BBr (Rosenthaler 1940): in the present instance its formation arises from the fact that whereas $F'(J) > F''(J)$ for small J, $F'(J) < F''(J)$ for larger J, i.e. $B_0' > B_0''$, but $D_0' > D_0''$.

Much less information was obtained about the longer wavelength systems, but a sufficient number of bands was observed to confirm the ground-state vibrational intervals deduced from the analyses of the C–X systems. The weakness of the systems A, B–X and the observation that the A–X bands possess only one head, whereas the B–X bands have two, support their identification as $A\,^3\Pi_{0^+}$, $B\,^3\Pi_1 - {}^1\Sigma^+$ as in other molecules of this group (see, for example, Wehrli and Miescher 1934).

The vibrational analyses are given in tables 1–6: the measurements given for the B, C–X systems are for the Q heads, where resolved; those for the A–X systems are for the P heads.

Table 1. Deslandres Scheme for the System $A\,^3\Pi_{0^+} - X\,^1\Sigma^+$ of GaF

P heads.

v' ↑ / v'' →	0		1		2	3
4						33858·6 (0) *2952·60*
3					33831·1 (1) *2955·00*	
					653·8	
2			33800·8 (2) *2957·65*	605·5	33195·3 (1) *3011·60*	
			642·7			
1	33767·7 (2) *2960·55*	609·6	33158·1 (3) *3014·98*			
	651·7					
0	33116·0 (5) *3018·81*					

Table 2. Deslandres Scheme for the System $B\,^3\Pi_1 - X\,^1\Sigma^+$ of GaF

Q heads, except where the measurements are in parentheses, indicating unresolved heads, Q+P.

v' ↑ / v'' →	0		1		2		3	4
5								(34220·2) (1) *2921·40*
4							(34190·5) (2) *2923·94*	
3					(34160·2) (3) *2926·53*			
					(636)			
2			34137·2 (2) *2928·50*	608·8	33528·4 (2) *2981·68*	(609)	(32915·8) (0) *3037·17*	
			647·2		647·2			
1	34107·1 (3) *2931·09*	617·1	33490·0 (5) *2985·10*	608·8	32881·2 (0) *3040·37*			
	658·2		655·2					
0	33448·9 (10) *2988·77*	614·1	32834·8 (0) *3044·67*					

Table 3. Deslandres Scheme for the System $c\,^1\Pi - x\,^1\Sigma^+$ of GaF

Q heads, except where the measurements are in parentheses, indicating unresolved heads, R+Q.
All bands are degraded to longer wavelengths, except those marked V.
l: line-like head.

v′ ↑ / v″ →	0		1		2		3		4		5		6		7		8
6																	(45259·7) (0) *2208·78*
																	(350·9)
5					(48426·1) (2) *2064·34*						(46639·2) (6) *2143·44*				(45479·4) (2) *2198·11*	(570·6)	(44908·8) (0) *2226·04*
					(397·3)						(397·1)						
4			(48634·8) (2) *2055·48*	(606·0)	(48028·8) (1) *2081·42*	(601·2)	(47427·6) (6) *2107·81*	(594·5)	(46833·1) (8) *2134·57*	(591·0)	(46242·1) (5) *2161·85*	(582·2)	(45659·9) (4) *2189·42*				
			(434·5)		(437·5)		(435·9)		(440·3)		(434·7)						
3	(48818·4) (1) *2047·75*	(618·1)	(48200·3) (4) *2074·02*	(609·0)	47589·6 (8) *2100·61*	601·0	46988·6 (8) *2127·50*	600·4	45388·2 (6) *2155·04*	588·4	45799·8 (5) *2182·73*						
	(472·8)		(467·6)		471·2		474·8		469·1								
2	48342·2 (4) *2067·93*	613·7	47728·5 (7) *2094·52*	610·1	47118·4 (9) *2121·64*	604·6	46513·8 (7) *2149·22*	594·7	45919·1 (6) *2177·06*								
	497·3		500·4		497·9		495·9										
1	47844·9 (6) *2089·42*	616·8	47228·1 (10) *2116·71*	607·6	46620·5 (8) *2144·30*	602·6	46017·9 (5)*l* *2172·38*										
	522·4		521·6		522·5												
0	47322·5 (10) *2112·49*	616·0	46706·5 (7)V *2140·35*	608·5	46098·0 (4)V *2168·61*												

Table 4. Deslandres Scheme for the System $A\,{}^3\Pi_{0^+} - X\,{}^1\Sigma^+$ of InF

P heads.

v′ ↑ / v″ →	0		1		2	3
4						31106·8 (0) *3213·81*
3					31081·6 (1) *3216·41*	
					550·4	
2			31054·1 (1) *3219·26*	522·9	30531·2 (1) *3274·40*	
			558·4			
1	31023·5 (1) *3222·44*	527·8	30495·7 (1) *3278·21*			
	563·9					
0	30459·6 (2) *3282·10*					

Table 5. Deslandres Scheme for the System $B\,{}^3\Pi_1 - X\,{}^1\Sigma^+$ of InF

Q heads, except where the measurements are in parentheses, indicating unresolved heads, P+Q.

v′ ↑ / v″ →	0		1		2		3	
5								(31940·4) (0) *3129·93*
4							31925·6 (0) *3131·38*	
3					31900·0 (2) *3133·89*			
					552·8			
2			31871·2 (3) *3136·72*	524·0	31347·2 (1) *3189·16*	(528)	(30816·0) (1) *3244·13*	
			558·5		(560)			
1	31841·9 (2) *3139·61*	529·2	31312·7 (5) *3192·67*	(526)	(30783·9) ?(1) *3247·52*			
	565·5		(571)					
0	31276·4 (6) *3196·38*	(535)	(30738·6) (0) *3252·30*					

Table 6. Deslandres Scheme for the System $c^1\Pi - x^1\Sigma^+$ of InF

Q heads, except where the measurements are in parentheses, indicating unresolved heads, R − Q.
All bands are degraded to longer wavelengths, except those marked V.
l: line-like head. *also the 1,0 band.

v' ↑ / v'' →	0		1		2		3		4		5		6		7		8		9		10		11
8															(42026·6) (0) *2378·72*								
															(238·9)								
7							(43819·0) (0) *2281·41*	(513·4)	(43305·6) (0) *2308·46*						(41787·7) (0) *2392·32*				(40811·3) (0) *2449·56*	(484·0)	(40327·3) (0) *2478·96*	(479·3)	(39848·0) (0) *2508·78*
							(281·5)								(276·1)				(283·8)		(282·3)		(282·9)
6							(43537·5) (2) *2296·16*						42008·4 (4) *2379·75*	498·1	41510·3 (1) *2408·31*	494·4	41015·9 (3) *2437·34*	491·1	40524·8 (0) *2466·88*	(484·5)	(40045·0) (0) *2496·44*	(479·9)	(39565·1) (0) *2526·72*
							(319·2)						320·9		322·6		321·6		321·2				
5					43732·9 (4) *2285·90*	(516·6)	[43218·3] (7) *2313·12**				42190·2 (15) *2369·38*	502·7	41687·5 (3) *2398·07*	499·8	41187·7 (5) *2427·17*	493·4	40694·3 (0) *2456·60*	490·7	40203·6 (1) *2486·59*				
					352·2		(354·7)				351·8		354·5		353·6		353·6						
4			(43909·2) (1) *2276·72*	(528·5)	43380·7 (5) *2304·46*	519·6	42861·1 (5) *2332·40*	515·4	42345·7 (20) *2360·79*	507·3	41838·4 (4) *2389·42*	505·4	41333·0 (6) *2418·64*	498·9	40834·1 (1) *2448·19*	493·4	40340·7 (0) *2478·14*						
			(382·6)		381·5		381·7		380·3		382·5		380·1		377·0								
3			43523·1 (8) *2296·92*	523·9	42999·2 (5) *2324·91*	519·8	42479·4 (30) *2353·36*	514·0	41965·4 (9) *2382·19*	509·5	41455·9 (8) *2411·47*	503·0	40952·9 (1) *2441·09*	495·8	40457·1 (0) *2471·01*								
					407·2		406·5		405·6		406·2												
2	43647·6 (6) *2290·37*				42592·0 (40) *2347·14*	519·1	42072·9 (1) *2376·10*	513·1	41559·8 (8)*l* *2405·44*	510·1	41049·7 (1)V *2435·33*												
	429·3				427·9		427·6																
1	43218·3 (7) *2313·12*	528·8	42689·5 (50) *2341·78*	525·4	42164·1 (12)V *2370·96*	518·8	41645·3 (10)V *2400·50*																
	446·7		448·4		447·0																		
0	42771·6 (100)V *2337·28*	530·5	42241·1 (12)V *2366·64*	527·0	41717·1 (7)V *2396·37*																		

(iii) *Rotational Constants*

An attempt may be made to interpret the R–Q and P–Q head separations in these systems as follows. We first estimate the value of r_e''. Let us consider AlF. Now the increase in internuclear distance on going from the diatomic molecule BX to AlX is almost constant: we find (from Herzberg 1950) AlH–BH, 0·413 Å; AlCl–BCl, 0·422 Å; AlBr–BBr, 0·408 Å; AlO–BO, 0·413 Å. The mean difference is 0·414 Å, which, with $r_e''(\mathrm{BF}) = 1{\cdot}262$ Å, gives $r_e''(\mathrm{AlF}) = 1{\cdot}68$ Å. For InF, InH–BH, 0·605 Å; InCl–BCl, 0·602 Å, giving $r_e''(\mathrm{InF}) = 1{\cdot}87$ Å. No internuclear distances have been measured for diatomic gallium compounds: we should guess, however, that r_e''(GaF) lies between the values for AlF and for InF, and that it probably lies nearer to the value for AlF (see, for example, Sidgwick 1950, p. xxix). We take $r_o''(\mathrm{GaF}) = 1{\cdot}75$ Å. Then $B_e''(\mathrm{GaF}) = 0{\cdot}369$; $B_e''(\mathrm{InF}) = 0{\cdot}295_5$ cm^{-1}.

Table 7. Band-head Separations, Q – P, in the System B – X of GaF

Band (v', v'')	1,0	2,1	0,0	1,1	2,2	0,1	1,2
$\Delta\nu$(cm^{-1})obs.	15·2	10·7	11·0	10·2	8·1	11·1	10·2
calc.	14·9	11·1	14·0	10·6	8·5	10·2	8·2

Table 8. Band-head Separations, R – Q or Q – P, in the System C – X of GaF

Band (v', v'')	2,0	1,0	2,1	3,2	0,0	1,1	2,2	3,3
Degradation	R	R	R	R	R	R	R	R
$\Delta\nu$(cm^{-1})obs.	6·8	15·8	8·4	3·6	49·1	28·6	14·7	6·2
calc.	6·8	12·4	8·4	6·3	53·6	18·5	10·9	7·6

Band (v', v'')	0,1	1,2	2,3	3,4	0,2	1,3	2,4	3,5
Degradation	V	R	R	R	V	V	R	R
$\Delta\nu$(cm^{-1})obs.	large	40·7	22·3	9·1	50·8	large	31·4	15·1
calc.	large	37·8	15·7	9·7	27·9	large	28·6	13·5

Table 9. Band-head Separations, Q – P, in the System B – X of InF

Band (v', v'')	1,0	2,1	3,2	4,3	0,0	1,1	2,2
$\Delta\nu$(cm^{-1})obs.	8·5	7·2	7·7	8·5	5·9	6·5	6·9
calc.	7·7	7·8	8·1	8·3	6·2	6·3	6·4

With these assumed values of B_e'', values of α'' were derived from the head–head separations, $\Delta\nu$, in the v'-constant progressions of the C–X systems, using $\Delta\nu = (B' + B'')^2/4(B' - B'')$. Values calculated from $B_v'' = B_e'' - \alpha''(v'' + \frac{1}{2})$ were then used to obtain B'_v, and hence B_e' and α' for the systems C–X and B–X. The values of the rotational constants derived in this way are given in table 11.

The observed and calculated band-head separations are compared in tables 7–10. It will be seen that the calculated values reproduce quite well the general trends observed in the values of the separations with v', v''.

It should be emphasized that this agreement means no more than that a self-consistant set of rotational constants has been obtained on the basis of the assumed values of B_e''. The values of B_e'' can be varied in fact within quite wide limits to give other sets of rotational constants which in turn give reasonably satisfactory separations. If there were a convenient criterion of best fit, it would of course be possible to determine B_e'' by a trial-and-error method. This can hardly be expected to be a fruitful procedure, however, since for the small separations, the error in the experimental values is proportionately large, while for the large separations, of which there are good experimental values, the calculated values—because of the importance of *D*-terms—are no longer well represented by $\Delta\nu=(B'+B'')^2/4(B'-B'')$. In the case of GaF, the effect is still further complicated by small isotope displacements.

Table 10. Band-head Separations, R – Q or Q – P, in the System of c – x of InF

Band (v', v'')	Degrad.	$\Delta\nu$(cm^{-1}) obs.	$\Delta\nu$(cm^{-1}) calc.	Band (v', v'')	Degrad.	$\Delta\nu$(cm^{-1}) obs.	$\Delta\nu$(cm^{-1}) calc.
5,2	R	4·0	3·2	4,5	R	7·2	7·3
				5,6	R	4·9	5·1
2,0	R	9·9	8·6	6,7	R	2·5	3·9
3,1	R	6·9	5·9				
4,2	R	4·2	4·4	0,2	V	10·8	10·9
				1,3	V	~20	21·4
1,0	R	24·7	26·0	2,4	R	?42·7	large
3,2	R	7·2	7·1	3,5	R	20·8	19·2
4,3	R	5·0	5·1	4,6	R	10·4	9·4
				5,7	R	5·8	6·1
0,0	V	~35	28·2	6,8	R	2·9	4·4
1,1	R	37·5	large				
2,2	R	20·5	16·8	2,5	V	16·3	34·9
3,3	R	10·5	9·0	3,6	R	30·2	45·8
4,4	R	6·5	6·0	4,7	R	14·0	13·2
5,5	R	4·0	4·4	5,8	R	6·3	7·5
6,6	R	2·3	3·5	6,9	R	5·4	5·2
0,1	V	18·2	15·8	3,7	?	large	large
1,2	V	large	large	4,8	R	18·2	22·7
2,3	R	29·8	32·7	5,9	R	9·7	9·9
3,4	R	14·2	12·2				

Table 11. Summary of Constants for GaF and InF

GaF	State	ν_e	ω_e	$x_e\omega_e$	$y_e\omega_e$	B_e	α	r_e(Å)	D_0(ev)	κ_e(dyn/cm $\times 10^{-5}$)
$\mu=$	c $^1\Pi$	47362·3	542·3	7·7$_5$	—0·9$_2$	[0·368$_7$]	[0·008$_1$]	[1·75]	0·4$_4$	2·58
24·7$_8\times10^{-24}$g.	B $^3\Pi_1$	33430·5	661·$_8$	3·8	—	[0·377$_4$]	[0·0006]	[1·73]	—	3·85
	A $^3\Pi_{0+}$	33096·$_2$	663·$_6$	4·$_{15}$	—	—	—	—	—	3·87
	x $^1\Sigma^+$	0	623·2	3·4$_0$	—	[0·369$_0$]	[0·003$_6$]	[1·75]	6·1$_5$	3·41
InF										
$\mu=$	c $^1\Pi$	42807·5	463·9	7·3$_5$	—0·5*	[0·300$_6$]	[0·006$_4$]	[1·85]	0·4$_2$	2·06
27·0$_7\times10^{-24}$g.	B $^3\Pi_1$	31256·8	573·0	3·4$_6$	—	[0·310$_4$]	[0·002$_9$]	[1·83]	—	3·15
	A $^3\Pi_{0+}$	30441·$_1$	572·$_2$	3·4$_0$	—	—	—	—	—	3·14
	x $^1\Sigma^+$	0	534·7	2·56	—	[0·295$_5$]	[0·002$_4$]	[1·87]	5·4$_1$	2·74

Notes :

The rotational constants are of relative, rather than absolute significance: see text. The least certain value is that of α for B $^3\Pi_1$ of GaF : most probably the value given here is too small.

* There is some evidence that levels with $v'\geqslant 7$ in c $^1\Pi$ of InF begin to converge rather more rapidly than is given by this expression.

The constants have their usual significance : thus for InF, c—x,

$$\nu(\text{Q head})=42807{\cdot}5+[463{\cdot}9u'-7{\cdot}3_5u'^2-0{\cdot}5u'^3]-[534{\cdot}7u''-2{\cdot}56u''^2],$$

where $u=v+\frac{1}{2}$.

In spite of these limitations on the absolute accuracy of the rotational constants, it is more than probable that the values are correct relatively, i.e. that they show the correct trends from one electronic state to another of the same molecule. In particular, it may be concluded that (i) the equilibrium internuclear distances vary much less among the states of these molecules than do the force constants, (ii) the states C are anharmonic to a high degree, as shown both by the large values of $x_e\omega_e$, $y_e\omega_e$ and of α_e.

§ 4. ENERGIES OF DISSOCIATION

The vibrational levels in the states $C\,{}^1\Pi$ converge rapidly, both for GaF and for InF. Numerical extrapolation, using the vibrational constants given in table 11, gives $D_0'(\mathrm{C:GaF}) = 3\,545\ \mathrm{cm}^{-1}$; $D_0'(\mathrm{C:InF}) = 3\,465\ \mathrm{cm}^{-1}$. The dissociation limits above $v'' = 0$ are 50 870 and 46 240 cm^{-1} for GaF and InF respectively.

It remains to identify the atomic products of dissociation of the states C. When the molecules of this group are considered as a whole, it proves difficult to draw a consistent picture of their dissociation energies except on the assumption that the process is $\mathrm{MX}(C\,{}^1\Pi) = \mathrm{M}({}^2P_{3/2}) + \mathrm{X}({}^2P_{1/2})$. The arguments may be best illustrated by reference to the molecules InCl and InBr.

For InCl, an upper limit for D_0'' was found by Wenk (1941) from a study of atomic fluorescence. The effective wavelength for the process $\mathrm{InCl} \rightarrow \mathrm{In}({}^2S_{1/2}) + \mathrm{Cl}({}^2P_{3/2})$ was found to be 1 640 Å, i.e. 60 980 cm^{-1}. The interval In $({}^2S_{1/2} - {}^2P_{1/2})$ is 24 373 cm^{-1} so that $D_0'' \leqslant 36\,610\ \mathrm{cm}^{-1}$. Now $\nu_{0,0}$ for the C–X system of InCl is at 37 415 cm^{-1}: a very short extrapolation of the vibrational levels in C gives a limit at 37 950 cm^{-1}. The excitation energy of $\mathrm{Cl}({}^2P_{1/2})$ is 881 cm^{-1} so that if the products at this dissociation limits were $\mathrm{In}({}^2P_{1/2}) + \mathrm{Cl}({}^2P_{1/2})$, $D_0'' = 37\,950 - 880 = 37\,070\ \mathrm{cm}^{-1}$, which is higher than Wenk's upper limit. Thus one of the products of dissociation of state C must be $\mathrm{In}({}^2P_{3/2})$, with an excitation energy of 2 210 cm^{-1}, and D_0'' is at least as low as $37\,950 - 2\,210 = 35\,740\ \mathrm{cm}^{-1}$. It will appear that, with great probability, $\mathrm{InCl(C)} \rightarrow \mathrm{In}({}^2P_{3/2}) + \mathrm{Cl}({}^2P_{1/2})$, so that D_0'' $35\,740 - 880 = 34\,860\ \mathrm{cm}^{-1}$.

In the case of InBr, there is no indication that the state C possesses a potential minimum, the C–X system appearing as a set of fluctuation bands. Analysis of these absorption maxima leads to a dissociation limit at 33 940 cm^{-1} above $v'' = 0$. The atomic fluorescence of InBr has been studied by Sedov and Filippov (1934) and by Wenk (1941). The former give 1 960 ± 30 Å as the long-wavelength limit for production of the lines $\mathrm{In}({}^2S_{1/2} - {}^2P_{3/2,\,1/2})$: the latter finds that the most effective wavelength is 1 830 Å. With the last figure, $D_0'' \leqslant 30\,270\ \mathrm{cm}^{-1}$. Now it is reasonable to assume that the products of dissociation of the states C in InCl and InBr are in the same electronic states. It has been shown that the In atom is excited, ${}^2P_{3/2}$, from state C in InCl. For InBr, we have $D_0'' = 33\,940 - 2\,210 = 31\,730\ \mathrm{cm}^{-1}$, if $\mathrm{InBr(C)} \rightarrow \mathrm{In}({}^2P_{3/2}) + \mathrm{Br}({}^2P_{3/2})$. This figure is, however, compatible neither with the upper limit derived from Wenk's work, nor with $D'' \sim 26\,600\ \mathrm{cm}^{-1}$ from Sedov and Filippov's observations. It must therefore be concluded that $D_0'' = 33\,940 - (2\,210 + 3\,685) = 28\,040\ \mathrm{cm}^{-1}$ corresponding to the process $\mathrm{InBr(C)} \rightarrow \mathrm{In}({}^2P_{3/2}) + \mathrm{Br}({}^2P_{1/2})$.

It is likely that the other $C\,{}^1\Pi$ states in this group of molecules behave similarly, and indeed there is a good deal of evidence for this view, which however need not be considered here. For GaF and InF, assuming that the states C dissociate into $M(^2P_{3/2})+F(^2P_{1/2})$, we find $D_0''=6{\cdot}15$ and $5{\cdot}41$ ev respectively.

It appears then that the two major problems in determining the dissociation energies of these two molecules, (i) the precise measurement of a dissociation limit, and (ii) the identification of the atomic products at that limit, have been solved reasonably satisfactorily. It should however be noted that there is a possibility that the convergence limits correspond, not to dissociation limits at infinite separation of the atoms, but rather to potential maxima. According to our present information such a situation appears to arise in the case of AlF (see below, § 5). Thus it is possible that the true values of D_0'' for GaF and InF are somewhat lower than those given in table 11. It is hoped to elucidate this point, and to check the identification of the atomic products of dissociation of the $^1\Pi$ states, by thermochemical work on these molecules now in progress.

Finally, it is of interest to compare the values of D_0'' with those obtained by direct linear Birge–Sponer extrapolations for the ground-state vibrational levels. It is found that the latter are only some 57% and 63% of the above values for GaF and InF respectively. This supports Gaydon's view (1947) that ionic forces contribute appreciably to the binding in this group of molecules, and it must be concluded that linear extrapolations of vibrational intervals are quite without value in these cases.

§ 5. DISCUSSION: TlF AND AlF

The values of the constants derived in the present work are collected together in table 11. A comparison of these figures with those for the other gallium and indium halides (see, for example, Herzberg 1950) shows that GaF and InF have very much the properties that would have been expected. The binding in the states of the fluorides, as measured by dissociation energy or by the force constant, is appreciably stronger than for the corresponding states of the other halides. This effect is particularly marked for the C $^1\Pi$ states, where, for example, the force constants for GaF, GaCl, GaBr and GaI are $2{\cdot}58\times10^5$, $0{\cdot}20\times10^5$, ~ 0 and 0 dyn/cm respectively. The indium halides behave similarly. On the other hand, the multiplet splittings, $^3\Pi_1-{}^3\Pi_{0^+}$, vary little throughout the series of gallium halides (the values, $-$F to $-$I, are 334, 332, 370, 330 cm^{-1}) or indium halides (816, 796, 786, 649 cm^{-1}).

Finally, the present results throw some light on two anomalies existing in the literature of the molecules of this group.

(i) *The Electronic States of TlF*

The $^3\Pi-{}^1\Sigma$ absorption systems of GaF, InF and TlF appear to be closely analogous: for each molecule, the system at longest wavelength consists of single-headed bands, while the shorter-wavelength system shows two heads in each case. Thus, contrary to Howell (1937), the minimum of the potential curve for the $^3\Pi_{0^+}$ state of TlF lies, as for the other molecules, below that of the $^3\Pi_1$ state. Thus Howell's assignments of the components for TlF must be inverted (see also Herzberg 1950).

(ii) *The Dissociation Energy of AlF*

The present results suggest that the value D_0'' for AlF should lie somewhere between the value for GaF, 6·15 ev, and the rather less certain value, 8·4 ev, which can be derived by extrapolation of the vibrational levels in the state A $^1\Pi$

of BF (Chrétien 1950). Two values have been put forward for D_0''(AlF). Gaydon (1947), from an extrapolation of the ground-state vibrational levels, following Rochester's analysis (1939) of the absorption bands, gives $D'' = ?1{\cdot}8 \pm 0{\cdot}3$ ev, but notes that ionic forces may be important, i.e. that the true value may be higher. A second value, $D'' = 6{\cdot}3_5$ ev, may be derived from the measurements by Gross, Campbell, Kent and Levi (1948) of the standard heat of formation of AlF gas. A revised vibrational analysis of the $^1\Pi - {}^1\Sigma$ system of AlF, on the basis of emission spectrograms (Rowlinson and Barrow, unpublished work) leads in particular to a smaller value of $x_e''\omega_e''$ than was derived by Rochester, and a somewhat higher value of D'', 4·4 ev, is obtained by the ground-state extrapolation. We should expect, by analogy with GaF and InF, that this figure represents about two-thirds of the true value of D'', i.e. $D'' \sim 7$ ev. A better spectroscopic estimate of D'' may however be obtained by extrapolating the vibrational levels in the $^1\Pi$ state; this gives $D'' = 7{\cdot}2$ ev. It is thus established that the dissociation energy of AlF is somewhere around 6 to 7 ev, but there is still a small discrepancy, $0{\cdot}8_5$ ev, between the thermochemical value and what is considered to be the most reliable spectroscopic value. Levels in the $^1\Pi$ state are known high enough to give a lower limit for D'' at 6·65 ev, 0·3 ev above the thermochemical limit. This fact suggests that there is a small maximum in the potential curve for the $^1\Pi$ state of AlF. The potential curves for the $c\,^1\Pi$ states of GaF and InF may be similar, but work on the thermochemistry of these molecules is needed before any definite conclusions about the existence or otherwise of potential maxima in these states can be drawn.

REFERENCES

Chrétien, M., 1950, *Helv. phys. Acta*, **23**, 259.

Froslie, H. M., and Winans, J. G., 1947, *Phys. Rev.*, **72**, 481.

Garton, W. R. S., 1951, *Proc. Phys. Soc.* A, **64**, 509.

Gaydon, A. G., 1947, *Dissociation Energies and Spectra of Diatomic Molecules* (London: Chapman and Hall).

Gross, P., Campbell, C. S., Kent, P. J. C., and Levi, D. L., 1948, *Discussions of the Faraday Society*, No. 4, 206.

Herzberg, G., 1950, *Molecular Structure*: I. *Spectra of Diatomic Molecules* (New York: van Nostrand).

Howell, H. G., 1937, *Proc. Roy. Soc.* A, **160**, 242.

Miescher, E., and Wehrli, M., 1934, *Helv. phys. Acta*, **7**, 331.

M. I. T. Wavelength Tables, 1939, (London: Chapman and Hall).

Rochester, G. D., 1939, *Phys. Rev.*, **56**, 305.

Rosenthaler, E., 1940, *Helv. phys. Acta*, **13**, 355.

Sedov, J., and Filippov, A., 1934, *C.R. Acad. Sci., U.R.S.S.*, **4**, 376.

Sidgwick, N. V., 1950, *Chemical Elements and their Compounds* (Oxford: Clarendon Press).

Wehrli, M., and Miescher, E., 1934, *Helv. phys. Acta*, **7**, 298.

Wenk, W., 1941, *Helv. phys. Acta*, **14**, 355.

On the Utilization of Multiple Scattering Measurements

By D. S. SCHONLAND
Department of Mathematical Physics, University of Birmingham*

Communicated by R. E. Peierls; MS. received 12th March 1952

ABSTRACT. The determination of the product *pv* for particles leaving tracks in photographic emulsions is discussed on the basis of measurements of the scattering in the tracks made by the 'coordinate' method (Fowler 1950), allowing for errors of measurement due to grain size. The use of Fowler's method with the comparatively large interval lengths used in practice is shown to be justifiable in spite of its neglect of much information contained in the track. (This neglect increases the root mean square error in the estimation of the scattering over the minimum attainable error by a factor less than approximately 2·6.) A possible method of estimating *pv*, which approximates to the 'best possible', based on the use of mean squares, is considered, and the root mean square relative error in the estimation found, the necessity for cutting off the scattering distribution at large angles being taken into account. A possible method of estimation based on the use of mean moduli is also discussed.

§ 1. INTRODUCTION AND SUMMARY

When a charged particle passes through matter it undergoes multiple coulomb scattering and, over a region in which the loss of energy by the particle is negligible, the probability distribution of any quantity associated with this multiple scattering depends essentially on the value of the product *pv*, where p is the (relativistic) momentum of the particle and v is its velocity. For an ionizing particle leaving a track in a photographic emulsion a measurement of the multiple scattering in the track therefore affords a means of estimating *pv* for the particle: in conjunction with a measurement of its velocity (specific ionization) or energy (residual range), this estimate can be used to give complete information about the mass and energy of the particle. Scattering measurements are particularly useful for fast particles which do not come to rest in the emulsion or which produce a nuclear event before coming to rest, since for these the range–energy relation cannot be used. It is thus of importance to discuss ways of measuring the scattering and of estimating *pv* from the measurements, and to find the probable error in these estimates.

In discussing this problem, specific allowance must be made for the unavoidable errors caused by the finite size of the grains forming the track; a measurement of the position of the centre of a grain will give information about the position of a point on the actual path of the particle only within a certain accuracy, since developable grains off its direct path may be formed by the ionizing particle. It will be assumed here that these errors have a gaussian probability distribution, of width approximately equal to that of a grain diameter, and that this distribution is independent of the multiple scattering. No other sources of error will be considered, and it will be further assumed that the loss of energy by the particle is negligible along the portion of its track that is measured.

---

* Now at Department of Mathematics, University of Southampton.

The theory of multiple scattering has been discussed by several authors (Williams 1939, Molière 1948, Snyder and Scott 1949, 1950). The results of Snyder and Scott have been found to be in satisfactory agreement with experiment (Corson 1950) and will be used below when numerical estimates of quantities associated with the multiple scattering distribution are required.

The maximum amount of information about a track would be obtained if the position of every grain in it were measured. Apart from the practical difficulty of making such a measurement, the analysis of the results would be complicated (Moyal 1950). This paper will therefore be concerned with the treatment of the information obtained from the 'coordinate' method of measuring up tracks developed by Fowler (1950), which is the most accurate so far described and which can in principle be extended to yield almost all the information contained in the track.

In Fowler's method the projected angles between successive equal chords of the track are measured. These measurements give the true multiple scattering angles combined with errors due to the finite grain size, and since these effects are statistically independent, the obvious method of obtaining information about the multiple scattering is to use mean square values of the scattering angles. This introduces a difficulty, however, since, because of the Rutherford scattering law, the mean square value of the chord angle diverges logarithmically in small angle approximation, and to give it a well-defined meaning some method of cutting off the observations at large angles must be used. This difficulty would not arise directly if mean moduli were used instead of mean squares, but one would then be faced with great analytical difficulties in removing the effects of the errors of measurement, and some sort of cut-off would probably still be necessary in order to minimize the statistical errors. It has therefore seemed most practical to discuss the problem with the use of mean squares and to introduce an explicit method of cutting off the observations.

In §§2 and 3 of this paper, the problem is discussed on the (incorrect) assumption that the mean square quantities introduced are well defined. §2 is concerned with the 'minimum possible' error in the estimation of the scattering, while in §3 the corresponding 'best possible' equations are discussed. Their form leads to the consideration of a particular method of estimation which is shown to approximate to the 'best possible' when the interval length used in the measurements is not too small. The discussion also leads to a justification of the use of Fowler's method with comparatively large interval lengths, in spite of the consequent neglect of possible information about the scattering which might be obtained from the track.

In the remainder of the paper the effect of the introduction of a cut-off is considered. In §4 a cut-off criterion, depending on a cut-off parameter, is laid down and its effect on the results of §3 is discussed, resulting in the postulation of an equation for determining the cut-off mean square chord angle and an expression for the mean square error of this estimation. §5 is concerned with the estimation of the product pv and the determination of the best conditions for measurement, including the best value to choose for the cut-off parameter. Finally, in §6, a systematic error in the estimation of the scattering, due to the method of cut-off used, is discussed and shown to be negligible, and in §7 a possible method of using mean moduli is considered.

Notation. Apart from symbols defined in the text, the following general notation has been used. If β_n is an angle derived from the nth of the measurements of angle made on the track, its mean square expectation value is denoted by b_0, while the expectation value of the product $\beta_n\beta_{n+r}$ is denoted by b_r. The corresponding mean values taken over the actual measurements are indicated by enclosing the symbol in triangular brackets, thus $\langle b_r\rangle$. Finally, the relative root mean square error in the estimation of some quantity x from the measurements is denoted by $\mathbf{F}(x)$, so that the actual root mean square error is $x\mathbf{F}(x)$.

§ 2. THE 'MINIMUM POSSIBLE' ERROR*

(i) *Correlations between the Chord Angles and Statistically Independent Variables*

In Fowler's method the track, which is nearly straight for a fast particle, is aligned along the x axis of a microscope stage and its y coordinates, y_n, are read off at equal intervals τ along the x axis. Since the scattering angles are small, the quantities

$$\beta_n = \frac{1}{\tau}(y_{n+1} - 2y_n + y_{n-1}) \qquad \ldots\ldots(1)$$

are the projected angles between successive equal chords of the track. In accordance with the programme outlined above, one writes

$$\beta_n = \alpha_n + \epsilon_n, \qquad \ldots\ldots(2)$$

where α_n is the true chord angle due to multiple scattering, and ϵ_n is the error in its measurement. Then, since the α_n and ϵ_n are statistically independent (using the notation described in the introduction),

$$b_0 = a_0 + e_0, \quad b_r = a_r + r_r, \qquad \ldots\ldots(3)$$

on the assumption that the mean squares are well defined. With this assumption it can be shown (Appendix A) that, independently of the exact form of the α and ϵ distributions,

$$b_1 = a_0/4 - 2e_0/3;\; b_2 = e_0/6;\; b_r = 0,\; r > 2; \qquad \ldots\ldots(3\,a)$$

and that a_0 is proportional to τ and e_0 to τ^{-2}, so that the 'signal/noise' ratio $\nu = a_0/e_0$ is related to the interval length by

$$\nu = (\tau/\tau_0)^3, \qquad \ldots\ldots(4)$$

where τ_0 is the value of τ for which $\nu = 1$, and depends on the characteristics of the track under examination.

The calculation of probable errors is greatly facilitated by the introduction of certain linear combinations of the β_n which are almost statistically independent. If one adds to the set of measured angles β_n, $n = 1, 2, \ldots, N$ the fictitious angle $\beta_0 = 0$, one may regard this whole set of angles as coefficients in a Fourier expansion of a set of variables

$$\phi_p = \left(\frac{2}{N+1}\right)^{1/2} \sum_{n=0}^{N} \beta_n \sin\frac{2\pi np}{N+1},\; p = 0, 1, \ldots, N; \qquad \ldots\ldots(5\,a)$$

then

$$\beta_n = \left(\frac{2}{N+1}\right)^{1/2} \sum_{p=0}^{N} \phi_p \sin\frac{2\pi np}{N+1},\; n = 0, 1, \ldots, N, \qquad \ldots\ldots(5\,b)$$

and these equations allow one to express results either in terms of the ϕ_p or the measured angles β_n.

---

* Some of the results for the gaussian case given in this section were derived in unpublished calculations by Dr. M. Krook.

From eqns. (5) and (3) it is readily shown that the correlations between the ϕ_p are given by

$$\overline{\phi_p\phi_q} = \Phi_p{}^2\delta_{pq} + \frac{4}{N+1}\, b_2 \sin\frac{2\pi p}{N+1}\sin\frac{2\pi q}{N+1}, \qquad \ldots\ldots(6)$$

where

$$\Phi_0 = 0;\ \Phi_p{}^2 = b_0 + 2b_1\cos\frac{2\pi p}{N+1} + 2b_2\cos\frac{4\pi p}{N+1},\ p = 1, \ldots, N. \qquad \ldots\ldots(7)$$

If the second term on the right-hand side of (6), which is of order $1/N$, is neglected, the ϕ_p may be regarded as statistically independent, with a mean square value given by (7) which becomes, on substitution from (3 *a*),

$$\begin{aligned}\Phi_p{}^2 &= \tfrac{1}{2}a_0\left(2 + \cos\frac{2\pi p}{N+1}\right) + \tfrac{2}{3}e_0\left(1 - \cos\frac{2\pi p}{N+1}\right)^2\\ &= \frac{2}{3}\,\frac{a_0}{\nu}\left[\left(1 - \cos\frac{2\pi p}{N+1}\right)^2 + \frac{3\nu}{4}\left(2 + \cos\frac{2\pi p}{N+1}\right)\right]. \qquad \ldots\ldots(8)\end{aligned}$$

This approximation materially simplifies the calculation of probable errors, and is quite justifiable when N is large, since one does not require great accuracy in the estimation of probable errors.

(ii) *The 'Minimum Possible' Error*

In order to judge any particular method of estimating a_0 one must know what the inherent limitations on the accuracy of estimation are, as determined by the probability distribution of the measurements. Using the ϕ_p variables, let

$$\begin{aligned}&p(\phi_1, \ldots, \phi_N | a_0, e_0)\, d\phi_1 \ldots d\phi_N\\ &\quad = \text{constant} \,.\, \exp\{-\tfrac{1}{2}g(\phi_1, \ldots, \phi_N | a_0, e_0)\} d\phi_1 \ldots\ldots d\phi_N \qquad \ldots\ldots(9)\end{aligned}$$

be the probability of 'observing' $\phi_1, \ldots, \phi_N$ for given a_0 and e_0. Then, from the principle of inverse probability, the probability of a_0 and e_0 having specified values for a given set of observations $\phi_1, \ldots, \phi_N$ is

$$P(a_0, e_0 | \phi_1, \ldots, \phi_N)\, da_0 de_0 = A\exp\{-\tfrac{1}{2}g(\phi_1, \ldots, \phi_N | a_0, e_0)\} da_0\, de_0, \qquad \ldots\ldots(10)$$

where A contains the prior probabilities of a_0 and e_0.

The most probable values of a_0 and e_0 for given $\phi_1, \ldots, \phi_N$ will be those which make (10) a maximum. That is, assuming that the prior probabilities of a_0 and e_0 are constant or only slowly varying functions, the most probable values of a_0 and e_0 are the solutions of

$$\partial g/\partial a_0 = 0;\ \partial g/\partial e_0 = 0. \qquad \ldots\ldots(11)$$

These are the 'best possible' equations for estimating a_0 and e_0, making the maximum use of the observations.

Suppose the solutions of (11) are $a_0{}^{\mathrm{m}}$, $e_0{}^{\mathrm{m}}$, and put $x = a_0 - a_0{}^{\mathrm{m}}$, $y = e_0 - e_0{}^{\mathrm{m}}$. Then, in virtue of (11),

$$\begin{aligned}g(a_0, e_0) &= g(a_0{}^{\mathrm{m}}, e_0{}^{\mathrm{m}}) + \frac{1}{2}\left[\left(x\frac{\partial}{\partial a_0} + y\frac{\partial}{\partial e_0}\right)^2 g\right]_{\mathrm{m}} + \ldots\\ &= g_{\mathrm{m}} + (ax^2 + 2bxy + cy^2) + \ldots\end{aligned}$$

where $\quad a = \tfrac{1}{2}\partial^2 g/\partial a_0{}^2;\ b = \tfrac{1}{2}\partial^2 g/\partial a_0\partial e_0;\ c = \tfrac{1}{2}\partial^2 g/\partial e_0{}^2. \qquad \ldots\ldots(12)$

Thus $\quad P(a_0, e_0 | \phi_1, \ldots, \phi_N)\, da_0\, de_0 \simeq P_{\mathrm{m}}\exp\{-\tfrac{1}{2}(ax^2 + 2bxy + cy^2)\}\, dx\, dy.$

Using this expression for P, it is clear that the mean square error associated with the 'best possible' determination of a_0 is given by

$$[a_0\mathbf{F}_{\mathrm{M}}(a_0)]^2 \equiv \overline{x^2} = [a - b^2/c]^{-1}. \qquad \ldots\ldots(13)$$

The definition of a, b and c by (12) depends explicitly on the 'observed' values of the ϕ_p. It will, however, give rise to only a small error if these 'observed' values are replaced by their expectation values after the differentiations have been performed, and one may assume that this has been done in (13).

To proceed further one needs to know the function $g(\phi_1, \ldots, \phi_N | a_0, e_0)$ determined by the combined probability distribution of $\phi_1, \ldots, \phi_N$. The exact expression for the distribution cannot be put into manageable form, but one may obtain an approximate evaluation by assuming that the α_n have a gaussian distribution. On this assumption, the ϕ_p will also have a gaussian distribution since each ϕ_p is a linear combination of the α_n and ϵ_n. Then, because the ϕ_p are taken as statistically independent,

$$p(\phi_1, \ldots, \phi_N | a_0, e_0) = (2\pi)^{-N/2} \prod_{p=1}^{N} \Phi_p^{-1} \exp\{-\tfrac{1}{2}\phi_p^2/\Phi_p^2\}$$

which gives $$g(\phi_1, \ldots, \phi_N | a_0, e_0) = \sum_{p=1}^{N} \{\log \Phi_p^2 + \phi_p^2/\Phi_p^2\}, \qquad \ldots\ldots(14)$$

where Φ_p^2, given by (8), is a function of a_0 and e_0. The quantities a, b and c can be found from (14) and, on replacing the observations ϕ_p^2 by their expectation values Φ_p^2 after differentiation and transforming sums over p to integrals, one obtains from (13)

$$\mathbf{F}_{\mathrm{M}}^2(a_0) = \frac{32}{9}\,\frac{1}{(N+1)\nu^2}[I_{20} - I_{11}^2/I_{02}]^{-1}, \qquad \ldots\ldots(15)$$

where

$$I_{mn}(\nu) = \frac{1}{2\pi}\int_0^{2\pi} \frac{(2+\cos k)^m (1-\cos k)^{2n}}{[(1-\cos k)^2 + \frac{3}{4}\nu(2+\cos k)]^2}\,dk. \qquad \ldots\ldots(16)$$

To discuss the variation of the 'minimum possible' error as given by (15) with the interval length one must express the number of observations in terms of τ or ν. Suppose that the total length of track available for measurement is T. Then

$$N+1 = T/\tau = \nu^{-1/3}(T/\tau_0) \qquad \ldots\ldots(17)$$

and (15) can be written as

$$(T/\tau_0)\mathbf{F}_{\mathrm{M}}^2(a_0) = 32\nu^{-5/3}[I_{20} - I_{11}^2/I_{02}]^{-1}/9. \qquad \ldots\ldots(18)$$

For a given track, i.e. given T and τ_0, (18) exhibits the variation of $\mathbf{F}_{\mathrm{M}}(a_0)$ with $\nu = (\tau/\tau_0)^3$; the quantity $(T/\tau_0)^{1/2}\mathbf{F}_{\mathrm{M}}(a_0)$ is plotted as a function of τ/τ_0 in fig. 1 (the broken curve I).

It may happen that for a number of similar tracks in an emulsion an accurate estimation of the 'noise' e_0 is possible. In this case the 'best possible' equation for a_0 is simply $\partial g/\partial a_0 = 0$ and the corresponding 'minimum possible' error is given by (18) with the term in I_{11}^2/I_{02} (which arises from uncertainties in the estimation of e_0) omitted. This 'minimum possible' error is plotted in fig. 1 as the broken curve II. The two errors coincide for small values of τ/τ_0 as one would expect, and both show a very slow decrease in the 'minimum possible' error with interval length. Evaluation of the integrals in (18) for $\tau/\tau_0 \ll 1$ shows in fact that for small interval lengths

$$(T/\tau_0)^{1/2}\mathbf{F}_M(a_0) \simeq 2\cdot 1(\tau/\tau_0)^{1/8}. \qquad \ldots\ldots(19)$$

This slow decrease of the minimum possible error with small interval lengths will be shown, at the end of the next section, to justify the use of Fowler's method with the comparatively large interval lengths that are convenient in practice.

§ 3. THE ESTIMATION OF a_0

(i) *The 'Best Possible' Equations*

The explicit expression (14) for the function $g(\phi_1, \ldots, \phi_N | a_0, e_0)$ enables one to write down the 'best possible' equations (11) for a gaussian multiple scattering distribution. These equations are

$$\frac{\partial g}{\partial a_0} \equiv \sum_p \frac{1}{\Phi_p^4} \frac{\partial \Phi_p^2}{\partial a_0} [\phi_p^2 - \Phi_p^2] = 0 ; \quad \frac{\partial g}{\partial e_0} \equiv \sum_p \frac{1}{\Phi_p^4} \frac{\partial \Phi_p^2}{\partial e_0} [\phi_p^2 - \Phi_p^2] = 0, \qquad \ldots\ldots(20)$$

and, using the expression (8) for Φ_p^2, may be written in the form

$$(a_0)_{\text{est}} = \frac{1}{N+1} \sum_p k_p(\nu) \phi_p^2 , \qquad \ldots\ldots(21)$$

with a similar expression for $(e_0)_{\text{est}}$. The form of (21) and the explicit expression for the $k_p(\nu)$ obtained from (20) both result from the assumption of a gaussian scattering distribution. The 'best possible' equation for a general non-gaussian distribution will differ from (21), but one may assume that, provided the distribution has a well-defined mean square, an equation of the form (21) with suitable choice of the coefficients $k_p(\nu)$ will give results lying close to the 'best possible' with a statistical error of the order of magnitude of the 'minimum possible error'. The fact that (21) must become an identity when $(a_0)_{\text{est}}$ and the 'measurements' ϕ_p^2 are replaced by their expectation values a_0 and Φ_p^2 imposes general conditions on the k_p, namely that when in the right-hand side of (21) ϕ_p^2 is replaced by Φ_p^2 the coefficient of a_0 must be unity and that of e_0 must vanish. These conditions are, from (8),

$$\frac{1}{2(N+1)} \sum_p k_p(\nu) \left[2 + \cos \frac{2\pi p}{N+1} \right] = 1 ; \quad \sum_p k_p(\nu) \left[1 - \cos \frac{2\pi p}{N+1} \right]^2 = 0, \qquad \ldots\ldots(22)$$

and imply that (expanding $k_p(\nu)$ in a Fourier series) the 'best possible' equation (21) is necessarily of the form

$$(a_0)_{\text{est}} = \frac{1}{N+1} \frac{4}{4+\mu} \sum_p \left[1 + \mu \cos \frac{2\pi p}{N+1} + (4\mu - 6) \cos \frac{4\pi p}{N+1} + \sum_{n>2} \lambda_n \cos \frac{2\pi p n}{N+1} \right] \phi_p^2, \qquad \ldots\ldots(23)$$

where the actual values of the coefficients $\mu(\nu)$ and $\lambda_n(\nu)$ will depend on the scattering distribution. Application of the transformation (5) to (23) gives the general form of the 'best possible' equation for the estimation of a_0 in terms of the actual measurements β_n:

$$(a_0)_{\text{est}} = \frac{4}{4+\mu} \left\{ \langle b_0 \rangle + \mu \langle b_1 \rangle + (4\mu - 6) \langle b_2 \rangle + \sum_{r>2} \lambda_r \langle b_r \rangle \right\}. \qquad \ldots\ldots(24)$$

(Since the derivation of (23) neglected the small correlations that do exist between the ϕ_p, the application of (5) to (23) will produce some spurious terms; these are easily recognizable and have been dropped from (24).)

(ii) *A Possible Method of Estimation*

One would expect the terms in (24) involving $\langle b_r \rangle$ with $r>2$ to have a small effect on the estimation, since they have zero expectation value, and thus that a good approximation to the 'best possible' equation (24) would be*

$$(a_0)_{\text{est}} = \frac{4}{4+\mu}\{\langle b_0\rangle + \mu\langle b_1\rangle + (4\mu-6)\langle b_2\rangle\}, \qquad \ldots\ldots(25)$$

with the parameter μ suitably chosen. A particular form of (25) corresponding to $\mu=8/5$ is

$$(a_0)_{\text{est}} = \tfrac{1}{7}\{4\langle b_0''\rangle - \langle b_0\rangle\}, \qquad \ldots\ldots(25\,a)$$

where b_0'' refers to the angle between adjacent equal chords of the track of length 2τ. This form of the equation can be directly derived by considering the dependence of a_0 and e_0 on the interval length, and is particularly simple to use in practice.

The root mean square error associated with the estimation of a_0 by (25) can be evaluated by writing the equation in terms of the ϕ_p; neglecting small terms of order $1/N$ due to end effects, the equation is of the form (21) with

$$k_p = \frac{4}{4+\mu}\left[1+\mu\cos\frac{2\pi p}{N+1} + (4\mu-6)\cos\frac{4\pi p}{N+1}\right], \qquad \ldots\ldots(26)$$

and consequently the mean square error in the estimation of a_0 by (25) is

$$[a_0\mathsf{F}(a_0)]^2 \equiv \overline{[(a_0)_{\text{est}} - a_0]^2} = \frac{1}{(N+1)^2}\sum_p k_p^2(\overline{\phi_p^4} - \Phi_p^4), \qquad \ldots\ldots(27)$$

since the ϕ_p are taken to be statistically independent.

Now ϕ_p is the sum of two statistically independent parts depending on the α_n and ϵ_n respectively; $\phi_p = \phi_p(\alpha) + \phi_p(\epsilon)$. Hence

$$\overline{\phi_p^4} - \Phi_p^4 = \overline{\phi_p^4(\alpha)} - \Phi_p^4(\alpha) + \overline{\phi_p^4(\epsilon)} - \Phi_p^4(\epsilon) + 4\Phi_p^2(\alpha)\Phi_p^2(\epsilon), \qquad \ldots\ldots(28)$$

and, since the ϵ_n are assumed to have a gaussian distribution, $\overline{\phi_p^4(\epsilon)} = 3\Phi_p^4(\epsilon)$. Thus the part of (27) depending on the last three terms in (28) can be evaluated by using (26) and the appropriate expressions for $\Phi_p^2(\alpha)$ and $\Phi_p^2(\epsilon)$ obtained from (8). Since the gaussian assumption is *not* made for the α_n, however, no such simple calculation is possible for the remaining terms of (27). The best way to find these is to rewrite them in terms of the α_n; the various expectation values involved (of the type $\overline{\alpha_n^4}$, $\overline{\alpha_n^3\alpha_{n+1}}$, etc.) can be found by the methods of Appendix A, and expressed in terms of a_0 and the quantity

$$\kappa = \overline{\alpha_n^4}/\alpha_0^2, \qquad \ldots\ldots(29)$$

and the summation can then be carried out.

The final expression obtained for the relative mean square error in the estimation of a_0 by (25) is

$$\mathsf{F}^2(a_0) = \frac{1}{N+1}\,\frac{8}{(4+\mu)^2}\{A\mu^2 - B\mu + C\}, \qquad \ldots\ldots(30)$$

---

* This equation was suggested by Dr. F. J. Dyson.

where

$$\left.\begin{aligned} A &= \frac{367}{8} + \frac{\kappa}{6} + \frac{104}{3\nu} + \frac{361}{9\nu^2} \\ B &= 117 - \kappa + \frac{354}{3\nu} + \frac{1208}{9\nu^2} \\ C &= \frac{151}{2} + \frac{7\kappa}{3} + \frac{304}{3\nu} + \frac{1012}{9\nu^2}. \end{aligned}\right\} \qquad \ldots\ldots(31)$$

The actual shape of the scattering distribution thus affects the error only through the occurrence of the quantity κ in A, B and C.

(iii) *Comparison with the 'Best Possible' Method*

Expressing the number of observations N in terms of T, τ_0 and ν, as in (17), one may write (30) in a form analogous to (18):

$$(T/\tau_0)\mathbf{F}^2(a_0) = \frac{8}{(4+\mu)^2}\,\nu^{1/3}\{A\mu^2 - B\mu + C\}. \qquad \ldots\ldots(32)$$

Comparison of (32) with (18) will then show how near, in fact, the estimation of a_0 by (25) approaches the 'best possible' estimation. This comparison is made in fig. 1, taking $\kappa=3$ in (31), the value appropriate to a gaussian scattering distribution. In the figure the solid curve A shows the envelope of $(T/\tau_0)^{1/2}\mathbf{F}(a_0)$ calculated from (32) when the best value of μ is chosen for each value of ν, while the curve B is obtained from (32) with $\mu=8/5$, giving the error in the estimation of a_0 by (25 *a*).

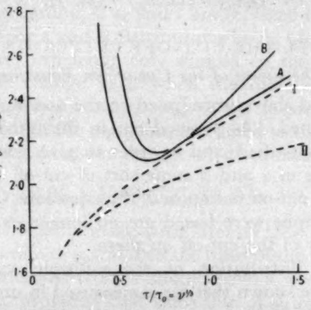

Fig. 1. I: The 'minimum possible' relative r.m.s. error in the estimation of a_0 when e_0 is unknown; II: the same quantity when e_0 is known from other measurements.
A: The relative r.m.s. error in the estimation of a_0 from (25) when the parameter μ is chosen appropriate to each value of ν; B: the same quantity when in (25) $\mu=8/5$. (All these curves assume a gaussian scattering distribution.)

Figure 1 shows that (25) gives results close to the 'best possible' provided $\tau/\tau_0 \gtrsim 0{\cdot}7$, while for smaller values of τ/τ_0 it becomes very bad. The general form (24) of the 'best possible' equation indicates that the estimation can be improved by adding terms in $\langle b_r \rangle$ with $r>2$ to the right-hand side of (25), and an analysis similar to that given above shows that if a term $\lambda\langle b_3 \rangle$ is added to (25) the resulting estimation, with proper choice of μ and λ, remains good down to $\tau/\tau_0 \simeq 0{\cdot}45$, after which the error again increases rapidly. Because of the slow decrease of the 'minimum possible' error with the interval length, this improved method of estimation can only increase the accuracy of an estimation based on the best use of (25) by 8%, and it is evident that to obtain any marked improvement on (25) very small interval lengths would have to be used, with a correspondingly great increase in the labour of estimation. Now the finite spacing of the grains forming the track imposes a lower limit $\tau_{\min}$ on possible values of τ and consequently on the minimum possible attainable error. If one uses (19) for this minimum error, taking $\tau_{\min}$ to be the average spacing of the grains in the track and τ_0, the interval length corresponding to unit 'signal/noise' ratio, to lie between 100–500 μ, it appears that the greatest possible improvement that can be made on estimates based on measurements with $\tau/\tau_0 \simeq 1$ is a reduction of the root mean square error by a factor lying roughly between 1·8 and 2·6. This comparatively small decrease in the error does not justify the elaborate technique that it would require for the estimation of a_0, and for practical purposes one may therefore conclude that Fowler's method with the comparatively large interval lengths implied by $\tau \simeq \tau_0$ is quite justifiable, and that for these intervals an estimation based on (25) will give good results.

This result has been obtained on the assumption of a gaussian scattering distribution, which is incorrect. Its qualitative aspect, however, should be largely independent of this assumption and may reasonably be applied to the cut-off scattering distribution.

In order to find the value of ν corresponding to a given interval length, it is necessary to estimate e_0. This can be done in a way analogous to (25); the equation for e_0 corresponding to (25 *a*) is

$$(e_0)_{\text{est}} = \tfrac{4}{7}\{2\langle b_0 \rangle - \langle b_0'' \rangle\}. \qquad \ldots\ldots(33)$$

§4. THE CUT-OFF CRITERION

(i) *The Effect of the Cut-off on Equation* (25)

The results obtained above were based on the assumption that the quantities a_0 and e_0 are well defined. As pointed out in the introduction, however, this assumption is quite unjustified, and in order to give a well-defined meaning to the mean square values of α and β some sort of cut-off must be applied to the observations. When a cut-off is imposed, the equations (3) on which the results of the previous paragraphs were based are no longer exact and it is necessary to investigate the effect of the cut-off on them.

If $W(\alpha)\,d\alpha$ is the distribution of the multiple scattering chord angle, Snyder and Scott* have shown that for α measured in units of the quantity

$$\rho = K\tau^{1/2}/pv \qquad \ldots\ldots(34)$$

(where K is a constant depending only on the properties of the emulsion and the charge of the ionizing particle) so that $\alpha = \rho\alpha'$, one may write

$$W(\alpha)\,d\alpha = w(\alpha')\,d\alpha',$$

where the distribution $w(\alpha')$ is very nearly independent of the interval length.

Suppose that the β distribution is cut off at $\beta = \pm\theta$. Then denoting angles measured in units of ρ by a prime, the cut-off β' distribution is

$$P(\beta')\,d\beta' = \begin{cases} \int_{-\infty}^{\infty} d\epsilon' q(\epsilon') w(\beta' - \epsilon') \,.\, d\beta'; & |\beta'| \leqslant \theta', \\ 0 & ; \; |\beta'| > \theta', \end{cases} \qquad \ldots\ldots(35)$$

---

* See Appendix B for a discussion of the Snyder–Scott results.

and the mean square value of β' over this cut-off distribution is

$$b_{0c}' = \int_{-\infty}^{\infty} d\epsilon' \int_{-\theta'}^{\theta'} d\beta' \beta'^2 q(\epsilon') w(\beta' - \epsilon') \bigg/ \int_{-\infty}^{\infty} d\epsilon' \int_{-\theta'}^{\theta'} d\beta' q(\epsilon') w(\beta' - \epsilon'), \quad \ldots (36)$$

where $q(\epsilon')$ is the probability distribution for the error ϵ'. Now $q(\epsilon')$ has a sharp maximum for $\epsilon' = 0$ and falls off very rapidly for large values of ϵ'. Thus if the cut-off angle θ is chosen so that $q(\theta')$ is small and if the 'signal/noise' ratio is not too small, one may assume that any value of the measured angle that is comparable with θ is due mainly to an exceptionally large multiple scattering, the error of measurement contributing only slightly to its size. Then a reasonable approximation to (36) is obtained by expanding the integrands in a Taylor series about $\epsilon' = 0$ and retaining only the first few terms. The result of this expansion gives

$$b_{0c}' = a_{0c}'[1 + (1-\gamma)/\nu_c], \quad \ldots\ldots(37)$$

where a_{0c}' is the mean square value of α' when the α' distribution is cut off at angle θ', $\nu_c = a_{0c}/e_0$ and γ is a quantity depending on θ' and ν_c, which is small for large θ' and ν_c not too small. (For the values of θ' and ν_c finally chosen as the best for measurements, $\gamma \simeq 0{\cdot}1$.)

This expression for b_{0c}' is to be compared with the first of equations (3) which, on writing $e_0 = a_0/\nu$, becomes $b_0' = a_0'[1 + 1/\nu]$. The only difference in the form of the two equations is the presence of the small number γ in (37), so that it appears that the results obtained on the basis of (3) will be approximately correct for the cut-off distribution, if a_0 and ν are replaced by their cut-off values a_{0c} and ν_c, the cut-offs for the α and β distributions being identical.

.A
5
2

In particular, since $w(\alpha')$ depends only slightly on the interval length, it is reasonable to neglect the change in it when the interval length is doubled. With this approximation, γ is a constant, $a_{0c} = \rho^2 a_{0c}'$ is proportional to τ and ν_c to τ^3, so that the form (25 *a*) of the equation developed in the previous paragraph for estimating a_0 may be retained for the cut-off distribution with confidence:

$$(a_{0c})_{\text{est}} = \tfrac{1}{7}[4\langle b_{0c}''\rangle - \langle b_{0c}\rangle], \quad \ldots\ldots(38)$$

where b_{0c}'' refers to measurements made with interval length 2τ. This equation will give a good approximation to a_{0c}, and on the basis of the arguments developed above, the value of a_{0c} estimated from it should have a mean square error close to the minimum possible, provided that the value of ν_c for the measurements is correctly chosen by suitable choice of the interval length. (From the way in which (25) was derived, it is evident that the procedure for using (38) is to cut off the original sample of values of β_n, and to form the β_n'' from those that are retained.)

The expression (30) for the error associated with an estimation by means of (25) may also be retained if ν is replaced by ν_c, N by N_c the number of observations kept in the cut-off set of measurements, and κ by κ_c, its value for the cut-off α distribution, while μ is put equal to 8/5, the value appropriate to (25 *a*). The approximations involved here are the postulation of equations (3) with a_0 replaced by a_{0c}, and the neglect of the local destruction of correlations caused by the rejection of a particular β_n. These approximations are reasonable since no very accurate estimate of the error is required.

(ii) *Postulation of a Cut-off Criterion*

The method of cut-off used is rather arbitrary. The criterion discussed below is simple and its consequences easily evaluated. Define

$$a_{0c}=\int_{-\theta}^{\theta}\alpha^2 W(\alpha)\,d\alpha\Big/\int_{-\theta}^{\theta}W(\alpha)\,d\alpha \quad \text{with} \quad \theta^2=\lambda a_{0c}, \qquad \ldots\ldots(39)$$

where λ is the cut-off parameter. (39) defines a_{0c} uniquely for each value of λ, and the estimation of a_{0c} from the measurements proceeds simply as follows, since one assumes that any large value of β_n arises from a large multiple scattering deviation, with a comparatively small contribution from the error of measurement: find $(a_{0c})_{\text{est}}$ from (38) for some arbitrary, small value of the cut-off and determine $\theta^2_{\text{est}}=\lambda(a_{0c})_{\text{est}}$. Then reject all the β_n for which $\beta_n^2>\theta^2_{\text{est}}$ and recalculate $(a_{0c})_{\text{est}}$ and θ^2_{est} with this new cut-off. Carrying on this process will eventually result in a steady state, and the final values of $(a_{0c})_{\text{est}}$ and θ^2_{est} are taken as estimates of a_{0c} and θ^2.

Suppose that δa_{0c} is the error in this estimate of a_{0c}. Then

$$\delta a_{0c}=(\delta a_{0c})_s+(da_{0c}/d\theta^2)\,\delta\theta^2, \qquad \ldots\ldots(40)$$

where $\delta\theta^2$ is the error in the estimate of θ^2, and $(\delta a_{0c})_s$ is the error due to statistical fluctuations in (38). Now $\theta^2_{\text{est}}=\lambda(a_{0c})_{\text{est}}$, therefore $\delta\theta^2=\lambda\delta a_{0c}$ and substituting for $\delta\theta^2$ in (40) gives

$$\delta a_{0c}=[1-\lambda(da_{0c}/d\theta^2)]^{-1}(\delta a_{0c})_s.$$

Thus the relative root mean square error, $\mathsf{F}_c(a_{0c})$, in the estimation of a_{0c} defined by (39), from (38) is

$$\mathsf{F}_c(a_{0c})=[1-\lambda(da_{0c}/d\theta^2)]^{-1}\mathsf{F}(a_{0c}), \qquad \ldots\ldots(41)$$

where $\mathsf{F}(a_{0c})$ is given by (30) with the changes described in (i) above. This equation will be used in the following section as the basis for deciding on the best value to choose for the cut-off parameter λ.

§ 5. THE ESTIMATION OF *pv* AND THE BEST CONDITIONS FOR MEASUREMENT

Expressing the equations (39) in terms of angles measured in units of ρ one has

$$a_{0c}=\rho^2 G(\theta'), \qquad \ldots\ldots(42)$$

where $$G(\theta')=\int_{-\theta'}^{\theta'}\alpha'^2 w(\alpha')\,d\alpha'\Big/\int_{-\theta'}^{\theta'}w(\alpha')\,d\alpha', \quad \theta'^2=\lambda G(\theta'). \qquad \ldots\ldots(43)$$

Now the distribution $w(\alpha')$ depends on the interval length by being a slowly varying function of n, the average number of scatterings suffered by the ionizing particle in the traversal of one interval length. This number can be determined if the velocity of the particle is known, and so can be estimated independently of the scattering measurements. Assuming it to be known, eqns. (43) can be solved to give the value of θ' and $G(\theta')$ corresponding to the value of the cut-off parameter λ chosen. Hence, by substituting the estimated value of a_{0c} in (42), ρ and so pv can be calculated.

The error $\delta\rho$ in the calculation of ρ from (42) is related to the error δa_{0c} in the estimation of a_{0c} by $\delta\rho/\rho=\frac{1}{2}\delta a_{0c}/a_{0c}$. Hence $\mathsf{F}(pv)$ the relative root mean square error in the determination of pv when a_{0c} is estimated in the manner indicated in § 4 is

$$\mathbf{F}(pv)=\mathbf{F}(\rho)=\tfrac{1}{2}\mathbf{F}_c(a_{0c}), \qquad \ldots\ldots(44)$$

where $\mathbf{F}_c(a_{0c})$ is the expression (41). Using (43), the term in (41) depending on $da_{0c}/d\theta^2$ can be expressed in terms of θ', $w(\theta')$ and λ and from (30) and (41) one finds

$$\mathbf{F}(pv)=\tfrac{1}{2}[1-(\lambda-1)\theta' w(\theta')/p(\theta')]^{-1}\left(\frac{8}{N+1}\right)^{1/2}\frac{1}{4+\mu}[A\mu^2-B\mu+C]^{1/2}, \qquad \ldots(45)$$

where

$$p(\theta')=\int_{-\theta'}^{\theta'} w(\alpha')\,d\alpha'. \qquad \ldots\ldots(46)$$

Here A, B and C are given by (31) with ν replaced by ν_c and κ by κ_c, and $\mu=8/5$ the value appropriate to an equation of the form (38). From the definition of $p(\theta')$, the number of β_n retained after the cut-off has been applied will be $N_c=p(\theta')N$ on the average. Then, writing N in terms of τ_0 and the total length T of measured track, and substituting the numerical values of A, B and C, (45) can be written explicitly as

$$(T/\tau_0)^{1/2}\mathbf{F}(pv)=\frac{5\sqrt{2}}{28}\,\frac{\{p(\theta')\}^{1/2}}{p(\theta')-(\lambda-1)\theta' w(\theta')}\left[\nu_c^{1/3}\left(4{\cdot}36\kappa+5{\cdot}74+\frac{1{\cdot}28}{\nu_c}+\frac{0{\cdot}27}{\nu_c^2}\right)\right]^{1/2}. \qquad \ldots\ldots(47)$$

This expression for the relative error in the estimation of pv depends on two parameters, viz. ν_c the 'signal/noise' ratio for the track and interval length considered and λ the cut-off parameter. For any particular track, the 'signal/noise' ratio can be made to take any value (within limits) by suitable choice of the interval length. The parameter λ, on the other hand, should be fixed once and for all for every track, to enable comparisons of different tracks to be made without the necessity of calculating pv from a_{0c} each time.

To find λ_m, the best value for the cut-off parameter λ, one first, for given λ, finds the minimum of the right-hand side of (47) with respect to ν_c; λ_m is then the value of λ for which this minimum is least. Carrying out this procedure, one finds (taking as a reasonable value of the average number of scatterings per interval length $n=1{\cdot}5\times10^3$) $\lambda_m=18$, and that λ can vary somewhat about this value without affecting the error appreciably.

Using $\lambda=18$, the quantity $(T/\tau_0)^{1/2}\mathbf{F}(pv)$ is plotted as a function of (τ/τ_0) in fig. 2. From this plot one can find the probable error in the estimate of pv when the value of ν_c corresponding to the interval length used for the measurements is known. It is evident that one should always try to work with interval lengths such that $\tau/\tau_0 \simeq 0{\cdot}75$. If this is done, the error, in terms of the total number of measurements N is

$$\mathbf{F}(pv)\simeq 1{\cdot}73N^{-1/2}. \qquad \ldots\ldots(48)$$

For purposes of comparison, the 'minimum possible' relative error in the estimation of pv, calculated from (18), is plotted in fig. 2 as well (curve B). Since the gaussian assumption made in deriving (18) probably does not affect the numerical values appreciably, the difference between the two curves (as compared with the similar curves B and I of fig. 1) shows the effect of the extra uncertainties resulting from the necessary introduction of a cut-off.

§ 6. SYSTEMATIC ERROR IN THE ESTIMATION OF a_{0c}

The method developed above for the estimation of a_{0c} is valid in the sense that the estimate of a_{0c} will tend to its correct value as the length of the track, and hence the number of observations, increases. One would expect, however, that if the estimates of a_{0c} obtained from a large number of similar finite tracks were averaged, the result would differ systematically from the true value of a_{0c} for the tracks, since the cut-off used for any one track depends on the scattering observed in that track.

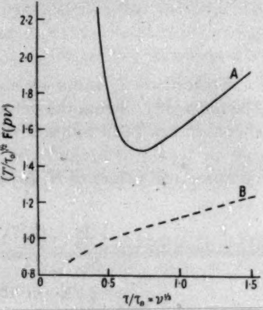

Fig. 2. A: The relative r.m.s. error in the estimation of *pv* by (38) and (42) when the large angle scattering is cut off. (Based on the Snyder–Scott distribution.)
B: The 'minimum possible' relative r.m.s. error in the estimation of *pv* for gaussian scattering with no cut-off. (For the use of these curves note that $T/\tau_0 = N(\tau/\tau_0)$.)

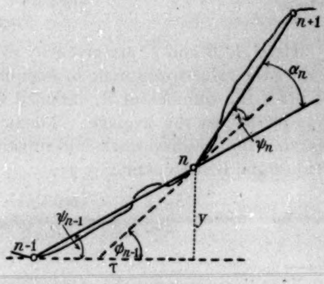

Fig. 3. Illustrating the notation of Appendix A.

Suppose that one has a very large number of similar tracks of the same energy and that a_i, θ_i are the estimates of a_{0c} and the cut-off angle θ for the ith track. Then, since for a large number of tracks the statistical fluctuations in the estimation of a_i from (38) after the cut-off has been applied will vanish on the average, one may write

$$a_i = f(\theta_i); \quad \theta_i^2 = \lambda a_i, \qquad \ldots\ldots(49)$$

with

$$f(\theta) = \int_{-\theta}^{\theta} \alpha^2 W(\alpha)\, d\alpha \Big/ p(\theta); \quad p(\theta) = \int_{-\theta}^{\theta} W(\alpha)\, d\alpha. \qquad \ldots\ldots(50)$$

Then

$$a_i = a_{0c} + \frac{df}{d\theta^2}(\theta_i^2 - \theta^2) + \tfrac{1}{2}\frac{d^2f}{d(\theta^2)^2}(\theta_i^2 - \theta^2)^2 + \ldots . \qquad \ldots\ldots(51)$$

and averaging over all the tracks, as the number of tracks tends to infinity, the systematic error in the estimation of a_{0c} is

$$\overline{\Delta a_{0c}} = \tfrac{1}{2}\frac{d^2f}{d(\theta^2)^2}\overline{[\delta\theta_i^2]^2}, \qquad \ldots\ldots(52)$$

since $\delta\theta_i^2 = \theta_i^2 - \theta^2$ will vanish on the average. Now from (49)

$$\overline{[\delta\theta_i^2]^2} = \lambda^2\overline{[\delta a_i]^2} = \lambda^2[a_{0c}\mathbf{F}_c(a_{0c})]^2.$$

Hence

$$\overline{\Delta a_{0c}}/a_{0c} = \tfrac{1}{2}\lambda^2 \frac{d^2f}{d(\theta^2)^2} a_{0c}\mathbf{F}_c^2(a_{0c}), \qquad \ldots\ldots(53)$$

and since for large $\theta W(\theta) \sim 1/\theta^3$

$$\frac{\overline{\Delta a_{0c}}}{a_{0c}} = \frac{\lambda}{4}\left[\theta' w(\theta') + \theta'^2 \frac{dw}{d\theta'}\right] \mathsf{F}_c^{\,2}(a_{0c}) \simeq -\tfrac{1}{2}\lambda\theta' w(\theta') \mathsf{F}_c^{\,2}(a_{0c}), \qquad \ldots\ldots(54)$$

writing θ and $W(\theta)$ in units of ρ, and putting $p(\theta)=1$, which is a reasonable approximation for large θ. Under the best conditions for measurement, the results previously obtained give $\mathsf{F}_c(a_{0c}) \simeq 3{\cdot}46 N^{-1/2}$, $\lambda\theta' w(\theta') \simeq 0{\cdot}23$, so that $\overline{\Delta a_{0c}}/a_{0c} \simeq -1{\cdot}4/N$.

Taking $N=50$ as a reasonable value for the average number of observations made on a track, $\overline{\Delta a_{0c}}/a_{0c} \simeq -3\%$. It therefore appears that while there is a systematic error in the estimation of a_{0c} using the cut-off procedure developed above, this error is small and is negligible in comparison with the inherent statistical error of the estimation.

§ 7. A POSSIBLE METHOD OF ESTIMATION FROM MEAN MODULI

The method of estimating a_{0c} developed above demands the calculation of mean squares from the observations. In practice, however, it is much simpler to evaluate mean moduli and it would therefore be advantageous to have a method for estimating the mean modulus of the scattering chord angle from a knowledge of that of the measured angles. The general treatment of this problem is difficult but a possible method can be postulated on the basis of the results obtained above.

Denoting the square of the mean modulus of the true chord angle taken over a cut-off distribution by $|a_{0c}|$, with a similar notation for the measured angle β, eqn. (38) suggests that one might assume an equation of the form

$$|a_0|_c = \frac{1}{7}[4|b_{0c}''| - |b_{0c}|] \qquad \ldots\ldots(55)$$

for the estimation of $|a_{0c}|$.

Now

$$|a_{0c}| - \frac{1}{7}[4|b_{0c}''| - |b_{0c}|] = |a_{0c}|\Gamma \qquad \ldots\ldots(56)$$

where

$$\Gamma = \frac{1}{7}\left\{7 + \frac{|b_{0c}|}{|a_{0c}|} - 4\frac{|b_{0c}''|}{|a_{0c}|}\right\}, \qquad \ldots\ldots(57)$$

and the postulation of (55) will therefore involve a systematic error in the estimation of $|a_{0c}|$ of amount given by

$$\Delta|a_{0c}|/|a_{0c}| = \Gamma. \qquad \ldots\ldots(58)$$

The calculation of Γ requires the evaluation of $|b_{0c}|$ as a function of the cut-off angle and the 'signal/noise' ratio ν_c. If the contribution of the error of measurement to large values of β near the cut-off angle is neglected, one may write approximately

$$(|b_{0c}|)^{1/2} = \int_{-\theta}^{\theta} d\alpha \int_{-\infty}^{\infty} d\epsilon\, |\alpha+\epsilon|\, W(\alpha) q(\epsilon) \Big/ \int_{-\theta}^{\theta} d\alpha \int_{-\infty}^{\infty} d\epsilon\, W(\alpha) q(\epsilon)$$

$$= \frac{4}{p(\theta)} \int_0^{\theta} d\alpha\, W(\alpha) \left\{\alpha \int_0^{\alpha} q(\epsilon)\, d\epsilon + \int_{\alpha}^{\infty} \epsilon q(\epsilon)\, d\epsilon\right\}, \qquad \ldots\ldots(59)$$

where $p(\theta)$ is defined by (50). (This approximation is equivalent to the neglect of the small number γ in (37) in the analogous calculation of b_{0c}. It is reasonable for the purpose of estimating the order of magnitude of Γ.) The integrations can be carried out if a definite form for $q(\epsilon)$ is assumed, the parameters occurring therein being expressible in terms of a_{0c}, and hence θ and ν_c. The integration in (59) was carried out for $\nu_c = 1$ using the Snyder–Scott results for $w(\alpha)$ (with $n = 1{\cdot}5 \times 10^3$) and assuming (i) a gaussian distribution and (ii) a rectangular distribution for the error ϵ; in both cases the resulting value of Γ was found to be less than 1%.

Thus it appears that (55) gives a reasonable basis for the estimation of $|a_{0c}| = (\overline{|\alpha|_c})^2$ provided that the 'signal/noise' ratio is of the order of unity and that the cut-off angle is large; the error of the estimation will be of the order of that found above for the estimation by mean squares. (If the cut-off criterion (39) is written in terms of mean moduli, the value $\lambda = 18$ for the cut-off parameter corresponds to a cut-off of approximately 5·5 times the mean modulus.)

ACKNOWLEDGMENTS

This investigation was suggested by Professor R. E. Peierls, and it is a pleasure to express my gratitude to him and to Dr. F. J. Dyson for many helpful suggestions and stimulating discussions. I would also like to thank the South African Council of Scientific and Industrial Research for the award of a research bursary.

APPENDIX A

CALCULATION OF CORRELATIONS

(i) *Evaluation of* a_r

Consider a typical portion of the track as shown in fig. 3. Using the angles as marked there, one has

$$\alpha_n = \phi_{n-1} - \psi_{n-1} + \psi_n \qquad \ldots\ldots\text{(A 1)}$$

and it is obvious that the angles ψ_i, ϕ_j are all statistically independent except for those with the same suffix. Thus

$$a_0 = \overline{\phi^2} + 2\overline{\psi^2} - 2\overline{\phi\psi}; \quad a_1 = \overline{\phi\psi} - \overline{\psi^2}; \quad a_r = 0, \ r > 1. \qquad \ldots\ldots\text{(A 2)}$$

On the assumption that the individual coulomb scattering angle has a well-defined mean square, one can evaluate $\overline{\phi^2}$, $\overline{\psi^2}$, $\overline{\phi\psi}$ as follows. Suppose that during the traversal of one segment of the track the ionizing particle is scattered n times, and that at the ith scattering it is deviated through an angle θ_i at a distance τx_i from the end of the segment. Then, using the small angle approximation

$$\psi = y/\tau = \sum_{i=1}^{n} \theta_i x_i; \quad \phi = \sum_{i=1}^{n} \theta_i. \qquad \ldots\ldots\text{(A 3)}$$

In (A 3) the θ_i are statistically independent, and since x_i varies from zero to unity, the mean value of x_i^{p+1} is $1/(p+1)$. Thus

$$\left.\begin{aligned} \overline{\psi^2} &= \sum_{i,j=1}^{n} \overline{\theta_i\theta_j x_i x_j} = \tfrac{1}{3} n\overline{\theta^2}, \\ \overline{\phi\psi} &= \sum_{i,j=1}^{n} \overline{\theta_i\theta_j x_j} = \tfrac{1}{2} n\overline{\theta^2}, \\ \overline{\phi^2} &= \sum_{i,j=1}^{n} \overline{\theta_i\theta_j} = n\overline{\theta^2}, \end{aligned}\right\} \qquad \ldots\ldots\text{(A 4)}$$

and from (A 2)

$$a_0 = \tfrac{2}{3} n\overline{\theta^2}; \quad a_1 = \tfrac{1}{6} n\overline{\theta^2} = \tfrac{1}{4} a_0; \qquad \ldots\ldots\text{(A 5)}$$

showing that a_0 is proportional to n and hence to τ.

(ii) *Evaluation of e_r*

Let z_n be the error made in measuring the actual coordinate y_n of the track. Then

$$\epsilon_n = \frac{1}{\tau}(z_{n+1} - 2z_n + z_{n-1}), \qquad \ldots\ldots(\mathrm{A}\,6)$$

and since the z_n are statistically independent with the same mean square

$$e_0 = \frac{1}{\tau^2}(6\overline{z^2}) \qquad \ldots\ldots(\mathrm{A}\,7)$$

and $$e_1 = -\tfrac{2}{3}e_0; \quad e_2 = \tfrac{1}{6}e_0; \quad e_r = 0,\ r > 2; \qquad \ldots\ldots(\mathrm{A}\,8)$$

while (A 7) shows that e_0 is inversely proportional to the square of the interval length.

APPENDIX B

ON THE SNYDER–SCOTT DISTRIBUTION

Let the mean free path for coulomb scattering of the particle in the emulsion be λ, and let $p(\eta)\,d\eta$ be the probability that in an individual scattering the particle is scattered through a projected angle η. Then the probability that after travelling a distance z into the emulsion the particle is moving at a projected angle η to its original direction and has suffered a lateral displacement x is (Snyder and Scott 1949)

$$W(\eta, x \mid z)\,d\eta\,dx = \frac{d\eta\,dx}{4\pi^2}\int_{-\infty}^{\infty} ds \int_{-\infty}^{\infty} dt \exp\{i(\eta s + xt)\} \exp\left[-\frac{1}{\lambda t}\{h(s+tz) - h(s)\}\right], \qquad \ldots\ldots(\mathrm{B}\,1)$$

where $$h(s) = \int_0^s [1 - q(u)]\,du; \quad q(u) = \int_{-\infty}^{\infty} p(\eta)\mathrm{e}^{-i\eta u}du. \qquad \ldots\ldots(\mathrm{B}\,2)$$

(If this is integrated over x, the resultant expression for $W(\eta \mid z)$ is identical with that obtained by Molière (1948) written in terms of the projected angle.) From (B 1) one obtains the probability distribution for the chord angle α (Scott and Snyder 1950) as

$$W(\alpha \mid \tau)\,d\alpha = \frac{d\alpha}{2\pi}\int_{-\infty}^{\infty} ds \exp(i\alpha s) \exp\left\{-\frac{2\tau}{s}\frac{h(s)}{s}\right\}. \qquad \ldots\ldots(\mathrm{B}\,3)$$

(Since small angles are assumed throughout, the chord length is equated with the length of the segment of the track cut off by the chord.) In order to evaluate this distribution, Scott and Snyder assume

$$p(\eta) = \tfrac{1}{2}\frac{\eta_0^2}{(\eta^2 + \eta_0^2)^{3/2}}; \quad \frac{1}{\lambda} = \frac{4\pi N Z^2 Z'^2 \mathbf{e}^4}{p^2 v^2}\frac{1}{\eta_0^2}, \qquad \ldots\ldots(\mathrm{B}\,4)$$

where η_0 is a 'screening angle', Z the atomic number and N the density of the scattering atoms and $Z'\mathbf{e}$ the charge of the scattered particle. (These expressions arise in Born approximation from a shielded coulomb potential of the form $V = Z(\mathbf{e}^2/r)\exp(-r/a)$.) Then expressing angles in units of $\rho = (2n\eta_0^2)^{1/2}$, where $n = \tau/\lambda$ is the average number of scatterings suffered by the particle in traversing one interval length, Scott and Snyder give numerical results from which the α distribution can be found for given n.

Molière (1947) has investigated in how far the actual state of affairs can be represented by the approximation (B 4) and, basing his results on an analytic representation of the Thomas–Fermi potential, concludes that if η_0 is chosen so that

$$\eta_0 = \chi_0(1{\cdot}13 + 3{\cdot}76\alpha^2)^{1/2}, \qquad \ldots\ldots(\mathrm{B}\,5)$$

where $\chi_0 = \lambda/2\pi a$, with λ the de Broglie wavelength of the scattered particle, a the Thomas–Fermi unit of length and $\alpha = ZZ'/137\beta$, then the mean square value of η over the distribution (B 4) will agree with its mean square value over the actual distribution when both are cut off in a region where the Rutherford scattering law applies.

With Molière's choice of the screening angle, the Snyder–Scott results are probably a good approximation since the unit of angle employed does not depend on η_0 and the distribution is very insensitive to the value of $n \sim 1/\eta_0^2$ if n is large.

REFERENCES

Corson, D. R., 1950, *Phys. Rev.*, **80**, 303.
Fowler, P. H., 1950, *Phil. Mag.*, **41**, 169.
Molière, G., 1947, *Z. Naturforsch.*, **2a**, 133 ; 1948, *Ibid.*, **3a**, 78.
Moyal, J. E., 1950, *Phil. Mag.*, **41**, 1058.
Scott, W. T., and Snyder, H. S., 1950, *Phys. Rev.*, **78**, 223.
Snyder, H. S., and Scott, W. T., 1949, *Phys. Rev.*, **76**, 220.
Williams, E. J., 1939, *Proc. Roy. Soc.* A, **169**, 531.

Decay Schemes of ^{151}Sm and ^{155}Eu

By H. W. WILSON and G. M. LEWIS
Department of Natural Philosophy, The University, Glasgow

Communicated by P. I. Dee ; MS. received 12th September 1951, *and in amended form* 15*th February* 1952

ABSTRACT. Examination of the relatively long-lived isotopes produced by pile irradiation of samarium using the proportional tube spectrometer leads to the elucidation of the decay schemes of ^{151}Sm and ^{155}Eu. The conclusions are supported by experiments involving β–e$^-$ and β–γ coincidences, utilizing Geiger–Müller and scintillation counters.

§ 1. INTRODUCTION

The object of the work described in this paper was to obtain information upon the long-period activities resulting from the bombardment of samarium with neutrons. The radiations from these isotopes appeared to be well suited to a detailed investigation by proportional counter and related techniques, and it was hoped that results might be obtained which would clarify the decay schemes for the two isotopes, ^{151}Sm and ^{155}Eu.

Neutron capture by pure samarium results directly in the formation of the radioactive isotopes ^{145}Sm, ^{151}Sm, ^{153}Sm and ^{155}Sm (Inghram, Hayden and Hess 1947). ^{145}Sm is a pure K-capture source of half-life 410 days (Butement 1951). ^{151}Sm is a β-emitter of many years half-life (Inghram, Hayden and Hess 1947, 1950, Marinsky 1949). ^{153}Sm is short-lived, decaying into stable ^{153}Eu. ^{155}Sm is short-lived, decaying into β-emitting ^{155}Eu of half-life 2 years (Hayden, Reynolds and Inghram 1949, Winsberg 1950). Since the capture cross sections of ^{152}Sm and its ultimate product ^{153}Eu are high, a relatively very small amount of β-emitting ^{154}Eu can also be expected.

Samarium in the form of oxide, spectroscopically pure, was irradiated at Harwell for eight weeks at a thermal neutron flux of $3{\cdot}5 \times 10^{10}$/cm^2/sec. The source was allowed to decay for several months. Preliminary absorption studies on the β-radiation showed that most of the β-rays were of energy less than 250 kev, approximately the limiting energy of the β-spectra of ^{155}Eu. A further well-defined end point showed at about 75 kev, agreeing well with the end point of ^{151}Sm as given by Agnew (1950) and Marinsky (1949), viz. 75·5 and 74 kev respectively. Evidence was obtained too of the presence of ^{145}Sm, which, being a pure K-capture source, is not an appreciable obstacle in the investigation of the radiations of ^{151}Sm and ^{155}Eu. The sources of radiation ^{151}Sm and ^{155}Eu were present with relative intensities of roughly 1 to 4. It had been hoped that one or other of these radioactive isotopes would be predominant, but in view of the involved nature of the chemistry, the two activities have been studied without chemical separation.

§ 2. APPLICATION OF THE PROPORTIONAL TUBE SPECTROMETER

(i) *Gamma Radiation*

A proportional tube, diameter 5·5 in., active length 8 in., filled with methane and argon (partial pressures 15 and 60 cm Hg respectively), was used to examine the energies of the soft γ-rays from the source. The histogram of fig. 1 indicates the presence of radiations of energies 19·3 kev and 15·2 kev. The peak at about 8 kev is due to copper K x-rays excited at the wall of the counter by the γ-rays of the source, and was eliminated when a glass counter with an aluminium cathode was used to examine the region below 10 kev (inset to fig. 1). Concerning the two γ-radiations of 19·3 and 15·2 kev, Scharff-Goldhaber *et al.* (1950) have detected γ-radiation of energy 21 kev emitted by ^{151}Sm. The radiation here estimated with energy 19·3 kev is presumably of this origin. Since they did not observe any radiation corresponding to the peak at 15·2 kev in fig. 1, we are naturally led to the conclusion that this softer radiation is emitted in the decay

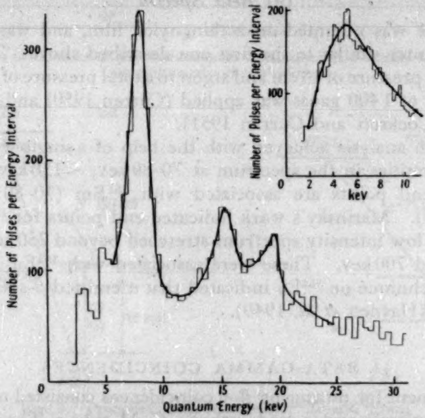

Fig. 1. γ-ray peaks at 15·2 and 19·3 kev as measured in proportional tube spectrometer. Inset : spectrum below 10 kev using counter with aluminium cathode.

of ^{155}Eu (their source was a fission product, presumably free of europium isotopes). Marinsky and others have found two γ-radiations of ^{155}Eu of energies 85 and 99 kev. These radiations were measured by means of internal conversion electrons in a magnetic spectrometer, and the very low energy radiation (15·2 kev) would presumably escape observation. It is natural to relate the radiation of energy 15·2 kev to the difference between 85 and 99 kev, in which case the 85 and 15·2 kev quanta would be emitted in cascade.

The inset to fig. 1, obtained with the second counter, shows a broad peak around 5 kev which can be tentatively ascribed to the L x-rays emitted by the source (in K-capture and internal conversion). Taking account of the absorption in the aluminium window, it must be concluded that the absolute intensity of this radiation is high.

An investigation of the region 20–70 kev showed the K x-radiations centred about 40 kev. The source peak was compared with a calibration peak obtained by exciting the Kα fluorescence x-radiations from a thin layer of samarium oxide with an x-ray equipment. The position and width of the source peak suggested that x-rays of higher and lower energy than Kα of samarium were emitted by the radioactive material. It is thought that the peak is mainly due to K-capture in ^{145}Sm and internal conversion of ^{155}Eu γ-rays (x-rays of Pm and Gd respectively).

(ii) *Beta Spectra*

A thin source was mounted on a thin nylon film, and was inserted into a proportional counter similar to the first one described above. The gas mixture was methane to a pressure of 10 cm and argon to a total pressure of 3¼ atmospheres. A magnetic field of 1400 gauss was applied (Curran 1950) and the counter was end corrected (Cockroft and Curran 1951).

The spectrum analysis achieved with the help of a single-channel kicksorter showed discontinuities in the spectrum at 70–80 kev, ~150 kev and ~250 kev. These various end points are associated with ^{151}Sm (70–80 kev) and ^{155}Eu (150 and 250 kev). Marinsky's work indicated end points for ^{155}Eu at 154 and 243 kev. A very low intensity spectrum stretched beyond 250 kev, showing end points at 400 and 700 kev. These were associated with ^{154}Eu. Previous work by absorption technique on ^{154}Eu indicated that it emitted β-spectra of energies 0·3 and 0·7 Mev (Hayden *et al.* 1949).

§3. BETA–GAMMA COINCIDENCES

The arrangement for measuring β–γ coincidences consisted of a thin window β-counter (1·7 mg/cm^2) and a lead cathode G–M tube. The latter was later replaced by a scintillation detector to improve the efficiency of γ-detection. This detector was shielded by 5/64 in. of copper to stop electrons and soft x-rays. In each case the resolving time was 0·7 μsec. The results obtained were similar, and a set using the scintillation detector is shown in fig. 2. Here β–γ coincidences per β-particle are plotted in terms of the thickness of aluminium between the source and the β-counter.

This coincidence absorption curve receives a ready interpretation in terms of the decay schemes proposed in fig. 3. The first steep rise to approximately 80 kev on the curve is due to the elimination of the β-rays of ^{151}Sm, for the 19·3 kev γ-radiation in cascade with the soft β-rays is not detected by the

γ-counter. The rather less steep rise to approximately 150 kev is probably associated with the absorption of the β-rays of higher energy ($\sim$250 kev) of ^{155}Eu since they do not contribute to the β–γ coincidences. The elimination of coincidences arising from the 150 kev spectrum of ^{155}Eu results in the break in the curve at approximately 150 kev, assuming the proposed decay scheme is correct. The gradual falling off to lower values is mainly due to the contamination of the source with ^{154}Eu, which gives rise to β-rays of energy as high as 0·7 MEV.

The results of work on β–e^- coincidences were consistent with the above interpretation.

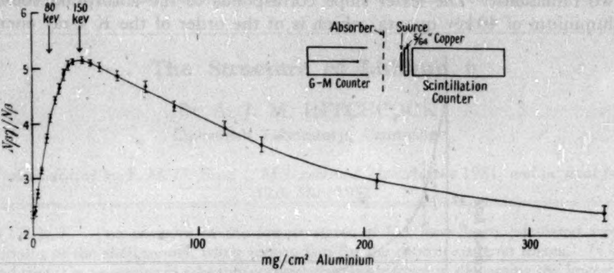

Fig. 2. Ratio of number of β–γ coincidences to number of β-counts as a function of aluminium absorber thickness.

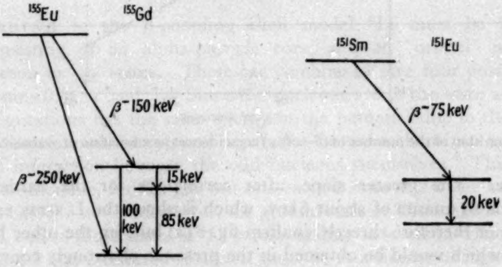

(a) *(b)*

Fig. 3. Proposed decay schemes of ^{155}Eu and ^{151}Sm.

Marinsky found that the lower energy β-rays of ^{155}Eu were coincident with γ-radiation, but he concluded that there were no γ–γ coincidences. We believe, as the result of the above work, that the 99 kev γ-ray corresponds to the difference in energy between the two β-spectrum end points and that the soft γ-ray detected here (15 kev) corresponds to the difference between the energies of the harder quanta.

It is easy to explain the difficulty of finding γ–γ coincidences with ^{155}Eu. The 15 kev quanta are not detected efficiently by most normal G–M counters, and, moreover, the presence of intense L-radiation and theoretical considerations suggest strongly that the quanta are very highly converted. However, a direct test of the scheme of fig. 3 (*a*) was arranged. This test sought to establish that the electrons of the softer β-spectrum of ^{155}Eu were followed by 15 kev γ-radiation. A β-counter was covered with sufficient material to stop the β-rays of ^{151}Sm (75 kev). Opposite this was placed a special G–M counter designed to detect soft quanta efficiently, containing argon to a pressure of one atmosphere together with ethyl alcohol (1·5 cm Hg). This second counter was covered with polythene of thickness 270 mg/cm^2, adequate to stop all β-particles from the source while transmitting quanta of 15 kev fairly efficiently. β–γ coincidences were recorded as a function of the thickness of aluminium placed between the source and the γ-ray counter. The results shown in fig. 4 indicate the predominance of two radiations. The lesser slope corresponds to the absorption coefficient in aluminium of 40 kev quanta, which is of the order of the K x-ray energy of the source. The greater slope, after corrections for the harder radiation, corresponds to quanta of about 6 kev, which is about the L x-ray energy. The test does not therefore directly confirm fig. 3 (*a*) but, on the other hand, this is the result which would be obtained in the presence of strongly converted 15 kev quanta. Removal of the absorber in front of the β-ray counter (total window thickness 1·7 mg/cm^2) showed that the number of β–γ coincidences per β remained almost constant ($1{\cdot}18\times10^{-2}$ and $1{\cdot}14\times10^{-2}$), although the β-count increased considerably. From this we deduce that the ^{151}Sm β-particles are likewise in coincidence with soft γ-quanta (19·3 kev) or with the L x-rays arising in their internal conversion. This affords direct support to the scheme of fig. 3 (*b*).

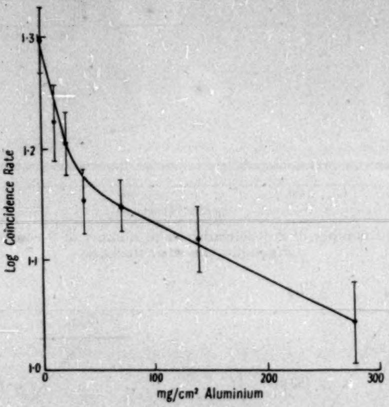

Fig. 4. Logarithm of the number of (β–soft γ) coincidences as a function of γ-absorber thickness.

ACKNOWLEDGMENTS

We should like to record our indebtedness to Dr. S. C. Curran for many suggestions contributing to the success of the investigation. We should like to acknowledge the assistance given by Mr. D. Dixon on the experimental side. Finally, we wish to thank Professor P. I. Dee for his encouragement in the prosecution of the work.

REFERENCES

AGNEW, H. M., 1950, *Phys. Rev.*, **77**, 655.
BUTEMENT, F. D. S., 1951, *Nature, Lond.*, **167**, 400.
COCKCROFT, A. L., and CURRAN, S. C., 1951, *Rev. Sci. Instrum.*, **22**, 37.
CURRAN, S. C., 1950, *Atomics*, **1**, 221.
HAYDEN, R. J., REYNOLDS, J. H., and INGHRAM, M. G., 1949, *Phys. Rev.*, **75**, 1500.
INGHRAM, M. G., HAYDEN, R. J., and HESS, D. C., 1947, *Phys. Rev.*, **71**, 643; 1950, Supplement 1, *Nuclear Data, Nat. Bur. Stand., Circular No.* 499.
MARINSKY, J. A., 1949, *Thesis*, Massachusetts Institute of Technology and Progress Report Lab. Nuclear Sci., Eng. (July).
SCHARFF-GOLDHABER, G., DER MATEOSIAN, E., MCKEOWN, M., and SUNYAR, A. W., 1950, *Phys. Rev.*, **78**, 325.
WINSBERG, L., 1950, *National Nuclear Energy Series* (Manhattan Project), paper 199.

The Structure of Lithium 6

BY A. J. M. HITCHCOCK
Cavendish Laboratory, Cambridge

Communicated by J. M. C. Scott ; MS. received 24th August 1951, *and in final form 12th May* 1952

ABSTRACT. The energies of the lowest states of ^{6}Li have been calculated from the standpoint of the shell model, using recent data for the proton–neutron forces. It is concluded that it is necessary to take into account the tensor force in discussing the lowest states of this and other odd–odd nuclei.

ACCORDING to the *jj*-coupling shell model ^{6}Li must be regarded as consisting of an alpha-particle core, and an 'orbital' neutron and proton in $p_{3/2}$ states. These can combine to give four possible ground states of spins 0, 1, 2 and 3. Since the nucleons are in the same shell, each of these configurations has the same energy in the potential due to the core (even including the coulomb force), and separation between them can only occur as a result of interaction between the odd nucleons themselves. This separation must be considerable, for ^{6}Li has but one excited state at 2·4 MEV and no others are known below 7 MEV. Moreover, the ground state of ^{6}He is about 3 MEV above that of ^{6}Li, and so those states of ^{6}Li corresponding to levels in ^{6}He, in particular those of spin 0 and 2 referred to above, must be at a similar or higher excitation above the ground state of ^{6}Li. It is the purpose of this note to show that the tensor interaction between nucleons must be taken into account to explain the observed spin 1 of the ^{6}Li ground state and the large separations between the four states of this multiplet.

The interaction

$$V(r)=V_0\frac{e^{-kr}}{r}\left\{1+\tfrac{1}{2}g(\boldsymbol{\sigma}^{(1)}\cdot\boldsymbol{\sigma}^{(2)}-1)+\gamma\left(\frac{3(\boldsymbol{\sigma}^{(1)}\cdot\mathbf{r}_{12})(\boldsymbol{\sigma}^{(2)}\cdot\mathbf{r}_{12})}{r_{12}^{2}}-(\boldsymbol{\sigma}^{(1)}\cdot\boldsymbol{\sigma}^{(2)})\right)\right\}$$

was assumed between two nucleons, and two cases were considered.

A. $V_0=81{\cdot}04\times10^{-13}$ MEV cm, $k=0{\cdot}8580\times10^{13}\,\mathrm{cm}^{-1}$, $g=0{\cdot}1602$, $\gamma=0$.

These are given as best values for proton–proton scattering by Jackson and Blatt (1950). These authors do not consider the tensor interaction, but as this has no effect in the singlet state it is reasonable to suppose that the value of k, which is deduced from these data, is correct in any case.

B. $V_0 = 46{\cdot}31 \times 10^{-13}$ Mev cm, $k = 0{\cdot}5755 \times 10^{13}\,\mathrm{cm}^{-1}$, $g = 0{\cdot}107$, $\gamma = 0{\cdot}73$.

These are given as permissible values from the deuteron data by Hu and Massey (1949). Qualitatively these authors expect that to assume the larger valued k given above requires that V_0 should be smaller and γ much larger, but no exact figures are given. After fitting the core potential to be consistent with the data in first approximation the additional binding energy, due to the interaction, for each of the four states was calculated to first order approximation.

The results are given in the table below:

Case A

State of spin	3	2	1	0
Contribution due to V_0 (Mev)	15·760	8·833	8·152	9·707
Contribution due to V_0g (Mev)	0	−1·120	+0·318	+0·606
Total binding (Mev)	15·760	7·713	9·707	10·313

Case B

State of spin	3	2	1	0
Contribution due to V_0 (Mev)	3·875	3·102	2·636	2·247
Contribution due to V_0g (Mev)	0	−0·276	+0·161	+0·484
Contribution due to $V_0\gamma$ (Mev)	−0·779	−0·472	+1·123	−0·185
Total binding (Mev)	3·096	2·354	3·920	2·546

It will be observed that the only effect tending to cause the state of spin 1 to be the lowest by a considerable margin is the tensor force (contribution of $V_0\gamma$), and that this effect is large in proportion to the size of γ.

For the reasons previously stated it is almost certain that an even larger separation may be obtained by choosing a value of k more in line with the proton–proton scattering data. It should be remembered, however, that Inglis (1937) obtained a ground state of spin 1 without using tensor forces, by employing, essentially, an L–S coupling scheme. This is inconsistent with the large departure from L–S coupling implied by modern shell model theories. The purpose of this note is fulfilled, however, by pointing out that, if the shell model is valid, it is necessary to take into account the tensor force in any consideration of the spins of odd–odd nuclei.

My thanks are due to Mr. J. M. C. Scott for suggestions and discussion.

REFERENCES

Hu, Tsi-Ming, and Massey, H. S. W., 1949, *Proc. Roy. Soc.*, **196**, 135.
Inglis, D. R., 1937, *Phys. Rev.*, **51**, 531.
Jackson, J. D., and Blatt, J. M., 1950, *Rev. Mod. Phys.*, **22**, 77.

The Photo-Ionization Cross Section of Methane

By A. DALGARNO
Department of Applied Mathematics, Queen's University, Belfast

Communicated by D. R. Bates; *MS. received* 14*th March* 1952

ABSTRACT. The photo-ionization cross section of methane is calculated using self-consistent wave functions. The value at the spectral head (105 850 cm^{-1}) is found to be $9{\cdot}4\times10^{-17}$ cm^2. An approximate general formula is employed to obtain results in a wave number range up to 200 000 cm^{-1} and the associated oscillator strength is computed. It is pointed out that exchange effects probably reduce the cross section. With the aid of the general formula an estimate is also made of the photo-ionization cross section of argon.

§1. INTRODUCTION

The method of self-consistent field, in which each electron is regarded as occupying a stationary state in the field of the nucleus and of the other electrons, has achieved considerable successes as far as atoms are concerned, but its extension to molecules is a matter of great difficulty because of the lack of spherical symmetry. Buckingham, Massey and Tibbs (1941) have shown, however, that in certain cases it is legitimate to average the nuclear distribution over all orientations about a central nucleus and so obtain a spherically symmetric potential field; thus they point out that for systems which possess a high degree of symmetry, such as the tetrahedral molecules CH_4, CCl_4 and SiH_4, the distributions of the electrons obtained using the averaged nuclear distribution should not differ greatly from the actual distribution. The self-consistent wave functions (without exchange) of methane, derived after making this approximation, were used by them to evaluate the diamagnetic susceptibility, the polarizability and the van der Waals force between two molecules. The elastic scattering of slow electrons by the calculated potential was also studied. From the results of these investigations, Buckingham, Massey and Tibbs concluded that the treatment for methane is only slightly less satisfactory than that for atoms.

Optical transition probabilities are sensitive to the detailed nature of the wave functions and hence provide a useful criterion for their accuracy. In this paper, the photo-ionization cross section of methane is evaluated using the self-consistent wave functions of Buckingham, Massey and Tibbs. It is understood that measurements of this cross section are being made by Professor R. W. Ditchburn of the University of Reading and by Professor G. L. Weissler of the University of Southern California, so that data should soon be available for comparison with the theoretical result. As Professor Ditchburn is also measuring the photo-ionization cross section of argon a preliminary estimation of this is made.

§2. THEORY

If χ_i and χ_f represent respectively the initial and final wave functions, suitably normalized, the photo-ionization cross section is given by (cf. Bates 1946 a)

$$a_\nu=\frac{32\pi^4 \boldsymbol{m}^2\boldsymbol{e}^2}{3\boldsymbol{h}^3\boldsymbol{c}}\,\frac{1}{\omega_i}\,\Sigma_i\,.\,\Sigma_f\,\nu\left|\int \chi_i^*\big(\sum_j \boldsymbol{r}_j\big)\chi_f\,dr\right|^2 \qquad \ldots\ldots(1)$$

where **e**, **m**, **c** and **h** have the customary meanings, ω_1 is the weight of the initial state, ν is the frequency of the incident radiation and $\mathbf{r}_j$ the position vector of the jth electron; Σ_1 denotes a summation over the initial states and Σ_f a summation over the final states. The averaging of the proton distribution effectively replaces the four protons of methane by a uniform shell about the carbon nucleus. Consequently the ground state may be represented by the configuration $(1s)^2$, $(2s)^2$, $(2p)^6$ and is closely similar to neon, except that the potential field of the nuclei is $-4-(6/r)$ or $-(10/r)$ according as r, the distance from the centre of symmetry, is less than or greater than the radius of the proton shell. This similarity enables (1) to be reduced as in the atomic case (cf. Bates 1946 b) giving the formula

$$a_\nu = 1{\cdot}71(I+\epsilon)\mathscr{C}_P(\Phi_{l-1}(\epsilon)^2 + 2\Phi_{l+1}(\epsilon)^2)10^{-18}\,\text{cm}^2 \qquad \ldots\ldots(2)$$

in which I is the ionization potential and ϵ the energy of the ejected electron in rydbergs; $\mathscr{C}_P$ is a factor, close to unity, allowing for the distortion of the passive electron wave functions by the transition; and

$$\Phi_{l\pm1}(\epsilon) = \left| \int_0^\infty rP(n,l\,|\,r)P(\epsilon, l\pm1\,|\,r)\,dr \right|,$$

where $r^{-1}P(n,l\,|\,r)$ is the radial part of the initial bound wave function, normalized to unity (n and l denoting the principal and azimuthal quantum numbers) and $r^{-1}P(\epsilon, l\pm1\,|\,r)$ are the radial parts of the final free wave functions, normalized so that $P(\epsilon, l\pm1\,|\,r)$ has an asymptotic amplitude of $1/\epsilon^{1/4}$. The transitions which must be considered are of course $2p \rightarrow \epsilon s$ and $2p \rightarrow \epsilon d$.

2.1. *Electron Wave Functions*

The radial equations for the ejected electron are

$$P'' + \left\{ V(r) - \frac{l(l+1)}{r^2} + \epsilon \right\} P = 0$$

where in the usual self-consistent field notation (Hartree 1946–47)

$$V(r) = \frac{2}{r}\left\{ 6 + 4r - 5Y_0\left(2p, 2p\,|\,r\right) - 2\sum_{n=1}^{2} Y_0\left(ns, ns\,|\,r\right)\right\}, \quad r<2$$

$$V(r) = \frac{2}{r}\left\{ 10 - 5Y_0\left(2p, 2p\,|\,r\right) - 2\sum_{n=1}^{2} Y_0\left(ns, ns\,|\,r\right)\right\}, \quad r>2,$$

the radius of the proton shell being 2 atomic units. The Y_0's depend upon the wave functions of singly ionized methane. These were obtained from the self-consistent wave functions of neutral methane and neutral and singly ionized neon by the method described in the following paragraph.

A scaling factor was applied to the 2p wave function of methane, chosen so that the magnitude of the maximum of this scaled function equalled the magnitude of the maximum of the 2p neon wave function. A unique correspondence could then be established between the radial distance at which the scaled function attained any particular value and the radial distance at which the neon wave function attained the same value. This correspondence was used to derive, from the 2p wave function of ionized neon, a wave function which, after application of the inverse of the scaling factor, should be a good approximation to the 2p wave function of ionized methane. The 1s and 2s wave functions were found in a similar way. It is unlikely that the procedure introduces any significant error; for the wave functions are required mainly for the calculation of the potential field in which the ejected electron moves and as will be seen later the cross section of methane is insensitive to the details of this potential field.

The radial equations of the ejected electron were solved by numerical integration for $\epsilon=0$, that is at the spectral head. Normalization was effected using the procedure suggested by B. Strömgren and described by Bates and Seaton (1949). The figure illustrates the form of $P(0,\mathrm{s}\,|\,r)$ and $P(0,\mathrm{d}\,|\,r)$ and includes for reference the function $rP(2\mathrm{p}\,|\,r)$ of Buckingham, Massey and Tibbs. It may be remarked that owing to the dominance of the centrifugal term $6/r^2$ $P(0,\mathrm{d}\,|\,r)$ approximates closely to the corresponding hydrogenic function.

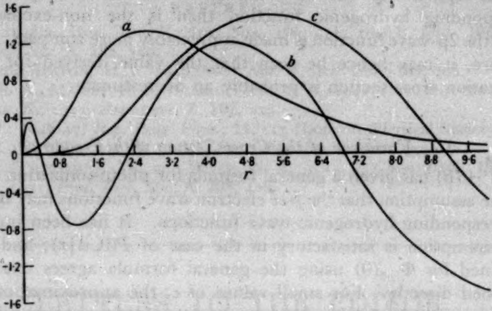

Wave functions for methane. Curve *a*: $rP(2\mathrm{p}\,|\,r)$; curve *b*: $P(0,\mathrm{s}\,|\,r)$; curve *c*: $P(0,\mathrm{d}\,|\,r)$.

§3. RESULTS AND DISCUSSION

3.1. *The Spectral Head Cross Section*

The wave functions described in the previous section were used to compute $\mathscr{C}_{\mathrm{P}}$ and $\Phi_{l\pm1}$. Taking the ionization potential of methane as 0·97 rydberg (Lossing, Tickner and Bryce 1951) and substituting in (2), the value of a_ν at the spectral head was thus obtained. The results are : $\mathscr{C}_{\mathrm{P}}=0{\cdot}98$, $\Phi_{l-1}(0)^2=4{\cdot}6$ atomic units, $\Phi_{l+1}(0)^2=26{\cdot}8$ atomic units, a_ν (spectral head) $=9{\cdot}4\times10^{-17}\,\mathrm{cm}^2$.

Each of the radial integrals $\Phi_{l\pm1}$ may be divided into two portions of opposing sign. Bates (1947) has shown that a convenient measure of the degree of cancellation is provided by the quantity $1-D$, where D is the ratio of the smaller to the larger of the two portions. For methane, $1-D$ for Φ_{l-1} is 0·65 and for Φ_{l+1} it is 0·98. The degree of cancellation in the greater of the two integrals is therefore slight and there appears no possibility of gross error in the value derived from the cross section (cf. Bates and Seaton 1949). However, it is apparent from the figure that a considerable part of the integrals $\Phi_{l\pm1}$ comes from large radial distances where the discrete function is ill-determined.* As a consequence high accuracy cannot be expected.

---

* In calculations which involve a single central potential, no advantage is gained by Chandrasekhar's device (1945) of reducing the contribution from large radial distances by transforming the transition matrix element from the dipole length to the dipole velocity form, since the two forms are exactly equivalent. In the calculations carried out here the difference between the potentials is trivial.

An obvious refinement would be to make allowance for exchange. Since the contribution of the transition 2p→εs to the cross section is small compared to that of the transition 2p→εd, we need discuss only the latter. Seaton (1951) has found that the Fock terms scarcely alter the εd wave functions of neon owing to the control exerted by the large centrifugal potential, and what little effect they have is repulsive so that the exchange solution is actually rather closer to the corresponding hydrogenic function than is the non-exchange solution. In contrast the 2p-wave function is made appreciably more compact. On referring to the figure, it may hence be seen that the value derived for the methane photo-ionization cross section is probably an overestimate.

3.2. *Variation of the Cross Section with Frequency*

Bates (1946 b) has given a general formula for photo-ionization cross sections based on the assumption that the *free* electron wave functions may be represented by the corresponding hydrogenic wave functions. It has been indicated above that this assumption is satisfactory in the case of $P(0, \mathrm{d}\,|\,r)$; and, indeed, the value obtained for $\Phi_{l+1}(0)$ using the general formula agrees exactly with the value obtained directly. For small values of ϵ, the approximation should still be satisfactory. As $\Phi_{l-1}(\epsilon)$ is relatively unimportant it was judged sufficient to apply the general formula multiplied by an external correcting factor chosen so as to make the value of the cross section at the spectral head equal to that given by the detailed computations. The results finally obtained are displayed in the table. For convenience the wave number of the incident radiation, rather than ϵ, is used as the independent variable.

Wave number of incident radiation ν/c (cm^{-1}).	105850*	120000	140000	160000	180000	200000
Photo-ionization cross section a_ν (10^{-17}cm^2).	9·4	7·7	5·7	4·2	3·3	2·4

* spectral head

For an N-electron system, the f-sum rule of Kuhn and Thomas states that $\Sigma_k f(i, k) = N$ where f is the oscillator strength of the transition $i \rightarrow k$ and the summation includes an integration over the continua for which the oscillator strength and the cross section are related by the formula $df = 1{\cdot}24 \times 10^{17}\, a_\nu\, d\epsilon$ with a_ν in cm^2 and ϵ in rydbergs. From the results given above the total oscillator strength associated with the 2p→εs and 2p→εd continua was found to be 6·3. The fact that this exceeds the number of 2p electrons is in no way anomalous since the discrete transitions 2p→2s and 2p→1s, whose oscillator strengths must be included in the summation (in spite of the fact that the inner shells are filled), give negative contributions.

3.3. *Photo-Ionization Cross Section of Argon*

The photo-ionization cross section of argon at the spectral head (127 110 cm^{-1}) was evaluated using the approximate formula mentioned earlier and the self-consistent wave functions with inclusion of exchange given by Hartree and Hartree (1938). The value $a_\nu = 3 \times 10^{-17}$ cm^2 was obtained.

ACKNOWLEDGMENTS

The wave functions for neutral and singly ionized neon respectively were generously supplied by Miss B. H. Worsley and Dr. M. J. Seaton to whom thanks are due. It is a pleasure to acknowledge the advice and encouragement of Professor D. R. Bates, who suggested this problem.

REFERENCES

BATES, D. R., 1946 a, *Mon. Not. R. Astr. Soc.*, **106**, 432; 1946 b, *Ibid.*, **106**, 423; 1947, *Proc. Roy. Soc.* A, **188**, 350.

BATES, D. R., and SEATON, M. J., 1949, *Mon. Not. R. Astr. Soc.*, **109**, 698.

BUCKINGHAM, R. A., MASSEY, H. S. W., and TIBBS, S. R., 1941, *Proc. Roy. Soc.* A, **178**, 119.

CHANDRASEKHAR, S., 1945, *Astrophys. J.*, **102**, 223.

HARTREE, D. R., 1946-47, *Rep. Prog. Phys.*, **11**, 113 (London: Physical Society).

HARTREE, D. R., and HARTREE, W., 1938, *Proc. Roy. Soc.* A, **166**, 450.

LOSSING, F. P., TICKNER, A. W., and BRYCE, W. A., 1951, *J. Chem. Phys.*, **19**, 125.

SEATON, M. J., 1951, *Proc. Roy. Soc.* A, **208**, 408.

LETTERS TO THE EDITOR

The Cupric Ion in a Trigonal Crystalline Electric Field

.A
5
2

The paramagnetic resonance spectra of single crystals of cupric salts have been extensively studied. The results are expressed as parameters in the usual spin Hamiltonian, with $S=\frac{1}{2}$:

$$\mathscr{H}=\beta g_{\parallel}H_zS_z+\beta g_{\perp}(H_xS_x+H_yS_y)+AS_zI_z+B(S_xI_x+S_yI_y).$$

Here we have assumed axial symmetry, and have omitted the terms due to the nuclear electric quadrupole moment of copper, and the term due to the direct effect of the external magnetic field on the nucleus; these have no effect on the point which we wish to make in this letter.

The spectra are usually anisotropic, with g varying from 2·4 to 2·1. But in the case of copper fluosilicate hexahydrate $CuSiF_6.6H_2O$, diluted with the isomorphous zinc salt, the spectrum is found at 90° K to be nearly isotropic (Bleaney and Ingram 1950). The experimentally determined parameters are $g_{\parallel}=g_{\perp}=2{\cdot}24$, $|A|=2\times10^{-3}$ cm^{-1}, $|B|=3\times10^{-3}$ cm^{-1}. Similar results have been obtained at 90° K with copper bismuth double nitrate $3Cu(NO_3)_2.2Bi(NO_3)_3.24H_2O$, diluted with the isomorphous magnesium salt, and with copper bromate $Cu(BrO_3)_2.6H_2O$, diluted with the isomorphous zinc salt.

The crystal structures of the fluosilicate, double nitrate and bromate are hexagonal, trigonal and cubic respectively. The structure of the bromate is similar to that of the alums, with four ions in the unit cell, each subject to a field of trigonal symmetry. Thus in each of these three salts one would expect that the static crystalline electric field has no components of symmetry less than trigonal. The consequence of this has been considered by Abragam and Pryce (1950). A field of trigonal symmetry does not split the degeneracy of the lower orbital doublet left by the cubic field; however, a general theorem of Jahn and Teller (1937) shows that the energy of the system will be lowered if the degeneracy is lifted. This requires a distortion of the octahedron of water molecules surrounding the cupric ion, and there is a continuous set of configurations all giving the same reduction in energy. The system resonates between these, and the experimentally determined parameters represent the average of the rapidly fluctuating values.

Recent experiments have revealed that in each of these three cases there is a radical change in the spectrum at low temperatures, the spectrum becoming complex and anisotropic. In the case of the fluosilicate and the double nitrate the change occurs between 60° K and 20° K, and in the bromate between 20° K and 12° K. The change from one spectrum to the other occurs over a rather wide temperature range, and it is possible to see the two different spectra simultaneously. The change is reversible with temperature.

The spectrum of the fluosilicate at 20° K has been fully analysed, using 0·8 cm^{-1} radiation to obtain better resolution. The fluosilicate has normally only one ion in the unit cell (Pauling 1930), but at 20° K the spectrum is that of three ions in the unit cell. If the trigonal axis of the crystal is considered as the space diagonal of a cube, then the three ions have each axial symmetry about one of the three mutually perpendicular cube edges. The following values are obtained for the parameters in the spin Hamiltonians: $g_{\parallel}=2{\cdot}46$, $g_{\perp}=2{\cdot}11$, $|A|=11\times10^{-3}$ cm^{-1}, $|B|\leqslant3\times10^{-3}$ cm^{-1}. These parameters are very similar to those obtained in the Tutton salts of copper (Bleaney, Bowers and Ingram 1951), and a nuclear electric quadrupole effect is also visible. Thus it seems probable that in this case we have a field of tetragonal symmetry, corresponding to the fourfold symmetry associated with the edges of a cube.

These results show that at low temperatures the rapidly fluctuating distortions associated with the Jahn–Teller effect are replaced by static distortions. The nature of this transition is obscure, but further information may be obtained from a careful study of the resonance spectrum at intermediate temperatures. At present no satisfactory theory of the mechanism involved has been suggested.

The authors wish to thank Professor M. H. L. Pryce for helpful discussion. The work on the double nitrate was carried out by Mr. R. S. Trenam, who very kindly informed us of his results prior to publication.

The Clarendon Laboratory,
Oxford.
17th June 1952.

B. BLEANEY.
K. D. BOWERS.

ABRAGAM, A., and PRYCE, M. H. L., 1950, *Proc. Phys. Soc.* A, **63**, 409.
BLEANEY, B., BOWERS, K. D., and INGRAM, D. J. E., 1951, *Proc. Phys. Soc.* A, **64**, 758.
BLEANEY, B., and INGRAM, D. J. E., 1950, *Proc. Phys. Soc.* A, **63**, 408.
JAHN, H. A., and TELLER, E., 1937, *Proc. Roy. Soc.* A, **161**, 220.
PAULING, L., 1930, *Z. Kristallogr.*, **72**, 482.

The M_V Absorption Edges of Tm and Er and the Origin of the Er M_V Absorption Lines

We have recently obtained a series of photographs of the absorption spectrum of ^{69}Tm in the M_V region by means of a bent crystal focusing spectrometer, using an absorbing film of thulium oxide approximately 0·1 mg/cm^2 thick. The photographs show no sign of the M_{IV} absorption edge, while in the M_V region a narrow absorption line only is apparent. This result may be compared directly with Lindberg's result for the two neighbouring elements ^{68}Er and ^{70}Yb. Lindberg (1931) found no M_{IV} edges for either of these elements, a single M_V absorption line for Yb, and a close pair of absorption lines in the M_V region for Er. Density curves of the Tm absorption line taken with a recording microphotometer, however, show that the line is definitely asymmetrical, having a steeper profile on the long wavelength side, which suggests that this is actually the M_V edge. A tracing of a typical density curve is shown in curve (*a*), where A is the point of minimum density (i.e. maximum absorption). Closer examination of these curves reveals that the long-wave side changes its gradient rather abruptly by a small but noticeable amount at the point B. This effect appears so consistently in approximately the same position on the microphotometer recordings of all the photographs taken that it must be considered to be real, and indeed suggests that we are dealing with two close unresolved absorption lines of unequal intensity of the type indicated by the dotted curves in (*b*). Our measurements show that these two lines would be separated by approximately 10 X.U. which would fall between the measured separation of 17 X.U. found by Lindberg for the two Er lines, and the zero separation for the Yb line. Assuming this analysis, the longer wavelength would be ascribed to a transition from the M_V level to an unoccupied 4f level, and the long wavelength profile of the shorter wavelength line would represent the M_V edge modified by the presence of the absorption line. The conventional wavelength of the M_V edge would then be that of the point K in (*b*), the point of inflection of the reconstructed M_V edge. Using Kα lines of Zn, Mn, Al, Ti and Ni in high order spectra as reference lines we estimate the wavelength of this point as 8469·5 ± 3 x.u. and of the point A as 8461·4 ± 2 x.u. The value of ν/R for the edge is then found to be 107·59 ± 0·07. A computed value of 107·65 is obtained from the wavelengths of the L_{III} edge found by Coster (1923) and of $L\alpha_1$ by Coster, Nishina and Werner (1923) (these are the wavelengths given in the tables of Cauchois and Hulubei 1947), so that the discrepancy is effectively zero, in contrast to the small but definitely negative values found in the case of other rare earth elements (Stewardson and Zandy 1950, Lee and Stewardson 1951). A modified Moseley plot of all relevant frequencies (L_{III}, $L\alpha_1$ and M_V) for the rare earths shows that the accepted value of Tm$L\alpha_1$ is rather low compared with that of neighbouring elements and the low value of the L–M_V discrepancy might well arise from this fact. The wavelength of the assumed absorption line accompanying the edge cannot be arrived at with any great reliability but will obviously differ from that of the edge by a few x.u. only.

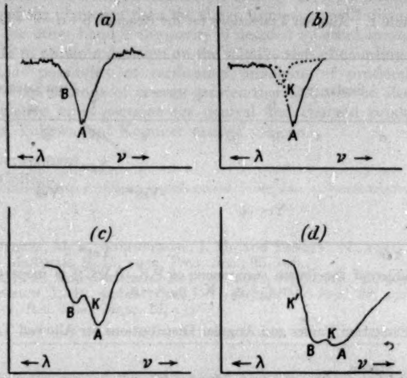

This result for Tm suggests that the results of Lee and Stewardson for the M_V edge of Er can be reconciled with those of Lindberg if it be assumed that Lindberg's two lines have the significance suggested here for the supposed Tm doublet, i.e. the longer wavelength corresponding to a transition to a 4f level, and the edge being given by some wavelength between the two lines at approximately 8813 x.u., instead of 8829 x.u. as found by Lee and Stewardson for a very thick absorption film. The hypothetical curves (*c*) (thin film) and (*d*) (thick film) show how this difference could arise, K′ being taken for the edge in the thick film, whereas the true edge is at K. Such progressive changes in appearance of an edge accompanied by a line absorption have been observed by Rule (1945) for ^{62}Sm, and by Zandy, working in this laboratory, for various rare earths. The modified value of the ErM_V wavelength suggested here would reduce the L–M_V discrepancy from −15 ev as previously found by Lee and Stewardson to the still large but more reasonable value of −12 ev approximately. Further experiments on the M_V and M_{IV} edges of these two elements are in progress.

Physics Department,
University College of Leicester.
16th May 1952.

P. A. Lee.
E. A. Stewardson.
J. E. Wilson.

Cauchois, Y., and Hulubei, H., 1947, *Constantes selectionées: Longueurs d'onde des émissions X, etc.* (Paris : Hermann).
Coster, D., 1923, *Phil. Mag.*, **46**, 956.
Coster, D., Nishina, Y., and Werner, S., 1923, *Z. Phys.*, **18**, 207.
Lee, P. A., and Stewardson, E. A., 1951, *Proc. Phys. Soc.* A, **64**, 318.
Lindberg, E., 1931, *Nova Acta Reg. Soc. Sci. upsal.*, Ser. 4, **7**, 68.
Rule, K. C., 1945, *Phys. Rev.*, **68**, 246.
Stewardson, E. A., and Zandy, H. F., 1950, *Proc. Phys. Soc.* A, **63**, 670.

The Nature of the Neutral π-Meson

It has been shown recently (Heckrotte, Henrich and Lepore 1952, Francis and Marshak 1952) that the π^0-meson would be expected to be produced much more readily in elastic photoproduction from deuterium, $\gamma + D = \pi^0 + D$, for a symmetrical meson theory than if the meson were coupled with the same sign to neutron and proton. It is the purpose of this note to consider the possibility of determining the relative sign of coupling, or indirectly of the parity, of the π^0-meson from differences to be expected in the reaction $n + p = \pi^0 + D$.

Table 1 shows the selection rules operative in this reaction for initial relative angular momenta 0, $\hbar$ or $2\hbar$ and for π^0-meson produced in s, p and d states. The differences that occur for the Yukawa neutral meson, where $g_N = g_P$, and the Kemmer neutral meson, $g_N = -g_P$ are due to the antisymmetry properties of the two fermion wave functions combined with the necessity of an isotopic singlet initial state for the Yukawa neutral meson, while since $\tau_3^{(i)}|{}^3(\tau)_0\rangle = -(-1)^i|{}^1(\tau)_0\rangle$, the Kemmer neutral meson is only produced from isotopic triplet initial n–p states. Qualitative differences are evident from consideration of this table and are verified by first-order perturbation calculations in many particle single time formalism. Table 2 gives the excitation function and expected angular distribution in the centre-of-mass system. Considering scalar mesons it is seen that the meson has to be created into d states if $g_N = g_P$ while p states are available for $g_N = -g_P$. The excitation function varies as $T^{5/2}$, where T is the meson kinetic energy in the centre-of-mass system, for Yukawa mesons, while the predicted cross section has a sharp forward peak, following an approximately $\cos^4\theta$ distribution. For Kemmer neutral mesons the cross section behaves as in the corresponding reaction $p + p = \pi^+ + D$; that is to say an excitation function of $T^{3/2}$ and a $\cos^2\theta$ angular law (Gunn, Power and Touschek 1951). For pseudoscalar mesons the selection rules are less effective. When accepting

Table 1. Allowed Transitions for the Reaction $p + n = \pi^0 + D$

Meson / n–p system	Scalar						Pseudoscalar					
	Y			K			Y			K		
	s	p	d	s	p	d	s	p	d	s	p	d
^{1}S											Yes	
^{3}S								Yes				
^{1}P							Yes*		Yes			
^{3}P					Yes					Yes*		Yes
^{1}D											Yes*	
^{3}D			Yes					Yes*				

* Forbidden if the fourth component of P.S. (P.V.C.) is inoperative.
Y : $g_N = g_P$; K : $g_N = -g_P$.

Table 2. Excitation Values and Angular Distributions for Allowed Transitions

Meson / n–p system	Scalar	Pseudoscalar
^{1}S	—	$T^{3/2}$: 1* (K, p)
^{3}S	—	$T^{3/2}$: $\cos^2\theta$ (Y, p)
^{1}P	—	$T^{1/2}$: 1 (Y, s)†
^{3}P	$T^{3/2}$: $\cos^2\theta$ (K, p)	$T^{1/2}$: 1 (K, s)†
^{1}D	—	$T^{3/2}$: $\cos^2\theta$ (K, p)
^{3}D	$T^{5/2}$: $\sim\cos^4\theta$ (Y, d)	$T^{3/2}$: $\cos^2\theta$ (Y, p)

* Small $\cos^2\theta$ term.
† Also $T^{3/2}$: $\cos^2\theta$ term from s–d interference.

the *ad hoc* assumption that the odd part of the pseudovector coupling is inoperative, the neutral and symmetric mesons must then come off in d or p states. This has been suggested by Francis and Marshak (1952) to explain the angular distribution for π^0-meson production in γ–p collisions and the forward cross section in $\pi+$ production by protons on protons (see also Chew, Goldberger, Steinberger and Yang 1951). It is only through a dominating fourth component in the interaction, for p-state mesons or from s–d interference that a non-isotropic distribution is favoured. This is necessary in the symmetric case to explain the observed behaviour in charged meson production.

The magnitudes of the cross sections are readily obtained. That for the Kemmer meson can be obtained from the charged meson results from which it differs by a factor two, except for the difference in rest mass of the π^+-meson and π°-meson. At 350 MeV the integrated cross section is approximately $1{\cdot}1\, g^2/\hbar c \times 10^{-28}$ cm², for neutral scalar mesons the cross section is approximately $3{\cdot}6\, g^2/\hbar c \times 10^{-30}$cm².

If other evidence, such as from the reaction $\gamma + \mathrm{D} = \pi^0 + \mathrm{D}$, gives information concerning the isotopic nature of the π^0-meson then the above interaction will distinguish scalar from pseudoscalar. On the other hand if the parity is decided by other means (Marshak 1951) it should be possible to obtain a decision on the relative sign of coupling. Other reactions with more immediate possibility of verification, involving π^0 production from nuclear collisions, such as from protons of energy greater than 200 MeV on deuterium, and also consideration of relative cross sections for neutral and charged production, will show differences between Yukawa and Kemmer neutral mesons.

Mathematics Department,
University College,
London.
8th May 1952.

E. A. Power.

Chew, G. F., Goldberger, M. L., Steinberger, J. M., and Yang, C. N., 1951, *Phys. Rev.*, **84**, 581.
Francis, N. C., and Marshak, R. E., 1952, *Phys. Rev.*, **85**, 496.
Gunn, J. C., Power, E. A., and Touschek, B. F. X., 1951, *Phil. Mag.*, **42**, 523.
Heckrotte, W., Henrich, L. R., and Lepore, J. V., 1952, *Phys. Rev.*, **85**, 490.
Marshak, R. E., 1951, *Rev. Mod. Phys.*, **23**, 137.

.A
5
2

Multiple Resonances in Photodisintegration Cross Sections

The reactions ^{16}O(γ, 4α) and ^{12}C(γ, 3α) have been studied by irradiating Ilford nuclear emulsions (200 micron E1 and C2) with bremsstrahlung, using peak energies from 20 to 70 MeV. Some 700 ^{16}O(γ, 4α) stars and 1 800 ^{12}C(γ, 3α) stars have been identified and analysed by techniques already described (Goward and Wilkins 1950), and the results reveal multiple resonances in the dependence of the cross sections on gamma-ray energy. These resonances suggest that the reaction should be interpreted in terms of the excitation of levels in a compound nucleus.

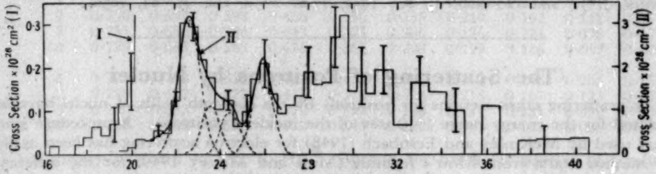

The figure illustrates the nature of the cross sections which have been found, and presents the ^{16}O(γ, 4α) cross section in the form of a corrected histogram. The uncorrected histogram recorded the gamma-quantum energy E_γ appropriate to each ^{16}O(γ, 4α) star, and was then corrected for the bremsstrahlung spectra, for ‘escape’ of stars from the emulsion layer and for other minor factors. Standard deviations are indicated by vertical lines and the experimental resolution (fairly closely known from experiments on the $^{12}C(\gamma, 3\alpha)$ reaction using $^{7}Li(p, \gamma)^{8}Be$ gamma-rays) by the dotted gaussian curves. At least three maxima, or resonances, are established, at gamma-ray energies of about 22·6, 25·8 and 29·5 Mev respectively. Comparison of the first two with the superposed dotted curves suggests real widths appreciably less than 1 Mev.

Making the assumption that the true cross section consists of a continuum of some form with relatively narrow resonances (<1 Mev) superposed thereon, it is clear that the present techniques cannot decide the relative contributions of continuum and resonances with any accuracy, although the continuum must be small near $E_\gamma=22{\cdot}6$ and 25·8 Mev. As an extreme illustration, the assumption of very narrow, discrete resonances at 22·6, 23·5, 24·5, 25·8, 27·2, 28·2 and 29·5 Mev, of relative magnitudes 1·00, 0·36, 0·29, 0·65, 0·32, 0·53 and 0·94 respectively (the values being obtained by trial curve fitting) would yield excellent agreement with the experimental data between 21·5 and 30·0 Mev without requiring any continuum.

The main trends of the $^{12}C(\gamma, 3\alpha)$ cross section have already been described (Wilkins and Goward 1951). Detailed study of results now available (Goward and Wilkins 1952) establishes at least four resonances at $E_\gamma=18{\cdot}4$, 21·8, 24·5 and 29·4 Mev respectively; the widths of the second and third must be appreciably less than 1 Mev. Several further resonances are strongly suggested by the results, particularly below $E_\gamma=18$ Mev. Again adopting the extreme illustration used in discussing the $^{16}O(\gamma, 4\alpha)$ results, the assumption of narrow, discrete resonances at 15·0, 16·1, 16·8, 17·4, 18·4, 19·5, 20·7, 21·8, 23·2 and 24·5 Mev, of relative magnitudes 0·30, 0·34, 0·28, 0·57, 1·00, 0·32, 0·08, 0·32, 0·23 and 0·70 respectively, gives excellent agreement with experiment between 14·5 and 25 Mev. Resonances at ^{12}C excitations of 16·1, 16·7, 19·4, 20·7 and 21·8 Mev have been reported in other reactions (Hornyak *et al.* 1950, Blaser *et al.* 1951). Such a series of discrete resonances is too drastic a simplification however, since it does not account for the known cross section at $E_\gamma=17{\cdot}6$ Mev (Nabholz *et al.* 1952, Goward and Wilkins 1952), or for certain forward/back asymmetries in the alpha-particle angular distributions (Wilkins and Goward, to be published) which indicate overlapping of ^{12}C states.

A significant feature of the results for both the $^{12}C(\gamma, 3\alpha)$ and $^{16}O(\gamma, 4\alpha)$ reactions is that the general trends of the cross sections show minima where the corresponding (γ, n) cross sections have maxima. This again suggests a compound nucleus interpretation.

Atomic Energy Research Establishment,
Harwell, Didcot, Berks.
23rd May 1952.

F. K. Goward.
J. J. Wilkins.

Blaser, J. P., Boehm, F., Marmier, P., and Scherrer, P., 1951, *Helv. Phys. Acta*, **24**, 465.
Goward, F. K., and Wilkins, J. J., 1950, *Proc. Phys. Soc.* A, **63**, 662; 1952, *A.E.R.E. Memorandum*, G/M 127.
Hornyak, W. F., Lauritsen, T., Morrison, P., and Fowler, W. A., 1950, *Rev. Mod. Phys.*, **22**, 291.
Nabholz, H., Stoll, P., and Waffler, H., 1952, *Helv. Phys. Acta*, **25**, 153.
Wilkins, J. J., and Gowapd, F. K., 1951, *Proc. Phys. Soc.* A, **64**, 1056.

The Scattering of Positrons by Nuclei

The scattering cross sections for positrons by the coulomb fields of nuclei have been calculated for the energy range 1–10 Mev of the incident positrons. A procedure similar to that used by McKinley and Feshbach (1948) for electron scattering has been applied. This method starts from Mott's formula (Mott and Massey 1949) for the differential scattering cross section $\sigma(\theta)$:

$$k^2\sigma(\theta)=q^2(1-\beta^2)FF^* \operatorname{cosec}^2 \tfrac{1}{2}\theta+GG^* \sec^2 \tfrac{1}{2}\theta, \qquad \ldots\ldots (1)$$

where $q=\alpha/\beta$, $\alpha=Ze^2/\hbar c=Z/137$, $\beta=v/c$, $k\hbar$ is the momentum of the incident positron and F and G are obtained by replacing α with $-\alpha$ in the similar quantities for electron scattering defined by Mott and Massey. F and G are expanded in powers of α, keeping terms up to α^4 and the coefficients in the expansion calculated. The ratios R of the differential cross sections so obtained for positron scattering to those obtained using the Rutherford formula,

$$\sigma_R(\theta)=(Ze^2/2mc^2)^2\{(1-\beta^2)/\beta^4\} \operatorname{cosec}^4 \tfrac{1}{2}\theta, \qquad \ldots\ldots (2)$$

were calculated.

The error in R due to this procedure is of the order of α^4 and should be reasonably small for values of Z less than 50 ($\alpha^4 = 0{\cdot}018$). To obtain values which should be accurate to within about 2% up to $Z=80$, the exact positron scattering calculations of Massey (1942) for $Z=80$ were compared with those calculated using the above expansion and the size of the necessary correction term thus obtained. (The extrapolation of Massey's values to higher energy was carried out by plotting his differential cross sections against β for each scattering angle.) It was then assumed that the correction to R should be proportional to Z^4 for Z less than 80 and in this way values of R were obtained.

These values are given in the table.

Values of $R = \sigma(\theta)/\sigma_R(\theta)$

θ = the angle of scattering in degrees, E = energy of the incident positron in MeV,
Z = the atomic number of the scatterer.

Z	*θ* / *E*	30	45	60	80	90	100	120	135	150	180
10	1	0·903	0·825	0·731	0·591	0·519	0·448	0·314	0·232	0·168	0·115
	2	0·897	0·812	0·711	0·558	0·480	0·403	0·258	0·169	0·099	0·042
	5	0·894	0·807	0·702	0·544	0·463	0·383	0·233	0·140	0·068	0·009
	10	0·893	0·806	0·700	0·541	0·460	0·379	0·229	0·134	0·063	0·0024
20	1	0·875	0·791	0·697	0·560	0·492	0·425	0·300	0·224	0·166	0·118
	2	0·867	0·777	0·675	0·526	0·452	0·379	0·243	0·159	0·096	0·043
	5	0·863	0·770	0·665	0·511	0·434	0·358	0·217	0·130	0·068	0·009
	10	0·862	0·769	0·663	0·507	0·430	0·354	0·212	0·124	0·058	0·0024
30	1	0·854	0·769	0·676	0·543	0·478	0·414	0·296	0·222	0·167	0·121
	2	0·845	0·752	0·651	0·507	0·436	0·365	0·236	0·155	0·095	0·044
	5	0·840	0·745	0·640	0·491	0·417	0·343	0·209	0·125	0·062	0·009
	10	0·839	0·744	0·638	0·487	0·413	0·339	0·204	0·119	0·056	0·0025
40	1	0·836	0·751	0·659	0·529	0·465	0·403	0·289	0·220	0·170	0·127
	2	0·826	0·733	0·633	0·490	0·420	0·352	0·227	0·156	0·095	0·047
	5	0·821	0·724	0·621	0·472	0·399	0·329	0·199	0·119	0·061	0·011
	10	0·820	0·723	0·618	0·469	0·396	0·325	0·193	0·113	0·055	0·005
50	1	0·823	0·741	0·651	0·522	0·460	0·400	0·291	0·224	0·175	0·134
	2	0·812	0·721	0·621	0·483	0·413	0·346	0·224	0·151	0·098	0·051
	5	0·806	0·711	0·610	0·463	0·392	0·321	0·194	0·119	0·063	0·014
	10	0·805	0·709	0·607	0·460	0·388	0·316	0·188	0·113	0·056	0·007
60	1	0·813	0·732	0·646	0·517	0·456	0·398	0·294	0·229	0·172	0·141
	2	0·800	0·710	0·610	0·476	0·407	0·341	0·222	0·156	0·102	0·057
	5	0·793	0·700	0·601	0·455	0·385	0·314	0·190	0·120	0·067	0·019
	10	0·791	0·698	0·597	0·450	0·379	0·309	0·184	0·113	0·060	0·013
70	1	0·803	0·722	0·635	0·508	0·446	0·394	0·297	0·237	0·191	0·149
	2	0·790	0·697	0·598	0·466	0·396	0·335	0·219	0·162	0·111	0·065
	5	0·781	0·686	0·586	0·443	0·373	0·306	0·186	0·124	0·076	0·027
	10	0·780	0·683	0·583	0·436	0·367	0·298	0·179	0·116	0·067	0·020
80	1	0·795	0·703	0·612	0·487	0·427	0·385	0·300	0·245	0·201	0·157
	2	0·780	0·677	0·577	0·445	0·376	0·322	0·215	0·167	0·123	0·077
	5	0·770	0·663	0·560	0·420	0·353	0·290	0·181	0·131	0·090	0·038
	10	0·768	0·660	0·556	0·413	0·345	0·280	0·173	0·123	0·080	0·032

I am greatly indebted to Dr. E. H. S. Burhop for his keen interest and valuable suggestions during the course of the present work. I also express my sincere thanks to Dr. M. M. Sengupta for providing me with every facility to complete the work.

Physics Department,
Patna University,
Patna, India.
22nd May 1952.

H. N. Yadav.

McKinley, W. A., and Feshbach, H., 1948, *Phys. Rev.*, **74**, 1759.
Massey, H. S. W., 1942, *Proc. Roy. Soc.* A, **181**, 14.
Mott, N. F., and Massey, H. S. W., 1949, *Theory of Atomic Collisions* (Oxford: University Press).

Neutron Energy Measurements with a Helium 3 Filled Proportional Counter

Fast neutron energies are usually measured by methods based on the scattering of the neutrons by hydrogen. The incident neutron energy spectrum is obtained either by differentiation of the complete recoil proton pulse height distribution or by measurement of the energies of the protons recoiling in the forward direction. Scintillation counters with organic phosphors are quite sensitive detectors which can be used for the first method, and recently satisfactory results have been obtained (Poole 1952). One way to accomplish the second method is by use of the photographic plate as detector (Nereson and Reines 1950). However, the grain size and sensitivity set a low energy limit of about 500 kev for this technique. It has, in addition, the disadvantage of being laborious and time-consuming.

The drawback of any method designed to measure neutron spectra which is based on scattering lies in the conversion of the definite energy of the incident neutron into a continuum of energies of the recoiling particle. For some considerable time a suitable nuclear transformation induced by neutrons has been sought, in which one energy release corresponds unambiguously to one neutron energy. In order to be successful the cross section of such a reaction should be fairly large and its variation with neutron energy should be smooth and free from sharp resonances. Also the energy release for zero neutron energy should be small, and there should be no low-lying excited states of the residual nucleus leading to the emission of particles of reduced energy. Of the various possibilities (^{14}N, ^{10}B, ^{6}Li, ^{3}He), some of which have been tested experimentally (Keeping and Roberts 1950), the most satisfactory is based on the disintegration of ^{3}He :

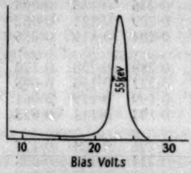

Fig. 1. Pulse height distribution obtained with ^{3}He counter when irradiated with thermal neutrons.

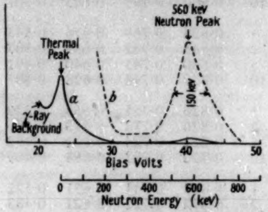

Fig. 2. Pulse height distribution obtained with ^{3}He counter when irradiated with ^{7}Li(p, n)^{7}Be neutrons (energy 560 kev).

$$ {}_2^3\mathrm{He}+{}_0^1\mathrm{n} \rightarrow {}_1^1\mathrm{H}+{}_1^3\mathrm{H}+770 \text{ kev}. \qquad \ldots\ldots (1)$$

The thermal neutron capture cross section of this reaction has been measured by Batchelor *et al.* (1949), 3 750 barns, King and Goldstein (1949), 5 000 barns, and Coon and Nobles (1949), 5 040 barns. The variation of cross section with neutron energy has been measured in the thermal energy region (King and Goldstein 1949) and in the 1 MEV energy region (Coon 1950). The value of the cross section for 1 MEV neutrons is about 1 barn which is comparable with the scattering cross section of neutrons of this energy by hydrogen. In reaction (1) the total energy of the proton and triton is $(E_n+0{\cdot}77)$ MEV, where E_n is the kinetic energy of the bombarding neutron.

The energy range of this detector is limited to a maximum neutron energy of 1 MEV because then the neutron–^{3}He elastic collision produces a maximum ^{3}He recoil energy of $\frac{3}{4}$ MEV, which event cannot be distinguished from a ^{3}He slow neutron disintegration. Above 1 MEV neutron energy the results of this method are ambiguous. However, if the neutron spectrum to be investigated has a definite upper energy limit E_m, then the maximum ^{3}He recoil energy will be $\frac{3}{4}E_m$. It follows that the energy release in the interval from $\frac{3}{4}E_m$ to $(E_m+0{\cdot}77)$ MEV can be assigned directly to the primary neutron spectrum in the range $(\frac{3}{4}E_m-0{\cdot}77)$ to E_m.

To put this scheme into operation a proportional counter containing ^{3}He and xenon to increase the stopping power has been constructed. Since the wall effect is a function of neutron energy, it is important to make it small. The presence of xenon unfortunately increases the γ-ray sensitivity of the counter and so increases the low energy background. The counter is 11 in. long and 3 in. in diameter and is filled to a pressure of 110 cm xenon and 5·4 cm of helium containing 10% ^{3}He. This helium was supplied by the Harwell Thermal Diffusion Group.

Figure 1 shows the pulse height distribution obtained with thermal neutrons for a gas amplification of 4. The width at half height is 55 kev. The counter was tested with approximately monokinetic fast neutrons from the ^{7}Li(p, n)^{7}Be reaction. Protons were accelerated by the Harwell Van de Graaff machine on to a lithium fluoride target. Curve *a* of fig. 2 shows a complete pulse height distribution including γ-ray background, thermal peak (due to thermal neutrons from wall scattering etc.) and a small fast neutron peak for neutrons of energy 560 kev. Curve *b* is drawn with a much increased ordinate scale to show the fast neutron peak more clearly. Part of the width of 150 kev is due to spread in the incident neutron energy introduced by target thickness and geometry (50 kev and 30 kev respectively). Similar response is obtained with neutrons of energies up to 800 kev, above which tests have not been made. With 350 kev neutrons, the peak is not completely resolved from the background.

I wish to thank Mr. P. Tunnicliffe for help at the start of this work, Dr. W. D. Allen for use of the Van de Graaff generator, and Dr. E. Bretscher for helpful guidance and discussion. I also thank the Director, Atomic Energy Research Establishment, for permission to publish this work.

Atomic Energy Research Establishment,
Harwell, Didcot, Berks.
19th May 1952.

R. BATCHELOR.

BATCHELOR, R., *et al.*, 1949, *Nature, Lond.*, **163**, 211.
COON, J. H., 1950, *Phys. Rev.*, **80**, 488.
COON, J. H., and NOBLES, R. A., 1949, *Phys. Rev.*, **75**, 1358.
KEEPING, G. R., and ROBERTS, J. H., 1950, *Rev. Sci. Instrum.*, **21**, 163.
KING, L. D. P., and GOLDSTEIN, L., 1949, *Phys. Rev.*, **75**, 1366.
NERESON, N., and REINES, F., 1950, *Rev. Sci. Instrum.*, **21**, 534.
POOLE, M. J., 1952, *Proc. Phys. Soc.* A, **65**, 453.

The Decay of the 2·4 Mev Level in ^{9}Be

The 2·4 Mev level in ^{9}Be has been studied through the reactions ^{9}Be(p, p′)^{9}Be* (Davis and Hafner 1948, Rhoderick 1950, and Browne *et al.* 1951) and ^{11}B(d, α)^{9}Be* (Buechner *et al.* 1951). Neutron emission from this level is energetically possible as an alternative to gamma radiation, and we have found that neutrons are indeed emitted.

A target of separated ^{11}B was bombarded with 425 kev deuterons. Alpha-particles emitted at 90° to the beam were detected by a thin anthracene screen and E.M.I. photomultiplier. A liquid phosphor (1·4 litres of a terphenyl solution in toluene) was used to detect the gamma-radiation or neutrons. It was mounted at a distance of about 50 cm from the target in a plane normal to the deuteron beam, and could be set at various angles to the first detector. The delay spectrum, i.e. the coincidence rate as a function of the delay between the pulses from the detectors (James and Treacy 1951), was studied using a circuit of 8 mμsec resolving time, similar to that described by Curling and Newton (1950) and modified later by Newton (1951).

If the reaction ^{11}B(d, α)^{9}Be* is followed by neutron emission to the ground state of ^{8}Be, recoil effects produce a variation in the neutron time-of-flight between 56 mμsec per metre at 180° to the alpha-particle direction and 187 mμsec per metre at 0°. For the same reason the rate of alpha–neutron coincidences should rise rapidly in going to 180°.

Such a sharp increase in the coincidence rate was indeed found in a preliminary study using a radiation detector placed close to the target. A delay spectrum with the radiation phosphor 40 cm away from the target and at an angle of 70° to the alpha detector gave only a single peak, at a delay of 8 mμsec in the radiation detector, and we must ascribe it to particle–gamma coincidences. (The 8 mμsec shift is to be expected if the gamma-ray pulses are larger than those from the other detector.)

The delay spectrum was next measured at 180° with the liquid scintillator 50 cm away from the target, giving curve 1 of the figure. Here a delayed group is clearly seen. The background (mainly from reaction $^{16}O(d, p)^{17}O^*(\gamma)^{17}O$) was obtained with a foil inserted to cut off the alpha-particles from $^{11}B(d, \alpha)^{9}Be^*$, and is shown in curve 2. The position of the particle–gamma coincidence group served to confirm the zero point of the delay spectrum. The two spectra were obtained in one session and under the same conditions; the average true-to-chance ratio for curve 1 was 1 : 1 and the true counting rate nearly one per second. The calculated delay of the alpha–neutron group is 28 mμsec. The observed value is 27 ± 5 mμsec. From these spectra we estimate the proportion of alpha–gamma coincidences at 180° to be $2{\cdot}5 \pm 2{\cdot}9\%$ of the total coincidence rate.

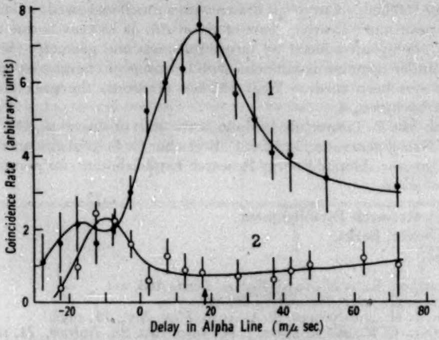

Arrow indicates expected delay of neutron group.

Assuming the alpha–gamma contribution to be small we studied, in steps of 10°, the correlation of the alpha-particles and neutrons with a radiation detector close to the target. (The background was determined as before and subtracted.) The rise towards 180° was confirmed, the intensity at this angle being about ten times that at 70°. This anisotropy, however, almost completely disappeared when the correction for the centre-of-mass effect was applied (disregarding the change of sensitivity of detection with neutron energy).

The small width of this level (< 3 kev, Browne *et al.* 1951) could be due to the angular momentum barrier for the low-energy neutrons emitted if a large spin change (2 or 3) is involved in the transition. Such small neutron widths have been observed (Bockelman *et al.* 1951).

We wish to thank Sir John Cockcroft and the Atomic Energy Research Establishment for providing the separated ^{11}B targets. We are much indebted to Professor W. E. Burcham for suggesting the experiment. One of us (G.A.D.) is grateful to the Ceylon Government for a scholarship, and the other (J.O.N.) to the Department of Scientific and Industrial Research for a grant.

Cavendish Laboratory,
Cambridge.
26th May 1952.

G. A. Dissanaike.
J. O. Newton.

Bockelman, C. K., Miller, D. W., Adair, R. K., and Barschall, H. H., 1951, *Phys. Rev.*, **84**, 69.
Browne, C. P., Williamson, R. M., Craig, D. S., and Donahue, D. J., 1951, *Phys. Rev.*, **83**, 179.
Buechner, W. W., Huang, K., Van Patter, D. M., Sperduto, A., and Strait, E. N., 1951, *Phys. Rev.*, **81**, 233.
Curling, C. D., and Newton, J. O., 1950, *Nature, Lond.*, **166**, 339.
Davis, K. E., and Hafner, E. M., 1948, *Phys. Rev.*, **73**, 1473.
James, D. B., and Treacy, P. B., 1951, *Proc. Phys. Soc.* A, **64**, 847.
Newton, J. O., 1951, *Proc. Phys. Soc.* A, **64**, 938.
Rhoderick, E. H., 1950, *Proc. Roy. Soc.* A, **201**, 348.

Internal Conversion Electrons from the ^{233}U Decay

In the artificially produced ($4n+1$)-series (Seaborg, Gofman and Stoughton 1947) previous investigations of γ- and X-rays indicate the existence of at least two excited states of the thorium resulting from the process $^{233}\mathrm{U} \rightarrow {}^{229}\mathrm{Th}$ (Studier 1947, West 1951). Using β-sensitive nuclear emulsions, a preliminary study has been made of the internal conversion electrons produced in this transition. Ilford G5 emulsions, thickness $200\,\mu$, were impregnated with uranium 233 in solution as the complex ammonium uranium citrate, adjusted to pH$=7$. The exposure time was 120 hours.

Out of 6 012 alpha-tracks, 548 ± 60 (i.e. $9{\cdot}1 \pm 1\%$) were associated with electron tracks. The uncertainty arises mainly from the difficulty of distinguishing the very short tracks. The grain count distribution of the electron tracks is shown in the diagram. Two groups of tracks are clearly resolved, the ratio of their intensities being 3·6 to 1.

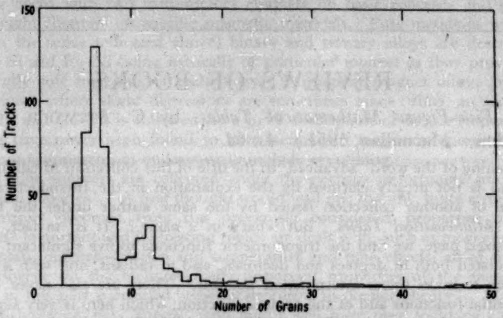

Grain count distribution for 548 electron tracks.

Using the relation between total grain count and energy established by Zajac and Ross (1949), the first group corresponds to an energy of about 20 kev, the second to one of about 33 kev. This is in agreement with the existence of an excited state of energy about 40 kev, assuming that the two groups mainly consist of L and (M+N) internal conversion electrons respectively. The interpretation is consistent with the observations by West (1951) of a γ-ray of $43 \pm 0{\cdot}5$ kev. There were 53 cases in which two electron tracks undoubtedly came from the origin of the same α-track. 44 of these could be interpreted as 43 kev conversion electrons associated with L Auger electrons. Eight events agree with the assumption that the weak $56 \pm 0{\cdot}5$ kev γ-line reported by West (1951) occurs in cascade with the 43 kev transition. The remaining double event consists of a 10 kev and an 82 kev electron track, which may be interpreted as due to an L Auger electron and an internal conversion electron arising from a direct transition with an energy of $43+56$ kev. This interpretation is supported by the existence of three single tracks attributable to L or M conversion of 99 kev. An alternative interpretation of this double event in terms of K Auger effect is somewhat less plausible. The intensities observed in this work are consistent with those published by West (1951). If then the 43 kev and 56 kev γ-rays are in cascade and if the 56 kev γ-ray is weak compared with the 43 kev ray both in emission and in internal conversion, then the first excited state is at 43 kev and the second at 99 kev. A check on the density of the background electron tracks showed that not more than four of all α-tracks might be wrongly interpreted as connected with an electron track because of chance superposition of the two events. The probability of a double electron event being spurious is negligible.

By using total grain counts instead of range measurements the time required for observation is much reduced. The use of grain counts as a measure of energy was justified by measuring both the three-dimensional range and the total number of grains for a limited number of tracks. Consistent energy values were obtained from the two measurements. An extended investigation of the electron energy distribution is contemplated.

The author wishes to thank Professor N. Feather for the opportunity of working in his department, for suggesting the problem and for his continued interest in the work. His thanks are also due to Dr. M. A. S. Ross for very helpful advice throughout the investigation. Valuable assistance has been given by Dr. N. Miller who prepared the uranium solution. A grant from the University of Aarhus enabled the work to be carried out.

Department of Natural Philosophy,
University of Edinburgh.
13th June 1952.

K. Maack Bisgård.*

* On leave from the Physical Institute, University of Aarhus.

Seaborg, G. T., Gofman, J. W., and Stoughton, R. W., 1947, *Phys. Rev.*, **71**, 378.
Studier, M. H., 1947, *NNES–PPR*, Vol. **17B**, Paper No. 1.3.
West, D., 1951, *Atomic Energy Research Establishment Progress Review*, No. 21.
Zajac, B., and Ross, M. A. S., 1949, *Nature, Lond.*, **164**, 311.

REVIEWS OF BOOKS

Advanced Five-Figure Mathematical Tables, by C. Attwood. Pp. v+69. (London: Macmillan, 1951.) 4*s*. 6*d*.

The meaning of the word 'advanced' in the title of this collection of tables is somewhat obscure, and is not greatly clarified by the explanation in the Introduction that it is a continuation of another collection issued by the same author under the title *Practical Five-Figure Mathematical Tables*. But what's in a name? It is, in fact, a handy set. On a good-sized page, we find the trigonometric functions to five significant (not decimal) figures, tabulated both in degrees and decimals, and in radians, and with a good deal of trouble taken to make linear interpolation possible. There are also tables of hyperbolic and exponential functions and of the gamma function, which here is very sensibly treated as the factorial function and written $x!$. Short tables of the complete elliptic integrals of the first and second kind take the square of the modulus as argument, an innovation which experience may well show to be advantageous. There are also short tables of the ordinate and of the area under the Gaussian curve; those interested in statistics would probably have wished for Student's t-distribution at least as often as they wish for the normal error curve.

The sources of the tables are not mentioned, but the author makes clear the great attention which he has given to the arrangement of them, with a view to reducing the occasions when linear interpolation is insufficient, and the care which he has given to avoiding numerical errors arising in the setting-up.

J. H. A.

Ferromagnetism (Bell Laboratories Series), by R. M. Bozorth. Pp. xvii+968. (New York: Van Nostrand; London: Macmillan, 1951.) £6 10*s*.

The subject of ferromagnetism nowadays pervades a wide field of pure and applied science. One of the oldest of the sciences, it is as important to the metallurgist, the chemist and the engineer, as to the physicist, whether an instrument designer or a student of the quantum mechanics of the solid state. Such an encyclopaedic subject needs an encyclopaedia to do it justice, and Dr. Bozorth's book succeeds in some measure to satisfy that need. The author is well qualified to carry out this monumental task. He is a member of the Bell Laboratories, whence so much of our recent knowledge of the nature and applicability of ferromagnetism has sprung, and his name is known wherever ferromagnetism is studied.

The book is written with emphasis on practice rather than on theory, although topics like domain theory and the molecular field concept also find their place. This accentuated practical approach may easily disguise the importance of phenomena which are of considerable interest in theoretical, and hence eventually, it is hoped, practical investigations. Thus, in discussing Ni–Co alloys we find the statement that "none of these alloys have any important industrial uses. Even the magnetic properties have no interesting peculiarities . . . ". To the theoretical student this very lack of interest, smooth curves rather than spectacular peaks, may be a substantial boon. Elsewhere in the book, especially where the author's own particular specialities are described, the approach is much happier. In fact, some theoretical sections, such as that on paramagnetism, could well have been omitted in favour of even more detailed experimental results, such as the important magnetic measurements by Sucksmith on the temperature variation of the magnetization of Fe–Ni–Al alloys, basic to modern permanent magnet materials. Many of the experimental sections, such as those on magnetic annealing of the permalloys and on the ΔE effect, are excellent and should prove to be most stimulating to teachers and investigators. The sections on powder patterns include photographs of the beautiful 'tree patterns'. These and other sections are frequently supplemented by useful practical hints, although it may be questioned whether they would be equally useful to one who was not a member of the Bell Laboratories.

The book opens with two introductory chapters on basic concepts and phenomena, followed by eight chapters on specific magnetic materials. Pure metals as well as many important (in the sense indicated above) binary and ternary alloys are described, those based on Fe–Si and Fe–Ni being naturally of particular interest as they provide most of the magnetically soft materials of technology. Permanent magnet alloys are discussed in a long chapter, where slight digressions are sometimes made : thus, an account of the systems Co–Pt and Co–Pd is followed by a brief description of the corresponding nickel alloys, which have never been found to have permanent magnet properties. Here and elsewhere there is apparent an endeavour to include everything.

The next nine chapters are collected under the perhaps unfortunate title 'Magnetic phenomena and theories'. A first thought would lead one to think, quite erroneously, that these are entirely divorced from the previously considered properties of materials. Actually, many important and interesting topics are dealt with, such as magnetic anisotropy of single crystals, magnetostriction and temperature and time effects, all of which have a profound influence on the technologically important properties of the materials. The final chapter in this part is entitled 'Special problems in domain theory'. Many of these problems are, however, not 'special' and might well have been included in the earlier parts of the book. Thus, a discussion of domain geometry could well have accompanied the section on powder patterns. The last chapter in the book deals with magnetic measurements, and in the main appendices are tables of the properties of soft and hard magnetic materials. The wide range of the characteristic properties of magnetic materials (for example, coercive force values ranging from 2×10^{-3}, supermalloy, to 6×10^{3}, silmanal) becomes particularly astonishing when these properties are presented tabularly.

Many of the disadvantages of the occasionally unsatisfactory arrangement of the subject matter and of incomplete cross references are offset by a detailed subject index. Here alloy systems are well arranged in alphabetical order and, since among the 800 or more figures there are very many binary and ternary phase diagrams, parts of the book constitute a miniature Hansen. The diagrams are consistently clear, but the captions are sometimes not sufficiently detailed. The author index refers the reader to the list of references containing some 1 700 publications between 1842 and 1951. The first of these is by Joule on 'A new class of magnetic forces' and the last by Weil on ferrites, in which magnetic forces of a new kind are again important. The wheel seems to have come full circle, but the reader of this book, if he can afford it at the exorbitant price, will have gained the impression that the wheel is capable of many more revolutions, leading through domains yet unexplored and fields yet untrodden. E. P. WOHLFARTH.

The Measurement of Radio Isotopes, by D. TAYLOR. Pp. viii+118. (London: Methuen, 1951.) 6*s*. 6*d*.

This little volume will be welcome to the rapidly growing number of people (engineers, biologists, doctors, etc.) who have to employ nuclear counting techniques without being nuclear physicists. Their job has become much easier now that nearly all the equipment required is manufactured, and [Dr. Taylor's book quite rightly refrains from describing any of the techniques for making counters and electronic circuits which constituted much of the art of nuclear physics in earlier days. Instead he briefly describes the physical principles involved in some of the commercial instruments (counters, scalers, counting rate meters, etc.) and gives common sense instructions for their use and testing. The book also contains in some detail the simple mathematics involved in the interpretation and planning of radioactive measurements; the elements of differential calculus are assumed and employed to derive formulae to allow for the effects of radioactive decay, self-absorption, solid angle, resolving time and statistical fluctuations. Most of the book refers to the use of Geiger–Müller counters, but proportional counters and scintillation counters are briefly described, and there is a chapter on monitors used for detecting contaminations and radiations dangerous to health.

The style of the book is pleasant and readable, and the mastery of the subject by the author is obvious throughout, occasionally from his use of terms or concepts which have not previously been explained. For this reason, and because of the stress on mathematical treatment, this is no book for bedside reading. But for the serious student it should not be difficult, and there are many numerical examples for the lovers of brass tacks.

O. R. FRISCH.

Facts from Figures, by M. J. MORONEY. Pp. 472. (Harmondsworth: Penguin, 1951). 5*s*.

Neither in scope nor price can this book be classed among the usual run of Pelican primers. To anyone who had not already some knowledge or interest in statistics its size might be discouraging. But to those who realize the possible value of statistical methods, and want a general introductory survey of the subject, this book should be most valuable.

Starting from the simpler ideas of probability, the earlier part of the book leads up to a descriptive account of the more important statistical distributions. Subsequent chapters show how these ideas lead to various applications, ranging from quality control to the analysis of variance ; a particularly interesting section describes the technique of sequential analysis. The author assumes that his reader has only a very slight knowledge of mathematics. This means that most of the formulae have to be given without proof. Instead, there is usually a careful explanation of the purpose of the technique under discussion and a fully worked out example showing its application.

The treatment throughout is remarkably entertaining. There are a large number of diagrams and tables to assist in the solution of the many examples, which are often both original and amusing. Sometimes the attempt to be easily understood is carried too far—it hardly seems necessary to explain how to square a number—but the reader can easily skip those parts which are too elementary for him. The author does not attempt to hide his political and other prejudices; this cannot be regarded as a fault since it adds to the general liveliness of the text. The treatment is particularly good in stressing both the error inherent in any statistical calculation and the many pitfalls which may be encountered in understanding the meaning of the results. Another virtue is that the author frequently points out that it would be dangerous to use the formulae which he gives without consulting a more advanced textbook. Even so, this book is likely to be worth a place in many research laboratories.

J. C. B.

The Challenge of Atomic Energy, by E. H. S. BURHOP. Pp. x+137. (London: Lawrence and Wishart, 1951.) 6*s*. 6*d*.

This booklet reviews the various aspects of atomic energy from the point of view of the general reader, and it fulfils its aim admirably. The physical introduction is written in a very simple and straightforward style, and it is no mean praise to say that the directness of the scientific approach is maintained in the later chapters discussing the economic, social and political aspects of the problem. The professional physicist concerned with this problem will find the first part useful if he has to prepare a popular lecture on the subject, and from the second part he will learn as much as anybody else.

L. ROSENFELD.

Elements of Thermodynamics and Statistical Mechanics, by E. O. HERCUS. Pp. ix + 153. (Melbourne, Australia: University Press; Cambridge: University Press, 1950.) 21*s*.

This book is divided into two distinct and separate halves, one on thermodynamics and the other on statistical mechanics, representing the lecture courses given to second and third year students respectively.

In the first half a review of the deductions which can be made from thermodynamics about systems of different sorts—chemical, radiating, electrochemical or purely mechanical—is made, preceded by a short review of the two main laws of thermodynamics themselves. The reviewer feels that this development is excellently carried out, but that the basis for the laws on which it rests is treated very scantly. In this he differs from the author and, since in fact the belief in the truth of the first law is one which grows up with each student during his study of mechanics, electricity, chemistry and other subjects, it must be conceded that it is not very important whether, before starting on formal thermodynamics, he is or is not given a summary of the evidence for a law which by that time is almost axiomatic to him.

The second part, on statistical mechanics, is very clear indeed, and can be recommended without any hesitation.

For the student there remains only the question whether he can afford the price, since he will in any case have to get a book on heat which will itself treat both these subjects. The answer depends on the depth of his purse and the amount of time he can devote to reading. If both conditions permit, he will do well to buy the book. J. H. A.

Heat and Thermodynamics, by MARK W. ZEMANSKY. Pp. xiv + 465. 3rd Edition. (London: McGraw-Hill, 1951.) 42*s*. 6*d*.

The author of this textbook is Professor of Physics in the City College of New York, and, therefore, has practical experience of teaching, and in fact says that the book represents an amplification of lecture notes. This is the third edition, which in itself shows that it must have been very popular in its country of origin.

To a reader who was not acquainted with the earlier editions it appears at the outset to attack the subject in a formal and rather pedantic way, but this impression disappears after the first ten or twelve pages. It has, in fact, quite a realistic and modern outlook, especially on the side where the subject approaches the field of physical chemistry. The chapter on heat transfer is also written from an extremely practical point of view.

The chapter on the physics of very low temperatures is quite masterly, and must have been re-written since the earlier editions, for its whole treatment of liquid helium II, supraconductivity and related matters reflects the ideas now current in this field, which had hardly crystallized when the earlier editions appeared.

The scope of the book is adequate for a degree course, and will often provide reference material for the research worker. It is well written and well produced, and if the price seems very high we may ask what commodity does not now seem very dear.

J. H. A.

Heat, by R. C. BROWN. Pp. ix + 270 + viii. (London: Longmans Green, 1952.) 13*s*. 6*d*.

This is one volume of a series which the author is writing to cover the branches of physics at the Intermediate Science level. At this stage the descriptive and experimental approach is called for, and the aim must be to give the student a broad familiarity with the terrain.

Dr. Brown writes well, and has given clear descriptions of the major phenomena usually treated under the heading of "Heat" and also of one hypothesis, the kinetic theory of gases. He has naturally not taken up the deductive side of the subject exemplified in thermodynamics.

His treatment of thermometry is particularly commendable for its accuracy in sorting out the concepts of heat and temperature, and in explaining why and how we formulate a scale of temperatures. The sections on calorimetry and on radiation are also particularly good, and the book can be confidently recommended. It has some examples for the student's practice. J. H. A.

Vektor- und Dyadenrechnung für Physiker und Techniker, by ERWIN LOHR. Pp. xv + 488. 2nd Edition. (Berlin: de Gruyter, 1950.) DM. 24.

Professor Lohr originally intended to carry out a complete revision of his book but, owing to the war, he has had to be satisfied with the addition of about 70 pages of supplementary material to an otherwise unchanged first edition. Being a physicist, the author writes primarily for physicists and engineers, but has provided at the same time a most adequate reference book for the applied mathematician working in a variety of fields.

In the first part a vector is defined geometrically in terms of its cartesian components, the idea of scalar products, complex vectors and dyads following in a simple manner. The quadric surface associated with a dyadic receives a fair amount of attention, including discussion of invariants and the Cayley–Hamilton equation.

The second part deals with differential operations together with a detailed treatment of vector and tensor fields, line, surface and volume integrals, sources, vortices and double layers.

The third part, which covers about half the book, deals with a wide range of physical applications, including theoretical mechanics, deformable media, differential geometry of curves and surfaces, elasticity, hydrodynamics of perfect and viscous fluids, electro-magnetic theory, optics, matrix and quantum mechanics. These are treated in surprisingly great detail considering the space at the author's disposal.

The additional material in the Supplement includes such topics as potential theory, special relativity, four-dimensional formulation of Maxwell's equations and Dirac's theory of the electron.

Although the book covers familiar ground and contains nothing substantially new, it must nevertheless be regarded as an advanced treatise, and its use to the beginner is further limited by the unfamiliar notation employed and by the fact that there are no exercises. There is a comprehensive 16-page index. A. N. GORDON.

Introduction to Modern Algebra and Matrix Theory, by O. SCHREIER and E. SPERNER. Pp. viii + 378. (New York: Chelsea, 1951.) No price given.

This book is the slightly shortened English version, in one volume, of the authors' work, originally in German, entitled *Introduction to Algebra and Analytical Geometry* and published in two volumes. It deals with the theory of vectors, determinants and the concept of field. It introduces briefly the theory of groups and ends with a long and more comprehensive chapter on linear transformations and matrices.

The authors are writing primarily for students of mathematics, but their demands of previous knowledge on the part of their readers is slight. Anyone who has mastered the chief operations of algebra and who has been introduced to the basic principles of geometry and the calculus will be able to follow the course presented here with ease and, indeed, with enjoyment.

Students of physics will find here a sound and very readable presentation of a notation which has in modern times become essential in their study.

They will find here an explanation of the terms and some propositions which are used, and often taken for granted, in textbooks of modern physics.

This is particularly true of the calculus of matrices and linear transformations which have come to be of fundamental importance to students of wave mechanics.

The book can be recommended with confidence to physics students in the final stages of their undergraduate course and in early postgraduate years. H. T. F.

Oeuvres scientifiques de Paul Langevin. Pp. 687. (Paris: Centre National de la Recherche Scientifique; London agents: H. K. Lewis, 1950.) In paper 44*s*.; in cloth 53*s*.

The appearance of most of the original papers of Paul Langevin collected together in one volume must be regarded as an event of great importance. This collection is not quite complete, as many papers which are readily accessible are not included; a list of these papers is given. In time this collection covers the entire first half of the twentieth century, for his first paper appeared in 1902 and his last in 1949: in substance it covers a range so wide as to include important papers on ionization of gases, kinetic theory, thermodynamics, electromagnetic theory, magnetism, relativity, radioactivity, ultrasonics, nuclear physics and gravitation. This is indeed a contribution to physics in the grand manner. An obituary notice of Langevin has been published in the *Proceedings of the Physical Society* (1947, **59**, 1041), where tribute to his immense range of achievement was made. His earlier work, coming as it did at a vital period in the development of physics, played a most important role in effecting the transition from the classical to the modern point of view, and can be regarded as forming a bridge between the statistical mechanics of the late 19th century and the early quantum ideas of the 20th century. In particular, Langevin's work is an excellent example of the power and scope of classical statistics in dealing with the fundamental collisional phenomena involved in the conduction of electricity through gases. Then, again, it is interesting to note that he was a pioneer worker in relativity, and also that Einstein first learned of de Broglie's original notions of wave mechanics from Langevin. For these reasons this volume of collected papers is, and probably will continue to be, of profound interest to the student of physics, and particularly to the young research worker, since, in addition to important theoretical papers, it also gives numerous papers describing his experiments.

Langevin's first papers dealt with the properties and motions of ions (the existence of free electrons in gases had not yet been demonstrated), and his interest in this subject no doubt originated during the time he spent at the Cavendish Laboratory under Sir J. J. Thomson. An outstanding problem which excited the interest of physicists at the turn of the century was that of the explanation of the electrical conductivity produced by X-rays or radioactive emanations. It was the application of classical kinetic theory to the experimental determinations of conductivity, and of current decay, which enabled the nature of the ion carriers to be found, the processes of ionization and recombination to be investigated, and the mechanisms of ionic transport, diffusion and recombination to be understood in terms of the collisions of elastic sphere atom models.

By consideration of the polarization of neighbouring neutral atoms produced by a charged ion, and also the resulting attraction effecting reduction of the free path, the consequent collection of molecules to form large clusters about a single ion was envisaged. These charged molecular groups, whether singly or in clusters, were shown to be the carriers of electricity. It was in this particular field that Langevin made his first outstanding contribution. In the series of papers in 1902–1905 (*Ann. Chim. Phys.*, **5**, 245), culminating in the famous paper *Une formule fondamentale de théorie cinétique*, he treated the motion of ions in gases, and rigorously derived the well-known formula for the drift velocity W:

$$W = 0{\cdot}815(Ze/m)(\lambda/C)\{(m+M)/M\}^{1/2},$$

of an ion of charge e, free path λ, r.m.s. velocity of agitation $C(\gg W)$, mass m moving under a field Z in a gas of molecular mass M in which the ion exerts no electric forces except at collision (low gas pressure). The ions are considered to be nearly in statistical equilibrium with the gas atoms: thus restriction is now known to be unnecessary, since the formula also applies to the motions of electrons under a regime of elastic conditions when the electrons are not in statistical equilibrium with the gas atoms, provided, however, that their energy distribution is Maxwellian. This latter consideration, again, only affects the numerical coefficient, which only varies from about 2/3 to unity over a wide range of electron energy distribution functions. Replacement of the force Ze by that due to the concentration gradient leads to Langevin's formula for the diffusion coefficient of ions. The application of his formulae to the measurements of the mobilities of clusters, single ions, or of electrons led to determinations of the mass factor and of the collisional cross sections of the ions: and, in fact, in the hands of Townsend and Tizard, such application suggested in 1913 the possibility of a variation of atomic cross section in collisions with slow electrons. That Langevin had peculiar insight in this subject is seen by the fact that his basic formula held the field for about 25 years, in fact until the discovery of exchange phenomena and the calculations of Mott and Massey based on quantum scattering, and was used in the interpretation of the experimental work of Tyndall and Powell.

The other great contribution with which Langevin's name is always associated is in the theory of magnetism, and this was made in 1905. The theory of electrons in the hands of Lorentz was making great strides, but doubt was expressed whether the magnetic theories of Ampère and Weber could be expressed adequately in terms of the new electron theory.

It was Langevin who set these doubts at rest. Curie's work on the temperature dependence of paramagnetism was almost completely explained by Langevin on the basis of the classical kinetic theory on the assumption that paramagnetic susceptibility was due to the reserve of permanent magnetic dipoles in each molecule. The results deduced that over a large range of temperature paramagnetic susceptibility is inversely proportional to the absolute temperatures—known as the Curie–Langevin law. This work today still forms a most valuable introduction to the electron theory of magnetism. The full explanation, however, had to await the application of the quantum theory of spin, with its restrictions on the orientations of the molecular magnets in a magnetic field.

This book of 687 pages gives a *curriculum vitae* of Langevin and a complete bibliography of his scientific works, and has altogether thirteen chapters. In spite of its size, this volume is quite pleasant to handle, and the print is clear and easy to read. The first chapter describes his experimental works on ionization of gases by X-rays, his experimental and theoretical work on ionic mobility and recombination, including the polarization of neutral atoms produced by the ion charge, and the properties of secondary X-rays ; he contributed to these subjects throughout his life. The second chapter is devoted to considerations of ionization in the atmosphere and the properties of ion clusters.

The next three chapters are of a theoretical character and give his papers on fundamental kinetic theory, electromagnetic inertia, relativity, and also his classic work in the theory of magnetism. The sixth chapter presents a collection of his papers on relativity, and this is followed by chapters on radioactivity and units. Then follow some twenty pages devoted to a critical review of classical, quantum and statistical mechanics. Chapters ten and eleven are concerned with his contribution to ultrasonics, under-water acoustics and divers technical problems : these represent his scientific work war in World War I. He originated and developed the piezoelectric under-water detector, and carried out trials in Toulon harbour. The two final chapters are devoted to his most recent work on nuclear physics and gravitation, and are of a fundamental nature.

It is not possible within the scope of a short review to discuss the chapters in detail : it is sufficient to stress the scope and quality and importance of the work described, to admire the clarity of its exposition, and very strongly to recommend this collection to all interested in the history and development of an important aspect of modern physics.

F. LLEWELLYN JONES.

Quantum Mechanics, by ALFRED LANDÉ. Pp. x + 307. (London : Pitman, 1951.) 40*s*.

In recent years there have appeared a fair number of good introductory treatises on Quantum Mechanics, each taking the student from the beginnings of quantum theory up to the description of relativistic electron theory and field quantization. It is typical of the many-sided aspects of quantum mechanics that these treatments all have considerable points of difference, not only in the detailed problems studied but also in the fundamental style of approach and in the order of treatment.

Professor Landé's book is an excellent addition to this series. As the author himself states in the Preface, the emphasis of his approach is placed on " the physical background of quantum mechanics and its close relation to classical experience, rather than on a rigid axiomatic formulation of the mathematical method ". The first three chapters are devoted to a study of the equivalence of waves and particles and of the older quantum theory. Schrödinger's equation for matter waves is then developed, and the next two chapters are devoted to some of the exact and approximate problems of wave mechanics. In chapter VI the transition is made to matrix mechanics based on the wave-mechanical representation. There follow treatments of some non-steady state problems, and of electronic spin leading to the helium atom and hydrogen molecule. There is also a brief discussion of atomic and molecular spectra and of quantum statistics. The last three chapters are concerned with Dirac's electron theory, and with the quantization of the electromagnetic and meson fields.

It will be seen that the ground covered in the book is very wide. The discussion is, however, generally clear, though at times rather condensed so that in places the mathematics is left to carry the argument. The inclusion of relativistic electron theory and field quantization in an elementary book poses severe problems, which cannot be said to have been completely solved by the author. However, it was no doubt right to include these topics, and the treatment offered at least forms an introduction to more advanced treatises.

In general, the book forms a reliable and well presented account of wave mechanics suitable for Honours Physics students of reasonable mathematical attainments, and for young research workers. An interesting feature is the short summaries at the end of each chapter, which preserve the main line of argument against the mathematical details.

J. C. G.

CONTENTS FOR SECTION B

PAGE

Dr. A. J. Goss and Mr. S. Weintroub. The Growth from the Melt of Single Crystals of Low Melting Point Metals 561

Mr. K. E. Puttick. The Growth from the Melt of Single Crystals of Low Melting Point Metals. (Discussion) 571

Dr. P. R. Rowland. Asymmetry of Texture in Cubic Crystals Grown from the Melt 572

Dr. K. M. Greenland. The Growth of Thallium-Bromo-Iodide Crystals 574

Dr. A. C. G. Menzies. Growth of Crystals of Caesium Bromide, and the Infra-Red Transmission Limit in Optical Materials 576

Dr. H. E. Buckley. Crystal Growth Ideas and Crystallographers . . . 578

Mr. J. Dyson. Optics of the Focusing X-Ray Microscope 580

Miss M. M. MacNaughton. The Focal Properties and Spherical Aberration Constants of Aperture Electron Lenses 590

Dr. U. F. Gianola. Investigation of Magnetic Lenses having the Axial Field $H(0, z)=\gamma/z^n$ 597

Dr. J. Woodrow, Mr. B. W. Mott and Mr. H. R. Haines. Analysis of Polarized Light Reflected from Absorbing Materials at Normal Incidence . . 603

Dr. R. Parker. The Magneto-Resistance of Ferromagnetic Al–Si–Fe Alloys . 616

Mr. J. M. Somerville. Sparking Potentials in a Transverse Magnetic Field . 620

Dr. E. Rabinowicz. Metal Transfer during Static Loading and Impacting . 630

Dr. D. R. Davies and Mr. T. S. Walters. Further Experiments on Evaporation from Small, Saturated, Plane Areas into a Turbulent Boundary Layer . . 640

Mr. A. N. Gent and Dr. R. S. Rivlin. Experiments on the Mechanics of Rubber: III—Small Torsions of Stretched Prisms 645

Letters to the Editor:

Mr. E. J. Gillham and Mr. J. S. Preston. Transparent Conducting Films . 649

Dr. J. W. Granville and Dr. H. K. Henisch. Area Contacts on Germanium 650

Dr. J. W. Granville, Dr. H. K. Henisch and Mr. P. M. Tipple. Contact Properties of p-Type Germanium 651

Reviews of Books 652

Contents for Section A 654

Abstracts for Section A 655

ABSTRACTS FOR SECTION B

The Growth from the Melt of Single Crystals of Low Melting Point Metals, by A. J. Goss and S. Weintroub.

ABSTRACT. The results of a series of experiments on the preparation of tin, lead, zinc, and bismuth single crystals in the form of rods are given. The effects on the crystallization of various thermal factors, in particular the temperature gradient and the rate of growth, are studied and the results for the four metals are compared.

Asymmetry of Texture in Cubic Crystals Grown from the Melt, by P. R. Rowland.

ABSTRACT. Careful electro-polishing of single crystal spheres of copper (face-centred cubic system) grown from the melt has revealed that they appear to consist of a number of parallel crystallites of square cross section with their lengths parallel to the [001] axis which lies nearest in direction to the ' direction of growth ' in the melt.

The Growth of Thallium-Bromo-Iodide Crystals, by K. M. Greenland.

ABSTRACT. Crystals of thallium-bromo-iodide, or KRS-5, are transparent to radiation of wavelengths between $0{\cdot}5\mu$ and about 40μ. This note briefly describes the growing of KRS-5 single crystals and their optical working. The crystals are grown in vertical cylindrical crucibles by a progressive freezing of the melt from bottom to top. The physical, chemical and mechanical properties of the material are summarized.

Growth of Crystals of Caesium Bromide, and the Infra-Red Transmission Limit in Optical Materials, by A. C. G. Menzies.

ABSTRACT. Following the development of methods for growing single crystals of materials having good optical properties, the search has been intensified for new substances. One such is caesium bromide, and this has been grown by the Kyropoulos–Pohl method of drawing from the melt; a modification of the standard process is described.

In the search for new materials, it is useful to have some way of predicting the useful long-wavelength transmission limit, and a rule is stated which forms a useful guide.

Optics of the Focusing X-Ray Microscope, by J. Dyson.

ABSTRACT. A brief description is given of Kirkpatrick and Baez' x-ray reflecting microscope. The types of aberration possible in optical systems without axial symmetry are discussed and the effect of spherical aberration on the diffraction pattern of an object point is evaluated. The resolving power of a circular mirror is calculated, and a method of correcting field obliquity is described. A method is given for the design of a figured mirror to give smaller spherical aberration with zero field obliquity.

Design equations are given for a system employing two circular mirrors in each plane, by which spherical aberration, obliquity and curvature of field can be corrected. The computed performance of the system is described.

The Focal Properties and Spherical Aberration Constants of Aperture Electron Lenses, by M. M. MacNaughton.

ABSTRACT. The focal properties and spherical aberration constants of a number of aperture electron lenses of varying diaphragm thickness and varying strength were determined numerically using potential distributions obtained (*a*) from a rigorous solution due to Ollendorff, and (*b*) on a resistor network analogue. The focal lengths of 'weak' aperture lenses of finite diaphragm thickness agree closely with those given by Davisson and Calbick's formula for the ' infinitely ' thin aperture lens; ' strong ' aperture lenses of all thicknesses show systematic deviations from this formula. The primary spherical aberration constants of diverging aperture lenses are small, and of such sign that they cannot be used for the correction of the spherical aberration of converging electron lenses.

Investigation of Magnetic Lenses having the Axial Field $H(0, z)=\gamma/z^n$, by U. F. Gianola.

ABSTRACT. Examination of the requirements for reducing the spherical aberration of an electron lens by modifying the field shows that the hypothetical lens field $H(0, z)=\gamma/z^n$ should have small aberrations.

It is shown that the properties of a certain class of this general field configuration can be described in terms of an exact analysis. In particular, the electron optical properties of the γ/z^2 field are described in detail.

The γ/z^2 field is found to have small aberrations, but practical conditions limit appreciable improvement in resolving power. The characteristics of the γ/z^3 field are also examined and are found to give little further advantage.

Analysis of Polarized Light Reflected from Absorbing Materials at Normal Incidence, by J. Woodrow, B. W. Mott and H. R. Haines.

ABSTRACT. Expressions are derived for the intensity of the analysed light reflected from absorbing crystals (*a*) under crossed polarizing units and (*b*) with the analyser slightly rotated from the crossed position. Four intensity maxima per complete rotation of the specimen are obtained when the polarizers are crossed, but under certain circumstances, as the analyser is rotated from the crossed position, the number of maxima may be reduced to two. These relationships are illustrated by experimental curves on specimens of tin, uranium, bismuth and stibnite.

The Magneto-Resistance of Ferromagnetic Al–Si–Fe Alloys, by R. Parker.

ABSTRACT. By extending the treatment in an earlier paper an equation is derived for the saturation magneto-resistance of some mixed ferromagnetic alloys as a function of composition and temperature. Results calculated from this equation are in good agreement with experiment for the Al–Si–Fe alloy system.

Sparking Potentials in a Transverse Magnetic Field, by J. M. Somerville.

ABSTRACT. A theory of sparking between parallel plates in a transverse magnetic field, put forward by Valle in 1950, is discussed and shown to be in qualitative disagreement with observation. By making allowance for the distribution of electron free paths, and for electron recapture by the cathode, a modified theory is produced which is in better agreement with observation. Further refinement of the theory requires an approximate expression for the first Townsend coefficient which is valid when a magnetic field is present. The possibility of obtaining such an expression is discussed.

Metal Transfer during Static Loading and Impacting, by E. Rabinowicz.

ABSTRACT. Experiments are described which investigate the metal transfer which takes place when a radioactive hemispherically ended slider is pressed normally into a flat surface of the same or another metal.

It is found that metal transfer in the form of a number of small fragments is always observed, and this supports the view that metallic junctions are formed between metal surfaces in contact. Experiments in which the load is varied suggest that at the higher loads the oxide layer on the metal surfaces is broken up to a larger extent than at lower loads, and a more than proportional increase in metallic interaction and transfer takes place. An analogous effect is observed in the presence of boundary lubricants.

When the surfaces are impacted together, very similar results are obtained. Somewhat less pick-up is observed than for static loading, and the difference is probably due to the fact that it takes time for strong junctions to be formed. Impact experiments with surfaces covered by lubricants show that a lubricant layer may be trapped between the surfaces, and this produces a large reduction in pick-up without greatly reducing the amount of plastic deformation.

Further Experiments on Evaporation from Small, Saturated, Plane Areas into a Turbulent Boundary Layer, by D. R. Davies and T. S. Walters.

ABSTRACT. This paper describes an experimental investigation designed to evaluate the effect of width and length on rates of evaporation from small, saturated, plane, rectangular areas placed in a turbulent boundary layer. An approach is made to the problem of estimating the distribution of temperature on the evaporating surface by using a number of thermojunctions situated at various points under the surface. The higher rate of evaporation near the edges of the area is well illustrated by this method, greater temperature differences between the surface and air stream being observed near the edges due to greater latent heat effects. Provided the crosswind width of the evaporating area is not less than about half the downwind length, Sutton's two-dimensional solution of this limited area problem is found to lead to tolerable accuracy in the circumstances tested.

Experiments on the Mechanics of Rubber—III: Small Torsions of Stretched Prisms, by A. N. Gent and R. S. Rivlin.

ABSTRACT. A theorem, relating the torsional modulus for small torsions of a rod of incompressible highly elastic material, held in a state of simple extension, to the extension ratio and force necessary to maintain the extension, is verified experimentally for rods of vulcanized rubber of rectangular cross section.

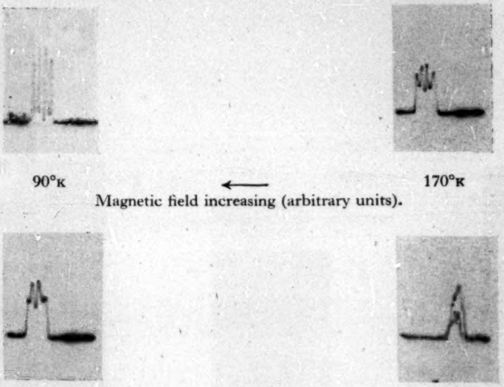

90°K ⟵ 170°K

Magnetic field increasing (arbitrary units).

240°K 290°K

(*a*) $K_2(Cu+Zn)(SO_4)_2 \cdot 6H_2O$

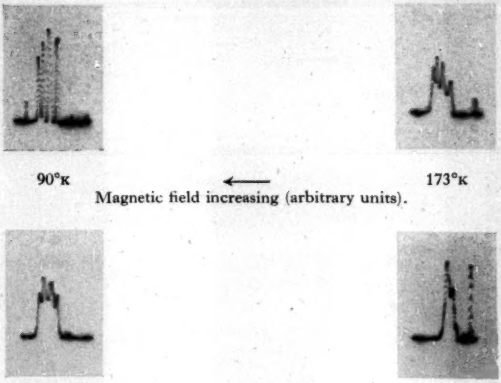

90°K ⟵ 173°K

Magnetic field increasing (arbitrary units).

215°K 290°K

(*b*) $Rb_2(Cu+Zn)(SO_4)_2 \cdot 6H_2O$

Fig. 2. Variation in width of hyperfine lines with temperature.

⟵

Magnetic field increasing (arbitrary units).

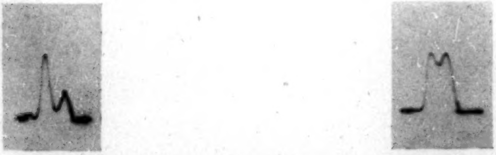

K_1K_3 K_2K_3

Fig. 3. Absorption lines in $K_2Cu(SO_4)_2 \cdot 6H_2O$ with magnetic field at 45° to *b* axis.

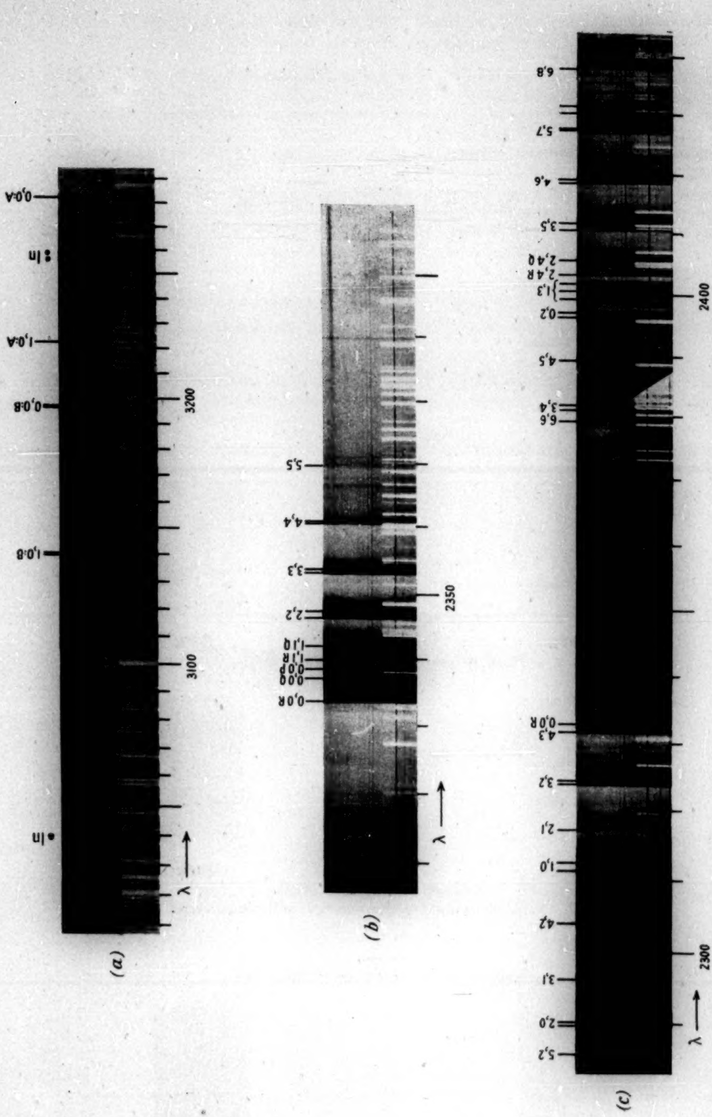

Fig. 2. The absorption spectrum of InF: (a) $A^3\Pi_{0^+}$, $B^3\Pi_1-X^1\Sigma$ systems; (b), (c) $C^1\Pi-X^1\Sigma$ system; Fe arc comparison spectrum.

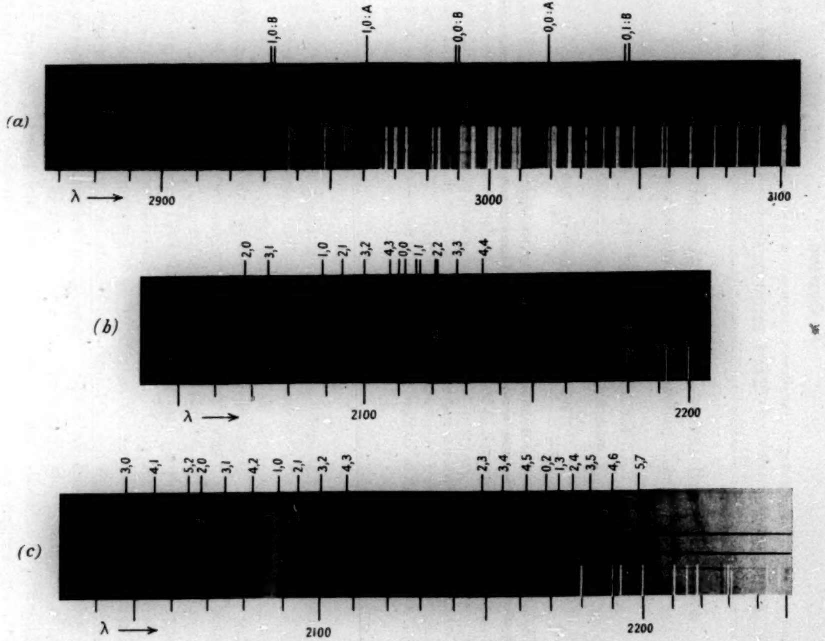

Fig. 1. The absorption spectrum of GaF: (a) $\mathrm{A}\,{}^3\Pi_{0^+}$, $\mathrm{B}\,{}^3\Pi_1 - \mathrm{X}\,{}^1\Sigma$ systems; Fe arc comparison spectrum; (b), (c) $\mathrm{C}\,{}^1\Pi - \mathrm{X}\,{}^1\Sigma$ system; Cu arc comparison spectrum.